2(mix)

NASA CR-120916

DESIGN OF A TF34 TURBOFAN MIXER FOR REDUCTION OF FLAP IMPINGEMENT NOISE

FINAL REPORT

by A. Chamay, D.P. Edkins, R.B. Mishler and W.S. Clapper

GENERAL ELECTRIC COMPANY
AIRCRAFT ENGINE GROUP
LYNN, MASSACHUSETTS/CINCINNATI, OHIO

Prepared for
NATIONAL AERONAUTICS AND SPACE ADMINISTRATION
February 2, 1972

NASA Lewis Research Center
Cleveland, Ohio
N.E. Samanich — Project Manager

CONTRACT NAS 3-14338 Modification 2

131 p

NASA CR-120916

FINAL REPORT

DESIGN OF A TF34 TURBOFAN MIXER FOR REDUCTION OF FLAP IMPINGEMENT NOISE

by

A. Chamay, D. P. Edkins, R. B. Mishler and W. S. Clapper

General Electric Company
Aircraft Engine Group
Lynn, Massachusetts/Cincinnati, Ohio

prepared for

NATIONAL AERONAUTICS AND SPACE ADMINISTRATION

February 2, 1972

CONTRACT NAS3-14338 Modification 2

NASA Lewis Research Center
Cleveland, Ohio
N. E. Samanich - Project Manager

TABLE OF CONTENTS

ABSTRACT

This portion of the TF34 Turbofan Quiet Engine Studies has been devoted to the selection and design of a special mixer exhaust nozzle system to reduce the maximum 150 m (500 foot) sideline noise generated by the impingement of four engine exhausts on a STOL wing flap system to less than 92 PNdB. The design concept selected consists of a 12-lobe internal mixer and a 12-lobe external mixer mounted in series. The internal mixer reduces maximum exhaust velocities by mixing the fan and turbine streams. The external mixer is designed to reduce the velocity of the exhaust stream striking the wing flap surfaces. A ground test version of this concept has been designed to be installed and tested on an acoustically treated TF34 engine nacelle, with flexibility to simulate a flight version of this concept which has also been defined. Estimated noise levels are 2 PNdB below the objective at approach and 2 PNdB above the objective at takeoff, with an uncertainty band of +3, -2 PNdB.

SUMMARY

A two-phase study program has been conducted to select and design a special mixer exhaust nozzle system for a quiet STOL TF34 engine ground test nacelle. This system is designed to reduce the engine exhaust-wing flap interaction noise of an externally blown flap TF34 engine installation. The selected design consists of a 12-lobe internal and a 12-lobe external mixer mounted in series. Two reference nozzle configurations have been designed to be used as a basis of a comparison and to assist in the diagnosis of additional potential noise sources. These three ground test exhaust nozzle designs, installed on the acoustically-treated nacelle are shown in Figure 1. The corresponding flight version of this acoustically treated nacelle and mixer nozzle design concept is illustrated in Figure 2.

The Task I studies to select this mixer nozzle design were initiated with a review of all available data on mixer nozzles, jet noise suppressors and the noise generated by exhaust jet impingement on wing and flap surfaces, and led to the identification of twelve potentially promising design concepts. Nine concepts were for engine cycles with mixed fan and turbine exhaust streams and three were for separate exhausts. Eight of the concepts had variable geometry, and four had fixed geometry, mixers. The fixed geometry multi-lobe design approach was selected as offering potential for the highest performance and lightest weight.

Multi-lobe mixer nozzle performance, velocity decay and flap interaction noise trade studies were conducted, using three new computer programs developed for this study:

(1) A generalized program for computing peak exhaust jet velocity decay as a function of mixer nozzle geometry and distance from the exhaust.

(2) A program to define minimum performance loss and minimum weight mixer nozzle geometry for a specified level of velocity decay.

(3) A generalized program for computing exhaust jet plus flap interaction noise as a function of exhaust velocity, engine power setting, and velocity decay.

Results from these studies along with engine exhaust velocity data from General Electric Proposal (M34-0170-006A System Proposal for Propulsion NASA Experimental STOL Transport Research Aircraft) led to the recommendation of a 12-lobe concept for detailed design in Task II.

The Task II ground test mixer nozzle design studies included engine cycle and systems studies to account for duct total pressure losses on nozzle jet area and exhaust velocity The effect of varying nozzle exit area was also investigated.

Mixer nozzle jet area trim capability was designed into the ground test hardware through replaceable contoured inserts that are a part of the outer surface of each lobe. A series of these contoured inserts have been designed to permit testing of symmetric and non-symmetric exit shapes.

The final selected mixer was designed to reduce the velocity of the exhaust gas to .68 and .58 of its peak value in 2.55 m (100 in.) and 4.1 m (160 in.), respectively. The associated thrust loss was estimated to be 1% at takeoff and 8% at cruise.

Acoustic analysis indicates that the 92 PNdB flap interaction noise objective at 150 m (500 foot) sideline (4 engines) will be bettered by 2 PNdB at approach and exceeded by 2 PNdB at takeoff, with an uncertainty band of +3 and -2 PNdB.

The flight version of this concept has been designed to have similar velocity decay and performance characteristics; however, it has a non-symmetric elliptical exit shape to minimize "scrubbing noise" from exhaust flow impingement on the wing lower surface. The top center lobe has been eliminated to avoid interaction with the large pylon structure anticipated for externally blown flap engine installations. The ground test mixer has been designed with sufficient trim capability to simulate this flight type mixer design.

BASE CONFIGURATION

- EXTERNAL MIXER
- INTERNAL MIXER

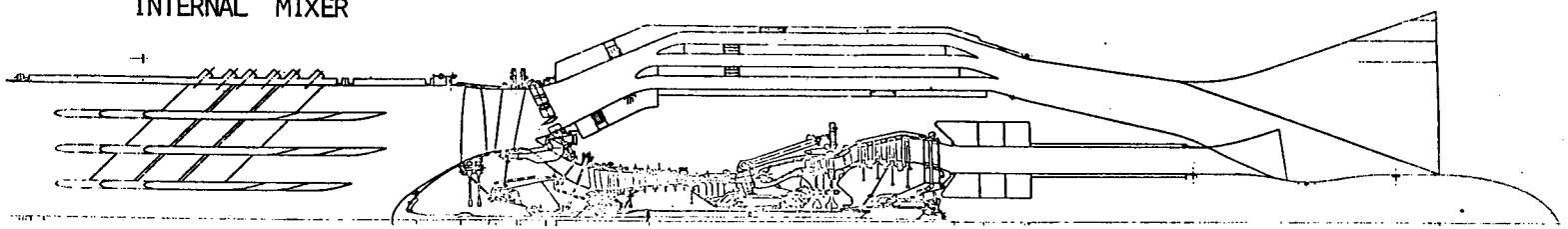

REF. CONFIGURATION

- CONVERGENT NOZZLE
- INTERNAL MIXER

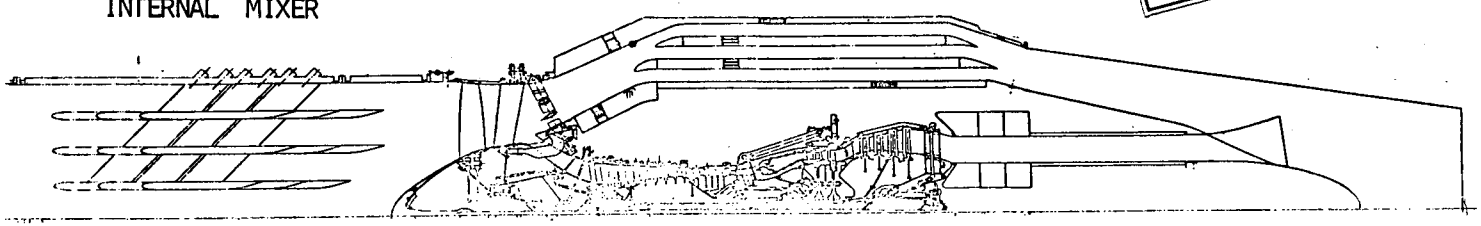

ALT. REF. CONFIGURATION

- CONVERGENT NOZZLE
- INTERNAL "FREE MIXER"

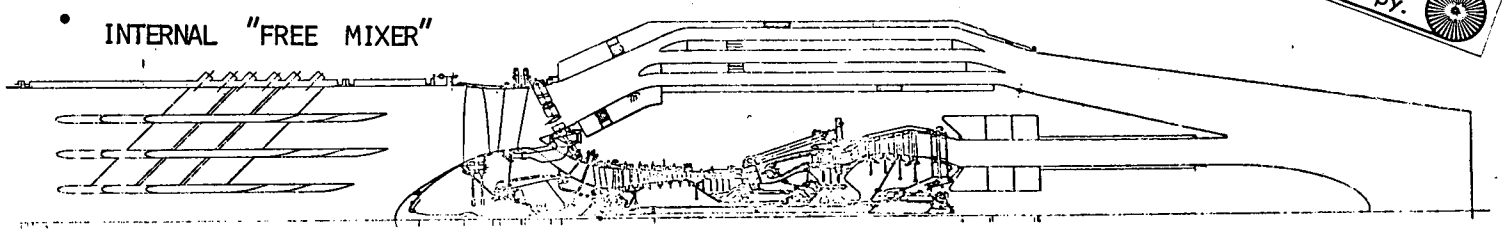

Figure 1. Ground Test Mixer Configurations.

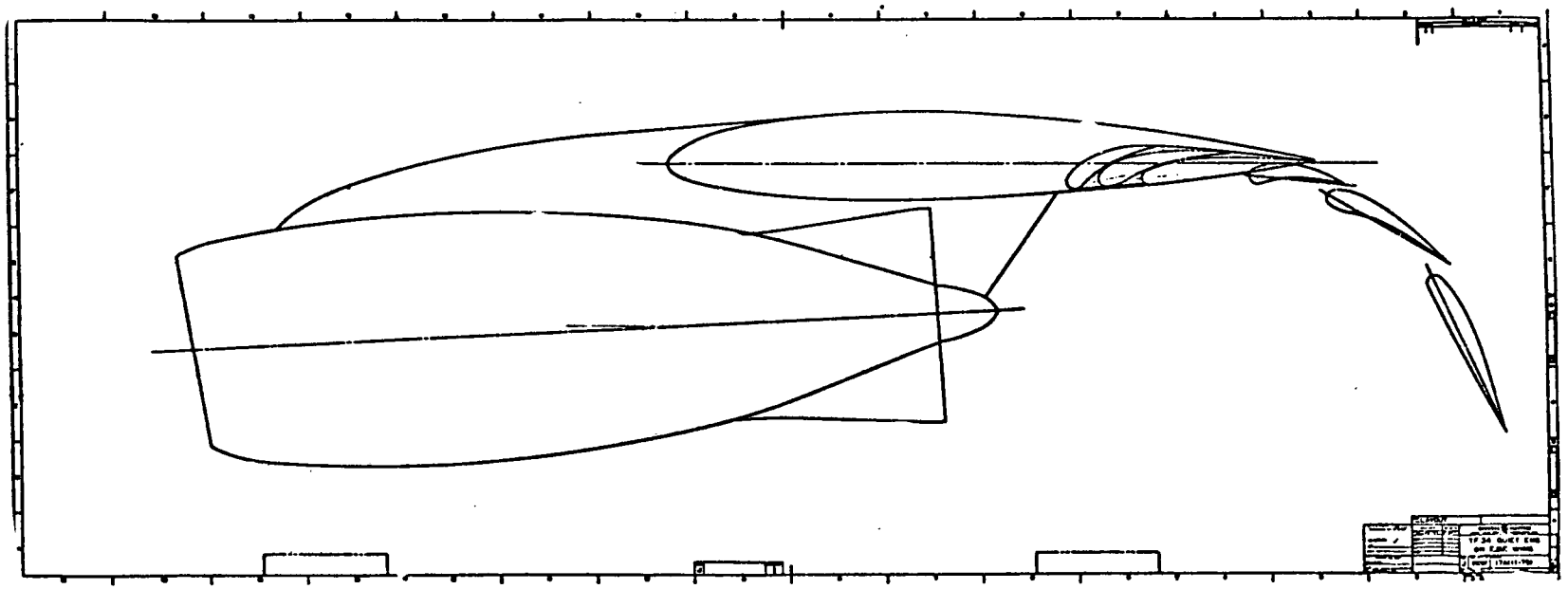

Nominal Flap Spacing $\sim$ 2.84m (112 inches)

Figure 2. Quiet TF34 Nacelle - Mixer Nozzle EBF Installation.

INTRODUCTION

The General Electric TF34 turbofan engine has been selected as the most promising propulsion system for the externally blown flap (EBF) version of the NASA Quiet Experimental STOL Aircraft. Under NASA contract NAS 3-14338, "TF34 Turbofan Quiet Engine Study" General Electric has been studying ways in which the installed engine noise can be reduced to satisfy a design overall noise goal of 95 PNdB at 150 m (500 foot) sideline conditions.

The EBF propulsion system generates the additional powered lift needed to satisfy STOL aircraft takeoff and landing requirements by deflecting the engine exhaust stream with the wing flap system. Recent test experience has shown that additional noise is generated by this exhaust wing flap interaction. The velocity of the exhaust striking the flap appears to be the dominant factor in creating flap interaction noise. For moderate bypass turbofan engines like the TF34, with exhaust velocities in the 200 to 300 m/s (650 to 1000 ft/sec) range, the flap interaction noise appears to be the dominant source of propulsion noise. In order to satisfy 150 m (500 foot) sideline, 95 PNdB noise objective, with four quiet TF34 turbofan engines, special steps must be taken to reduce flap interaction noise at takeoff and probably also at approach flight conditions.

This portion of the TF34 turbofan quiet engine study program has been devoted to the selection and design of a special mixer exhaust nozzle system with the objective of reducing the maximum 150 m (500 foot) sideline flap interaction noise to less than 92 PNdB. Other portions of the program are a study of TF34-based quiet engines and flight type nacelles, and the design of a ground test quiet nacelle.

SYMBOLS AND ABBREVIATIONS

A	area
AR	aspect ratio
C	flow coefficient - actual flow/ideal flow
C_f	friction drag coefficient
C_V	velocity coefficient - actual velocity/ideal velocity
D	diameter
F	thrust
H	lobe height
K4	mixing effectiveness parameter
M, Mn	Mach number
N	number of elements
P	pressure
P	perimeter
R	radius

S	spacing distance
SR	spacing ratio
T_F	100% mixed thrust
T_P	partially mixed thrust
T_U	unmixed thrust
V	velocity
W	lobe width
Y	radial distance
q	dynamic pressure
x	distance
γ	ratio of specific heats
Δ	change in value of parameter
θ	angle between lobes, injection angle of core stream flow
ρ	density
φ	angle of lobe

Subscripts

E	engine
N	net
R	relative
T	total
c	cowl
d	desired
e	equivalent
g	gross
h	hydraulic
i	inner
j	jet
o	outer
s	surface
in	inner
max	maximum
surf	surface

Abbreviations

EBF	externally blown flap
EGA	extra ground attenuation
HP	horsepower
LN	logarithm to base e
Log	logarithm to base 10
OASPL	overall sound pressure level
PNdB	perceived noise level in decibels
PNL	perceived noise level
SAE	Society of Automotive Engineers
S. L.	sea level
SST	supersonic transport
T/O	takeoff
in.	inches
rad	radians
s	seconds

TECHNICAL DISCUSSION

Program Objectives

To satisfy the total system noise objective of 150 m (500 foot) sideline maximum noise < 95 PNdB, the combined exhaust jet and flap interaction noise for four TF34 engines must not exceed a maximum value of 92 PNdB.

The two flight conditions at which flap interaction noise must be suppressed are: takeoff and approach. Both engine power setting and wing flap angle influence flap interaction noise. The nominal conditions specified for this study were:

- Takeoff - 100% power - 0/.35/.17 rad (0/20°/40°) flap angles
- Approach - 60% power - .25/.6/.8 rad (15°/35°/50°) flap angles

The nominal engine installation configuration shown in Figure 3 and 4 were included to be used as a guide in these studies.

Program Description and Schedule

The 21-week design study program was divided into two concurrent study efforts. The outline shown in Figure 5 presents the major elements of this study and their timing.

The 10-week Task I study effort was designed to select the most promising mixer nozzle design concept. These studies were initiated with a review of all available applicable design data. The concept selection and screeening studies included preparation of conceptual design drawings, takeoff and cruise performance estimates for 50 to 100% power settings and 150 m (500 foot) sideline flap interaction noise estimates.

The Task I concept selection consisted of an initial screening study that included fixed and retractable mixer concepts for both mixed and separate flow TF34 engine configurations. The latter portion of the concept selection studies were devoted to definition and optimization of six promising multi-lobe mixer nozzle designs.

The results of the Task I studies and General Electric's recommendation to select one of the 12-lobe mixer nozzle designs were presented to NASA.

The Task II studies were divided into two parallel efforts: (1) the design of a ground test version of the selected 12-lobe mixer nozzle concept for an acoustically-treated ground test nacelle, (2) the design of a flight version of this mixer nozzle concept.

Layout drawings of these designs plus the revised performance and noise estimates were then reviewed with NASA prior to preparation of the detailed manufacturing drawing of the ground test nozzle.

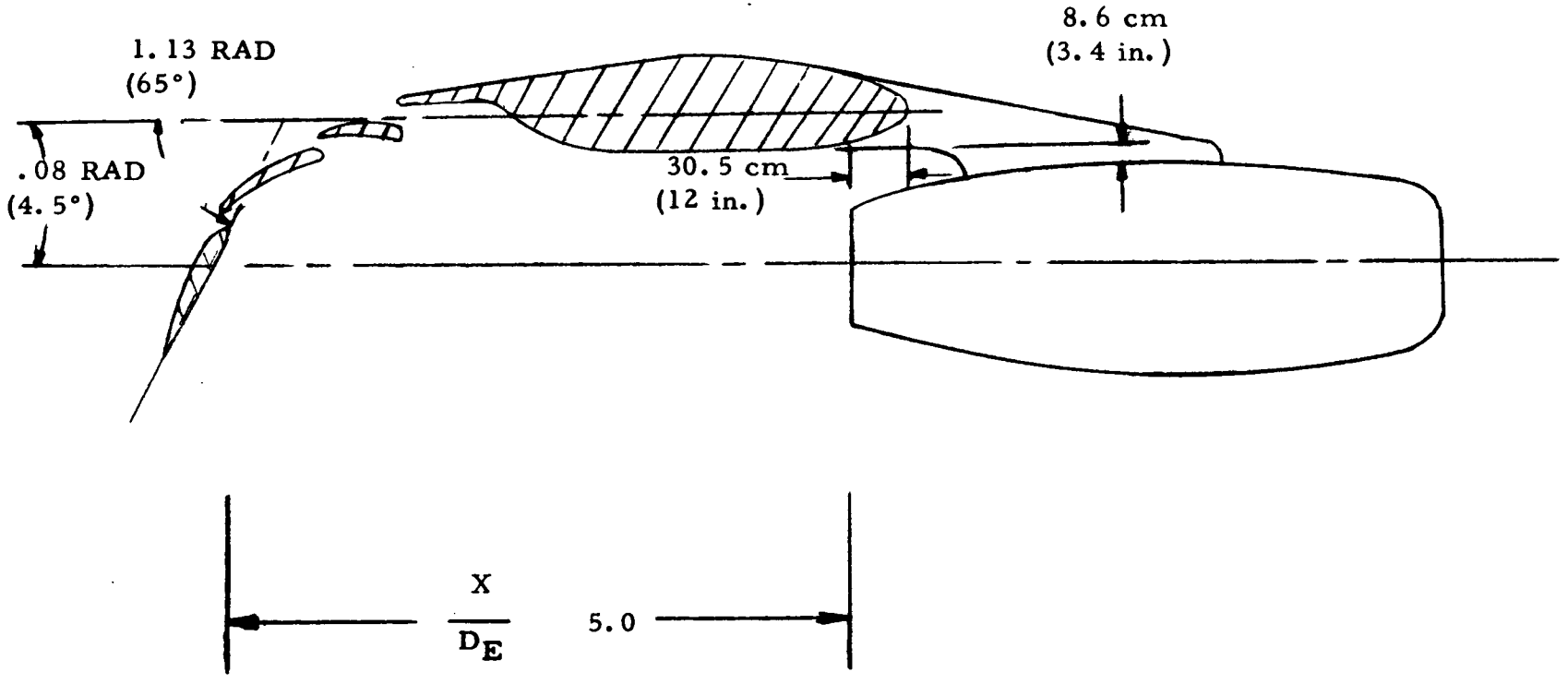

Figure 3. NASA Engine Installation.

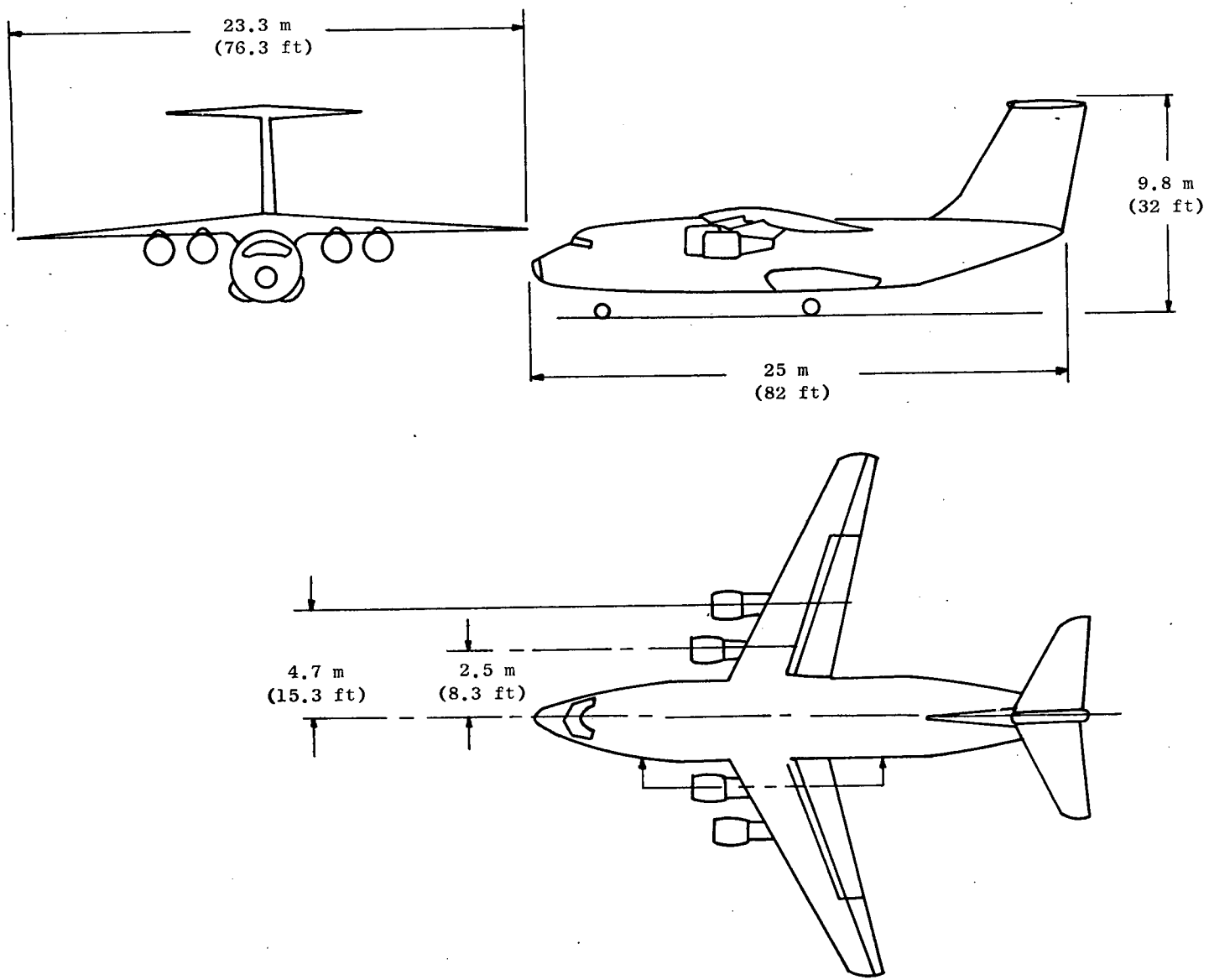

Figure 4. NASA EBF Airplane.

	TIMING
TASK I - CONCEPT SELECTION	START - 8 SEPT. 71
• REVIEW DESIGN DATA	
• IDENTIFY LIKELY DESIGN CONCEPTS	
- CONCEPT SKETCHES	
- PERFORMANCE AND NOISE ESTIMATES	
(NASA REVIEW AND SELECTION)	19 NOV. 71
TASK II - DESIGN	
• GROUND TEST VERSION	
- LAYOUT DRAWING	
- PERFORMANCE AND NOISE ESTIMATES	
• FLIGHT VERSION	
- CONCEPT SKETCH	
- PERFORMANCE AND NOISE AND WEIGHT ESTIMATES	
(NASA REVIEW OF TEST DRAWINGS)	22 DEC. 71
• GROUND TEST FABRICATION DRAWINGS	31 JAN. 72
• DRAFT OF FINAL REPORT	2 FEB. 72

Figure 5. Study Plan

Review of Design Data

The review of applicable design data included a survey of available information on -

- Flap Impingement Noise
  - Static Conditions
  - In-Flight Conditions
- Nozzle Exhaust Velocity Decay
  - Static Conditions
  - In-Flight Conditions
- Jet Noise Suppression
  - Static Conditions
  - In-Flight Conditions
- Nozzle Performance Characteristics
  - Internal Performance
  - In-Flight Drag

The number of data sources for convergent nozzles multi-tube, multi-lobe and multi-spoke suppressors and ejector nozzles are summarized in Figure 6. These tabulations illustrate that most of the available information is for static conditions. No data on in-flight velocity decay or flap interaction noise was found. A considerable quantity of static exhaust velocity decay data was available. However, the recent data in References 1 and 2 were found to be the most complete and directly applicable to the type of mixer nozzles considered in this program. Sufficient plots of the type illustrated schematically in Figure 7 had been generated so that the influence of mixer nozzle design variables like number of elements, element shape and element spacing on velocity decay characteristics could be readily predicted.

The mixer nozzle performance data located was not sufficiently complete to be used to estimate takeoff and cruise performance for a similar range of mixer nozzle design variables. It was determined that internal nozzle performance for takeoff conditions could be made with a reasonably high degree of confidence, using a simplified calculation procedure. General Electric CJ 805-23 8-lobe mixer nozzle wind tunnel test experience was used to establish afterbody design guidelines that would limit mixer nozzle cruise drag to additional skin friction drag only. This was done by limiting the maximum boattail conical angle to .25 rad (15^{o}).

Three sources of directly applicable data on engine exhaust flap interaction were:

- Published NASA Lewis small scale data ($\sim$50 cm (2") diameter jet)
- Published NASA Langley small scale data ($\sim$ 50 cm (2") diameter jet)
- Published NASA Edwards CF700-111 wing impingement data

*~Indicates direct G.E. Experience

	NUMBER OF ELEMENTS	REFERENCE	FLAP IMPINGEMENT NOISE CHARACTERISTICS		VELOCITY DECAY CHARACTERISTICS		NOISE SUPPRESSION CHARACTERISTICS		PERFORMANCE INTERNAL		EXT
			Static	Vo≠0	Static	Vo≠0	Static	Vo≠0	Static	Vo≠0	
• Standard Conical Nozzles	-	1*			X	X					
	-	2	X								
	-	3	X								
	-	4*					X		X		
	-	5					X		X		
	-	6					X				
	-	7	X								
	-	8	X								
	-	9*			X		X				
	-	10*			X						
	-	11					X		X		X
	-	12					X				X
	-	13*									X
	-	16			X	X	X				
	-	18					X	X			
	-	21	X								
	-	24			X				X		
	-	27			X						
	-	28	X				X				
	-	29*			X	X					
• Tube Suppressors	18	3	X								
	21	5					X		X		
	(7, 19, 43, 109, 253)	6					X				
	11, 19, 31	9*					X				
	72	10*			X						
	10, 11, 31	11					X		X		X
	9	12					X				X
	(5, 7, 21, 37, 72, 85)	15*			X		X		X		X
	12	17							X		X
	(9, 6, 12, 18)	14					X		X		
	2, 48, 55	20					X				
	1	24			X				X		
	6, 7, 13, 19	27			X						

Figure 6. Summary - Velocity Suppressor Literature Survey.

*~Indicates direct G.E. Experience

	NUMBER OF ELEMENTS	REFERENCE	FLAP IMPINGEMENT NOISE CHARACTERISTICS Static	FLAP IMPINGEMENT NOISE CHARACTERISTICS Vo≠O	VELOCITY DECAY CHARACTERISTICS Static	VELOCITY DECAY CHARACTERISTICS Vo≠O	NOISE SUPPRESSION CHARACTERISTICS Static	NOISE SUPPRESSION CHARACTERISTICS Vo≠O	PERFORMANCE INTERNAL Static	PERFORMANCE INTERNAL Vo≠O	PERFORMANCE EXT
• Chute (Lobe) Suppressors	32	4*							X	X	
	12	5					X		X		
	8	9*			X		X				
	12	11					X		X		X
	8	12					X				X
	8	13*									X
	3, 6, 12	14					X		X		
		15*							X		
	3, 12	16					X				
	8, 12	17							X		X
	6, 12	18					X	X	X		
	8	20					X		X		
	2, 4, 12	24			X				X		
	4, 6, 8, 12	27			X						
	8	28	X				X				
• Spoke Suppressors	24, 32, 48	4*					X		X		
	(12, 20, 24, 36)	15*					X		X		
• Ejector Suppressors		6					X				
A. Standard Nozzle with Ejector		11					X		X		X
		12					X				X
		17							X		X
B. Missing Nozzle with Ejector (tabs)		11					X		X		X
C. Lobed Nozzle with Ejector	8	12					X				X
D. Chutes and Scoops with Ejector	4, 8	19					X		X		
• Generalized Design Information for Noise Suppressors		6					X				
		9*					X				
		19							X		
		20					X			X	
		23*							X		
		24			X				X		
		27			X						

Figure 6. Summary - Velocity Suppressor Literature Survey (Concluded).

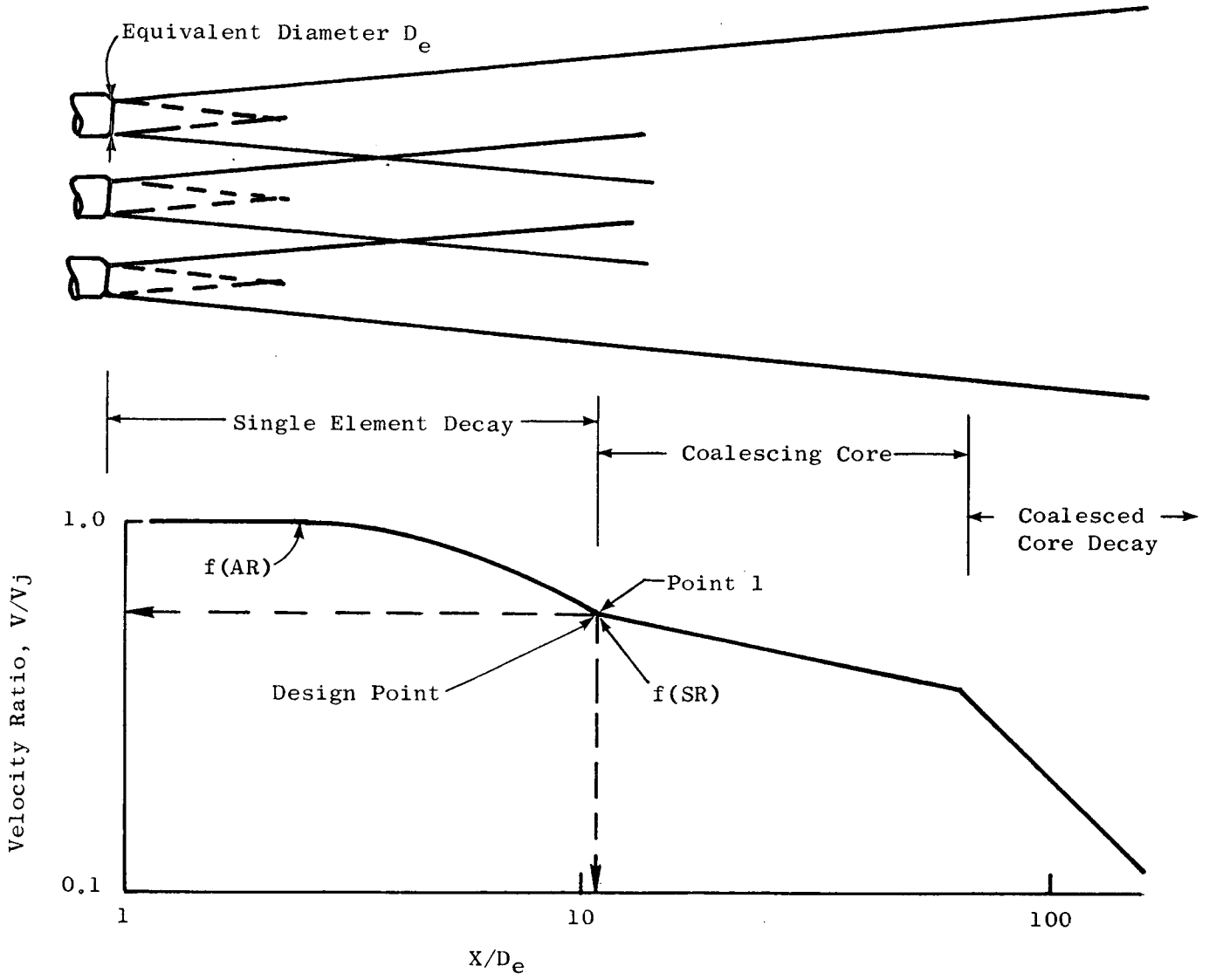

Figure 7. Task I Multi-Element Nozzle Velocity Decay.

- NASA LEWIS DATA CHOSEN FOR STATIC VELOCITY DECAY ESTIMATE
  - NO. OF ELEMENTS
  - ELEMENT SHAPE (TUBES, LOBES, WEDGES)
  - CIRCUMFERENTIAL SPACING
  - RADIAL SPACING AND NUMBER OF RINGS (SEPARATE FLOW)
- SIMPLIFIED CALCULATION PROCEDURES SELECTED FOR ESTIMATE OF
  - CRUISE DRAG (BASED ON CJ805 8-LUBE DAISY DESIGN EXPERIENCE)
  - THRUST LOSSES
- FLAP IMPINGEMENT NOISE TRENDS UTILIZE NASA LEWIS DATA
- NO APPLICABLE DATA ON IN FLIGHT FLAP INTERACTION NOISE.

Figure 8. Review of Available Design Data.

The NASA Lewis Research Center data was found to be the most complete and was selected for use in the study.

The information uncovered by this data review resulted in the conclusions outlined in Figure 8.

Engine Cycle Data

The engine exhaust velocity, airflow and thrust data for Task I design were based on the joint General Electric/Airframe Manufacturer Studies conducted during the preparation of the propulsion system proposal for the NASA Experimental STOL Transport Research Aircraft (Reference 32). The TF34 engine and acoustically-treated nacelle design concepts formulated for these studies were quite similar to those for the NASA-sponsored TF34 turbofan quiet engine studies. Representative suppression treatment and duct pressure losses estimates for the acoustic nacelle were developed along with representative estimates of installed engine power and bleed extraction required for a STOL aircraft.

The long mixed-flow exhaust ducts and jet nozzle areas for this EBF STOL engine installation were designed so that the basic TF34 fan operating line, at sea level static would not be noticeably different from the current TF34-2 base engine to be used in the S3A airplane. The acoustically-treated nacelle and the special STOL engine installation consideration result in sizeable reductions in takeoff thrust and exhaust velocity. Figure 9 presents a breakdown of these effects. The I (2) configuration was selected as being the most representative level of installation losses for the Task I studies.

The influence of engine power setting on exhaust velocity is shown in Figure 10. It is clear that quiet STOL engine installation considerations provide significant reductions in velocity. These effects help reduce flap interaction noise.

Initial Concept Screening Study

The first step in the mixer nozzle concept design studies was to identify a series of potentially promising concepts. These initial studies covered a broad range of engine and mixer nozzle possibilities.

- Initial Concept Definition (12)
  - Fixed Geometry (4)
  - Variable Geometry (8)
  - Mixed & Separate Flow Cycles
    - -- Separate Flow (3)
    - -- Mixed Flow (9)

MAX. THRUST
SEA LEVEL, STANDARD DAY, 50 M/S (100 KNOTS)

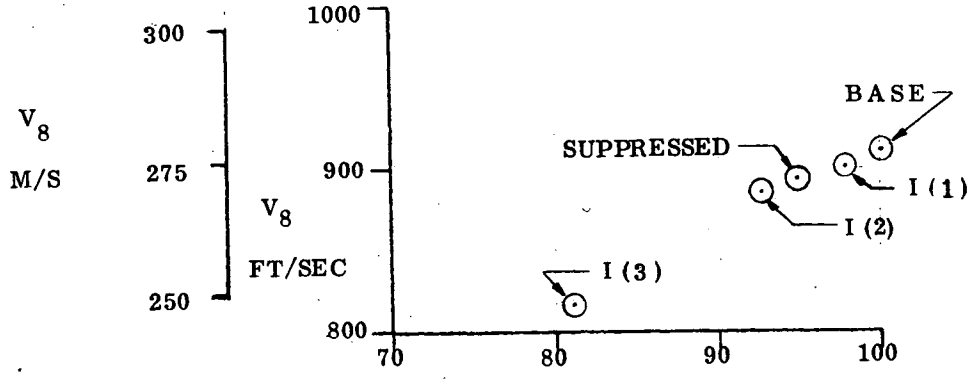

% OF BASE ENGINE MAX THRUST

CONFIGURATION	C_{V8}	$\Delta P/_{q}$ Inlet	$\Delta P/_{q}$ Fan Duct	$\Delta P/_{q}$ Core Duct	EXTRACTION POWER Watts	HP	AIR KG/S	LB/S
BASE	.995	0	.149	.153	0	0	0	0
SUPPRESSED (No Installation)	.993	.0895	.294	.163	0	0	0	0
INSTALLED (No Suppression) I (1)	.995	0	.149	.153	18650	25	0.14	0.3
INSTALLED I (2)	.993	.0895	.294	.163	18650	25	0.14	0.3
INSTALLED (No Suppression) I (3)	.995	0	.149	.153	48490	65	Maximum	

Figure 9. Influence of Typical Suppression and Installation Effects on Maximum Thrust and Jet Velocity.

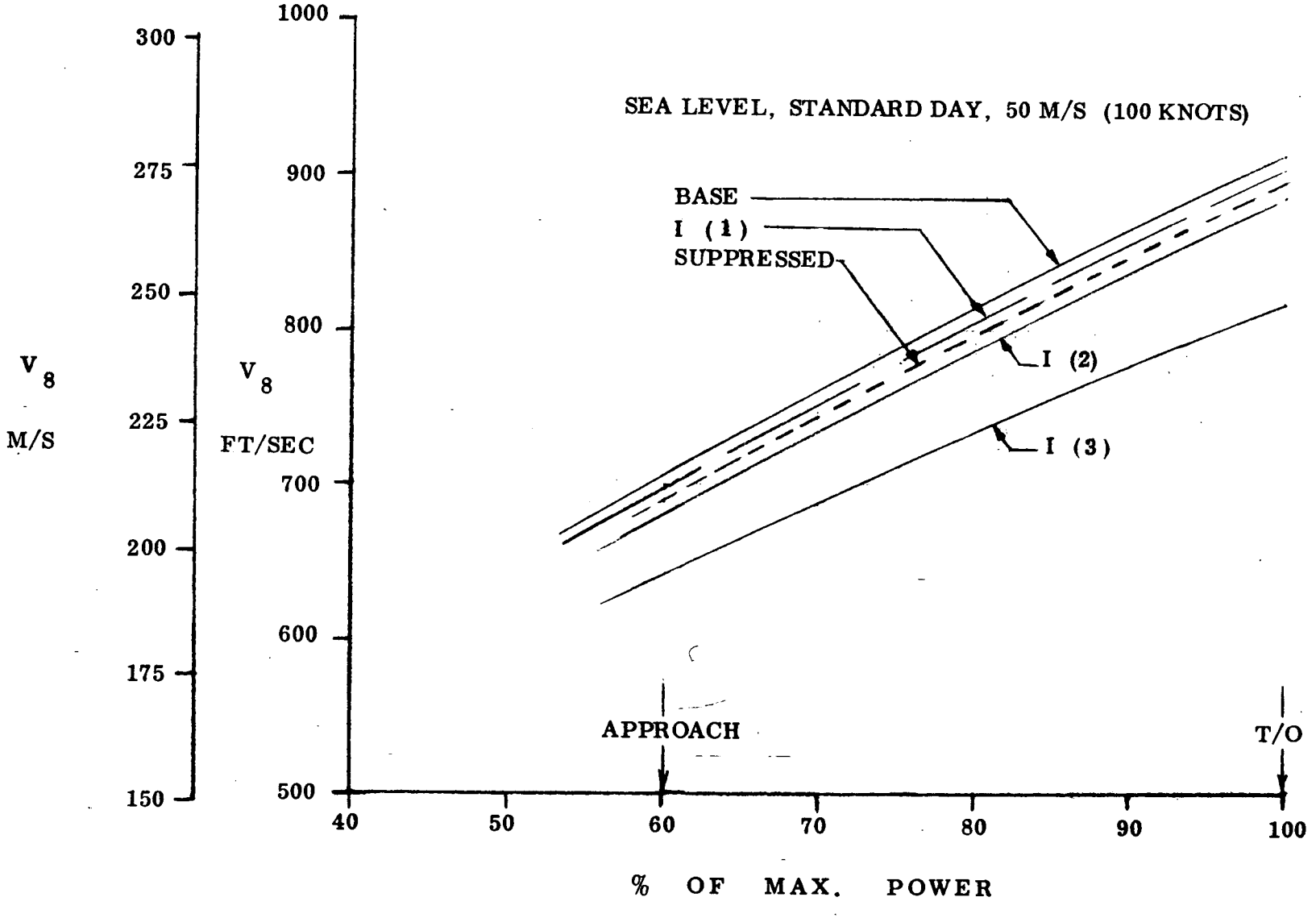

Figure 10. Influence of Typical Installation Effects on Jet Velocity.

The 12 potentially promising design concepts shown in Figures 11 - 22 were selected. The variable geometry retractable mixer concepts utilized much of General Electric's broad background of jet nozzle suppressor design experience developed during the supersonic transport engine development program.

An evaluation procedure was established to select the most promising design concept using the following 12 design considerations:

1. Velocity decay characteristics
2. Noise suppression characteristics
3. Lift augmentation
4. Cost and complexity
5. Weight
6. External drag
7. Internal performance
8. Risk/reliability/service life
9. Maintainability
10. Thrust reverser compatibility
11. Overall installation
12. Internal acoustics

Each item was given a good (3), fair (2) or poor (1) rating for each of the 12 design concepts.

- Weighing factors were applied to the evaluations as follows:
  - Two points were added for a configuration if it had no items below a 1.5 average.
  - Two points were subtracted if an average grade below 2.5 resulted for items 1 and/or 2.

The ratings were determined by a selected team of experienced designers and technical specialists.

The results of this "best judgement" type of evaluation study are presented in Figure 23. The fixed geometry multi-lobe mixer nozzle design concept was found to be clearly superior. It was anticipated that in a flight type of installation, the wing and pylon design considerations would favor a non-symmetric exhaust. In addition it was felt that the potential loss of flap turning effectiveness with a large diameter, low velocity mixer exhaust could be avoided by spreading the exhaust laterally to wash a larger segment of the wing flap.

Multi-lobe Mixer Nozzle Studies

The initial concept screening studies indicated that the fixed geometry multi-lobe mixer nozzle design approach was the most promising. Design, performance and noise trends needed to be most clearly defined to select the best mixer nozzle geometry. These studies included the four following major areas:

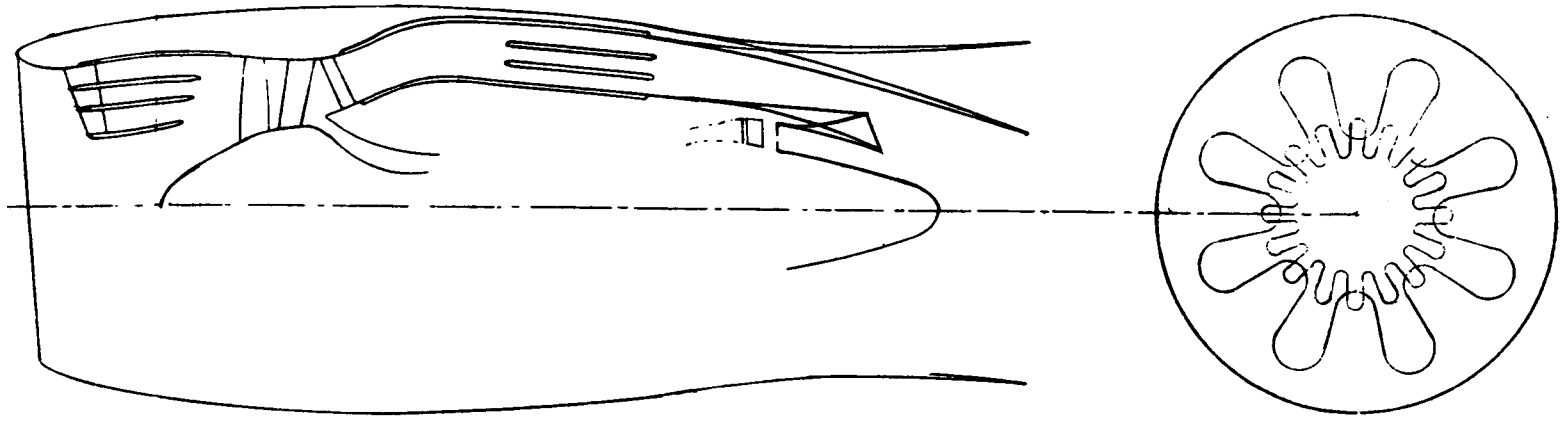

Evaluation

1.	Velocity decay characteristics	3.0
2.	Noise suppression characteristics	3.0
3.	Lift augmentation	2.0
4.	Cost and complexity	2.4
5.	Weight	2.0
6.	External drag	2.7
7.	Internal performance	3.0
8.	Risk/reliability/service life	2.5
9.	Maintainability	2.4
10.	Thrust reverser compatibility	2.8
11.	Overall installation	2.8
12.	Internal acoustics	2.7
		31.3

Good = 3, Fair =2, Poor =1

Comments

- All fixed geometry
- Plug could be made larger for more penetration and better mixer effectiveness.
- Compatible with interface plane requirements.
- Used on CJ-805 and on DC-8 with and ejector

Figure 11. Configuration 1 - Lobed Daisy with Partial Mixer; Circular.

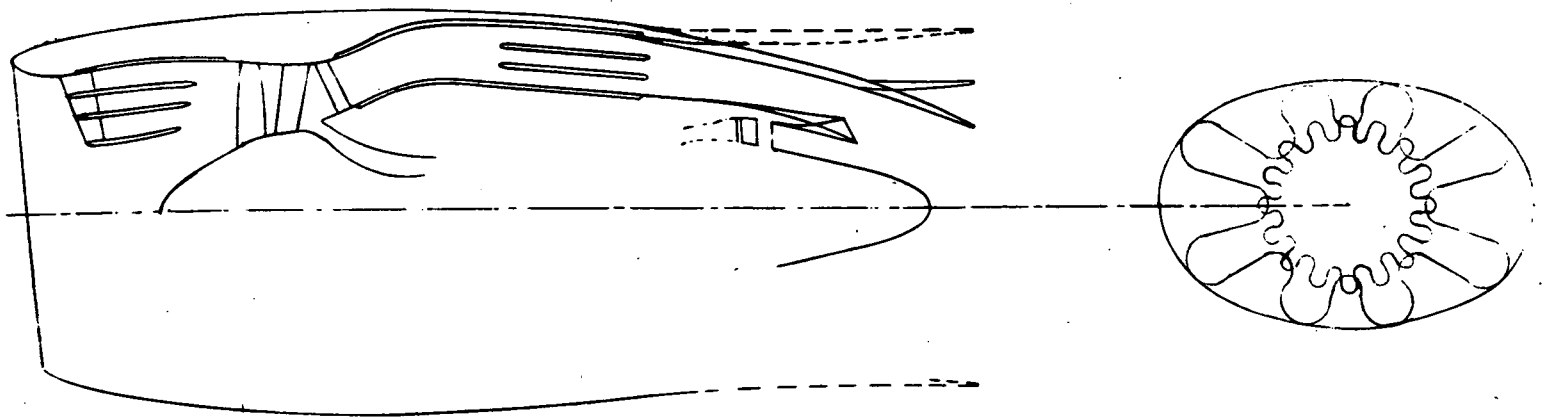

Evaluation

1.	Velocity decay characteristics	3.0
2.	Noise suppression characteristics	3.0
3.	Lift augmentation	3.0
4.	Cost and complexity	2.2
5.	Weight	2.0
6.	External drag	2.7
7.	Internal performance	3.0
8.	Risk/reliability/service life	2.3
9.	Maintainability	2.4
10.	Thrust reverser compatibility	2.7
11.	Overall installation	2.5
12.	Internal acoustics	2.7
		31.5

Good = 3, Fair = 2, Poor = 1

Comments

- All fixed geometry
- Plug could be made larger for more penetration and better mixer effectiveness.
- Compatible with interface plane requirements.

Figure 12. Configuration 2 - Lobed Daisy with Partial Mixer; Elliptical.

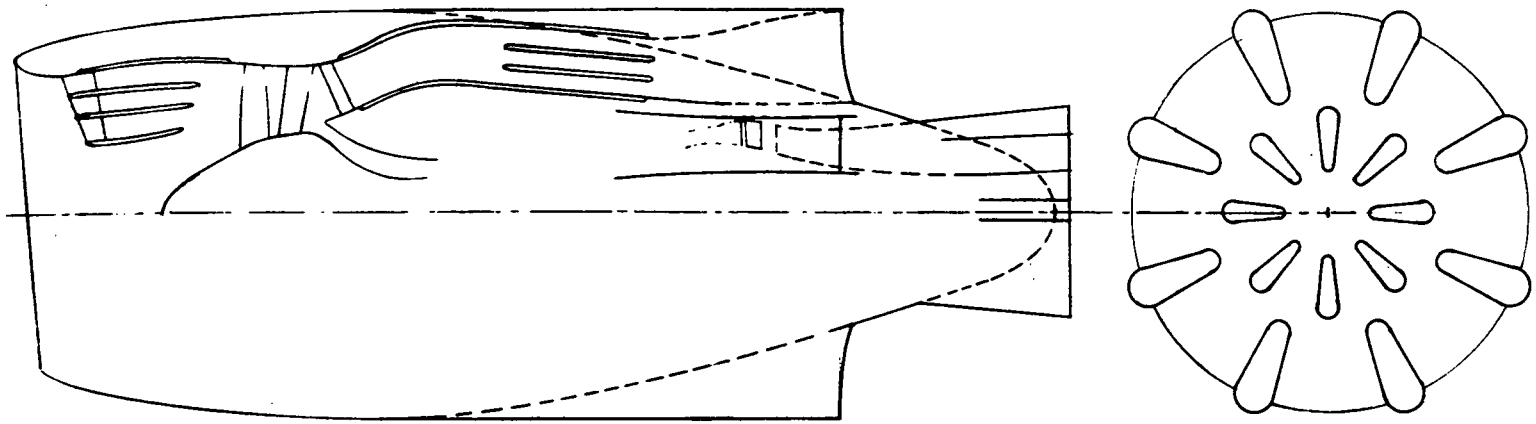

Evaluation

1.	Velocity decay characteristics	2.5
2.	Noise suppression characteristics	2.5
3.	Lift augmentation	2.0
4.	Cost and complexity	2.4
5.	Weight	2.0
6.	External drag	1.7
7.	Internal performance	2.0
8.	Risk/reliability/service	2.3
9.	Maintainability	2.2
10.	Thrust reverser compability	1.6
11.	Overall installation	2.3
12.	Internal acoustics	1.8
		25.3

Good = 3, Fair = 2, Poor = 1

Comments

- All fixed geometry
- Fan duct could be made shorter if acoustic splitters were removed.
- Similar to NASA Langley proposed design.
- Flap impingement velocity would be governed by decay characteristics of core nozzle.

Figure 13. Configuration 3 - Lobed Daisy with Separate Flow.

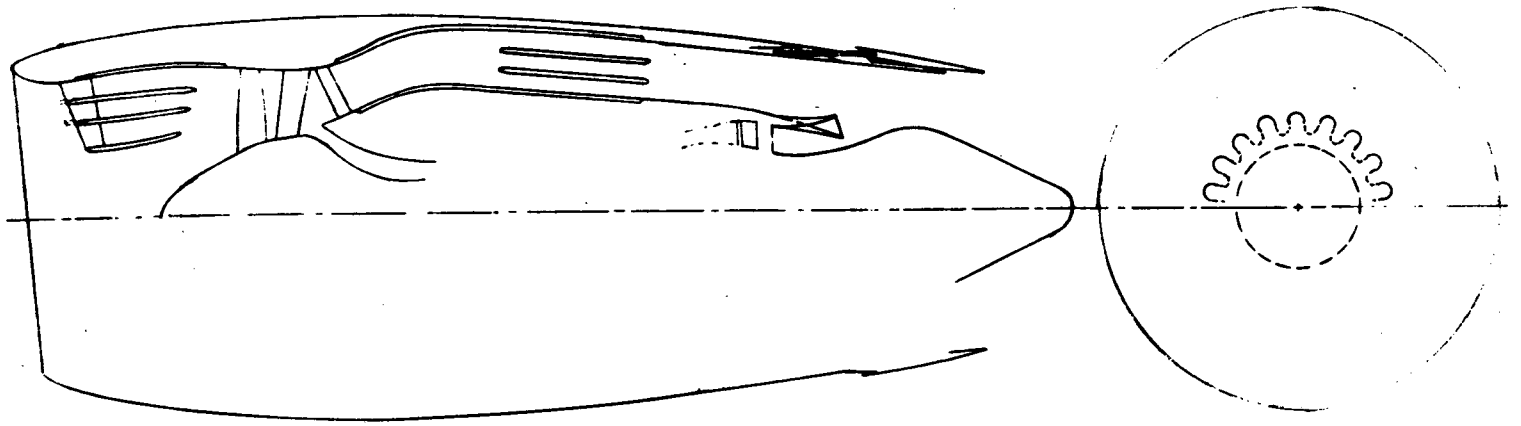

Evaluation

1.	Velocity decay characteristics	1.3
2.	Noise suppression characteristics	2.0
3.	Lift augmentation	1.7
4.	Cost and complexity	2.0
5.	Weight	2.2
6.	External drag	3.0
7.	Internal performance	3.0
8.	Risk/reliability/service life	2.3
9.	Maintainability	2.2
10.	Thrust reverser compatibility	2.8
11.	Overall installation	2.8
12.	Internal acoustics	2.3
		27.6

Good = 3, Fair = 2, Poor = 1

Comments

- Chutes could be added as on SST designs to increase penetration of external flow.
- Ejector retracted for cruise(secondary)
- Noise and performance tested by NASA.

Figure 14. Configuration 4 - Retractable Ejector with Partial Mixer.

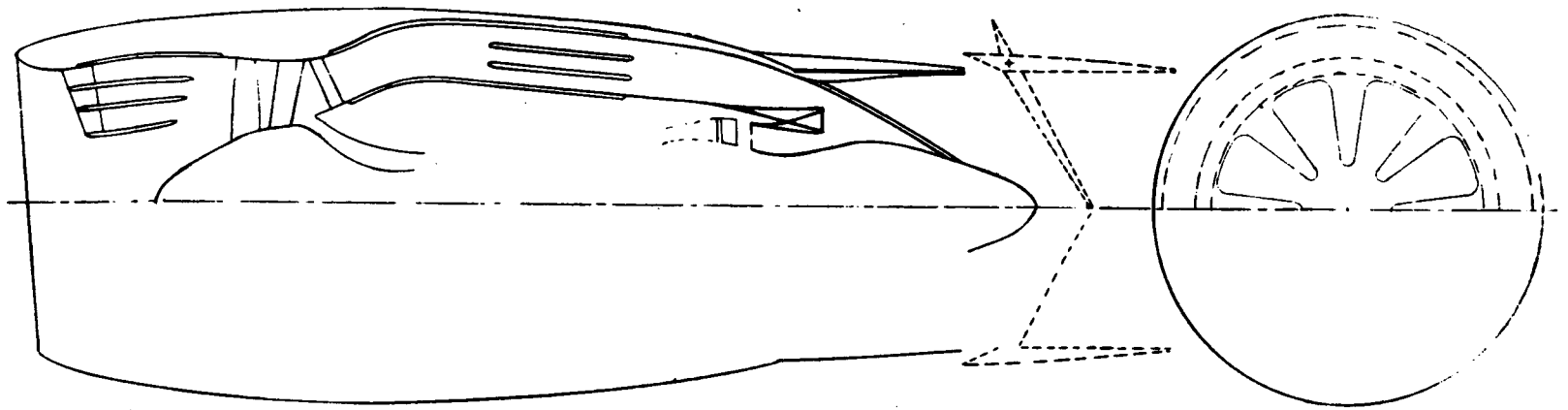

Evaluation

1.	Velocity decay characteristics	3.0
2.	Noise suppression characteristics	3.0
3.	Lift augmentation	2.3
4.	Cost and complexity	1.6
5.	Weight	1.7
6.	External drag	2.5
7.	Internal performance	2.3
8.	Risk/reliability/service life	1.8
9.	Maintainability	1.7
10.	Thrust reverser compatibility	2.8
11.	Overall installation	2.1
12.	Internal acoustics	2.7
		27.5

Good = 3, Fair = 2, Poor = 1

Comments

- Ejector should be retracted into cowl above daisy as on the DC-8. This eliminates base area but reduces penetration angle.
- Ejector could possibly become target or clam shell reverser.

Figure 15. Configuration 5 - Retractable Ejector with Lobed Daisy and Partial Mixer.

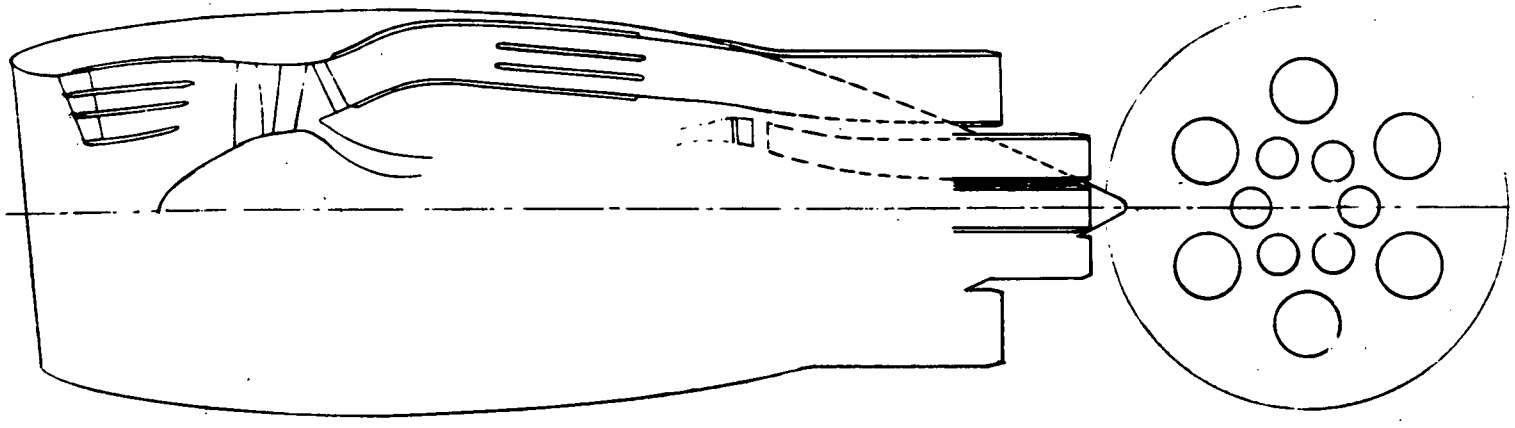

Evaluation		Comments
1. Velocity decay characteristics	2.2	• Test by Nasa
2. Noise suppression characteristics	2.2	
3. Lift augmentation	2.0	
4. Cost and complexity	2.4	
5. Weight	2.0	
6. External drag	1.5	
7. Internal performance	1.3	
8. Risk/reliability/service life	2.3	
9. Maintainability	2.3	
10. Thrust reverser compatibility	2.3	
11. Overall installation	2.3	
12. Internal acoustics	2.3	
	25.0	

Good = 3, Fair = 2, Poor = 1

Figure 16. Configuration 6 - Fixed Tubes with Separate Flow.

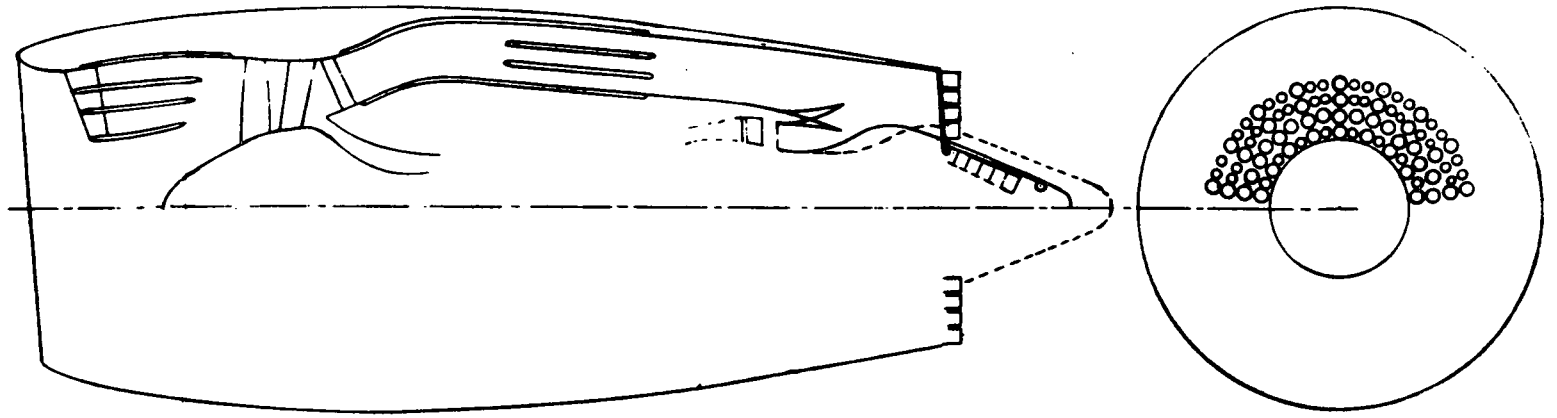

Evaluation		Comments
1. Velocity decay characteristics	3.0	• Similar to SST considered approach
2. Noise suppression characteristics	3.0	
3. Lift augmentation	2.0	
4. Cost and complexity	1.0	
5. Weight	1.3	
6. External drag	2.3	
7. Internal performance	1.7	
8. Risk/reliability/service life	1.0	
9. Maintainability	1.3	
10. Thrust reverser compatibility	2.1	
11. Overall installation	1.9	
12. Internal acoustics	2.7	
	23.3	

Good = 3, Fair = 2, Poor = 1

Figure 17. Configuration 7 - Retractable Tubes with Partial Mixer.

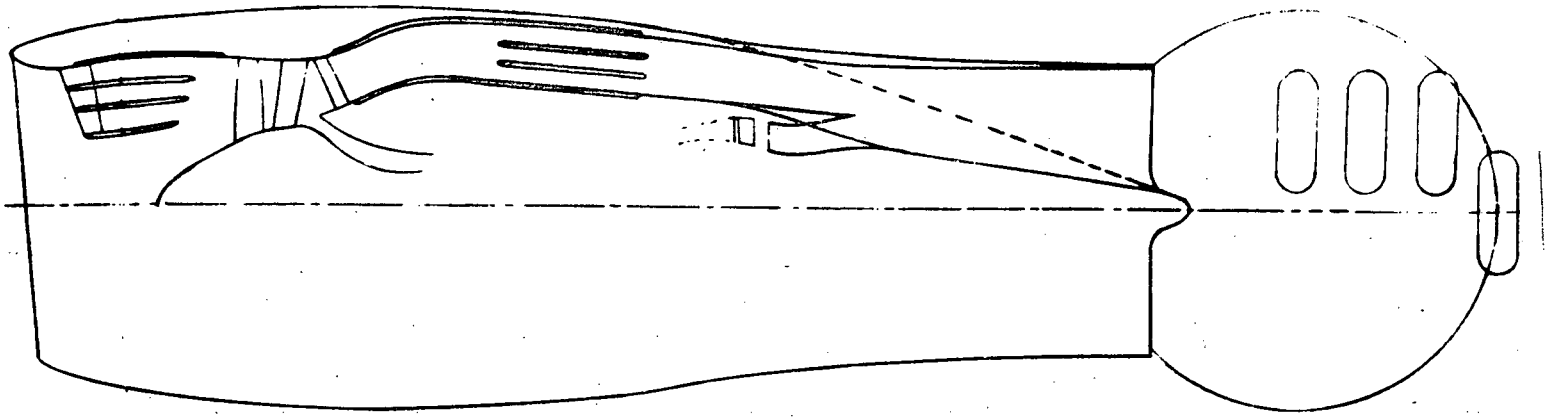

Evaluation

1.	Velocity decay characteristics	2.5
2.	Noise suppression characteristics	2.5
3.	Lift augmentation	2.3
4.	Cost and complexity	2.2
5.	Weight	1.8
6.	External drag	1.2
7.	Internal performance	1.7
8.	Risk/reliability/service life	1.9
9.	Maintainability	2.1
10.	Thrust reverser compatibility	2.3
11.	Overall installation	2.0
12.	Internal acoustics	2.5
		25.0

Good = 3, Fair = 2, Poor = 1

Comments

- Tested by NASA

Figure 18. Configuration 8 - Fixed Tubes with Partial Mixer; Rectangular.

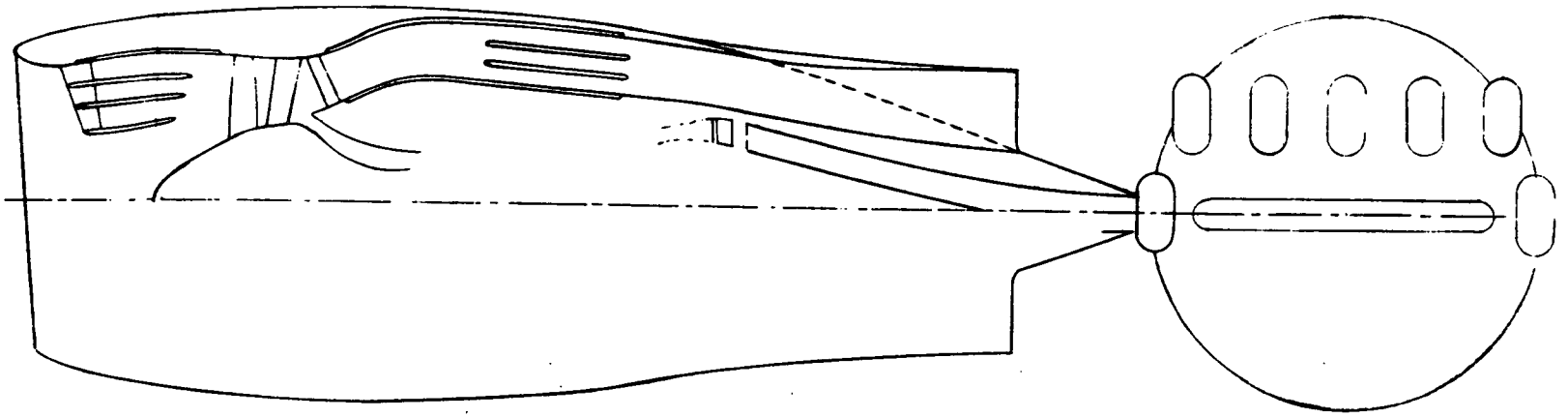

Evaluation

1.	Velocity decay characteristics	2.7
2.	Noise suppression characteristics	2.7
3.	Lift augmentation	2.3
4.	Cost and complexity	2.4
5.	Weight	1.8
6.	External drag	1.2
7.	Internal performance	1.7
8.	Risk/reliability/service life	2.1
9.	Maintainability	2.1
10.	Thrust reverser compatibility	2.1
11.	Overall installation	2.0
12.	Internal acoustics	2.2
		25.3

Good = 3, Fair = 2, Poor = 1

Figure 19. Configuration 9 - Fixed Tubes with Separate Flow-Rectangular.

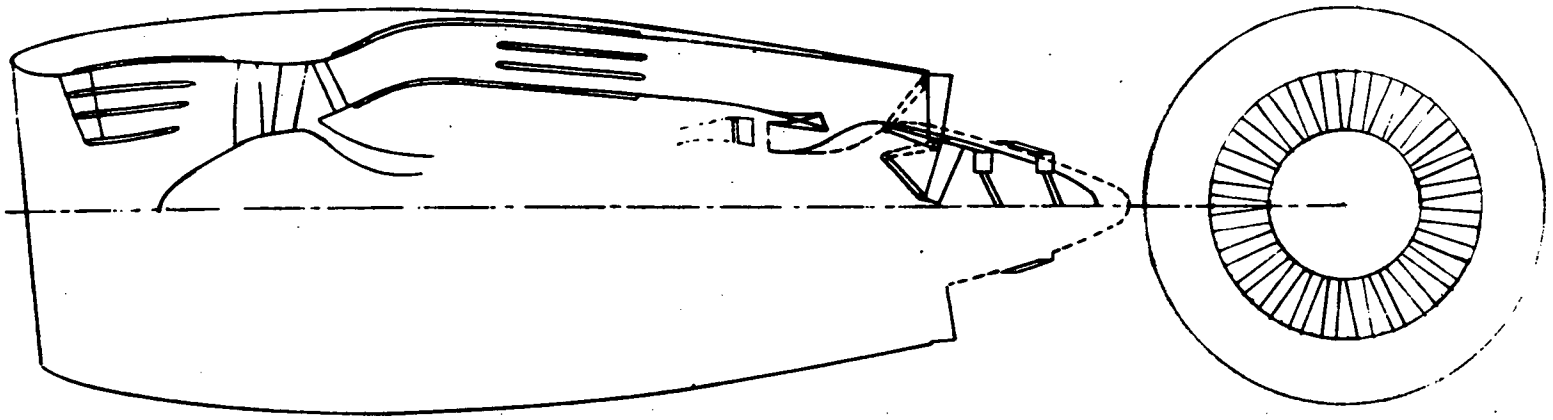

Evaluation

1. Velocity decay characteristics----------3.0
2. Noise suppression characteristics----------3.0
3. Lift augmentation----------2.0
4. Cost and complexity----------1.1
5. Weight----------1.2
6. External drag----------3.0
7. Internal performance----------2.7
8. Risk/reliability/service life----------1.1
9. Maintainability----------1.1
10. Thrust reverser compatibility----------2.4
11. Overall installation----------2.1
12. Internal acoustics----------2.7

Good = 3, Fair = 2, Poor = 1

Comments

- Considered seriously for SST

Figure 20. Configuration 10 - Stowable Chute System with Partial Mixer.

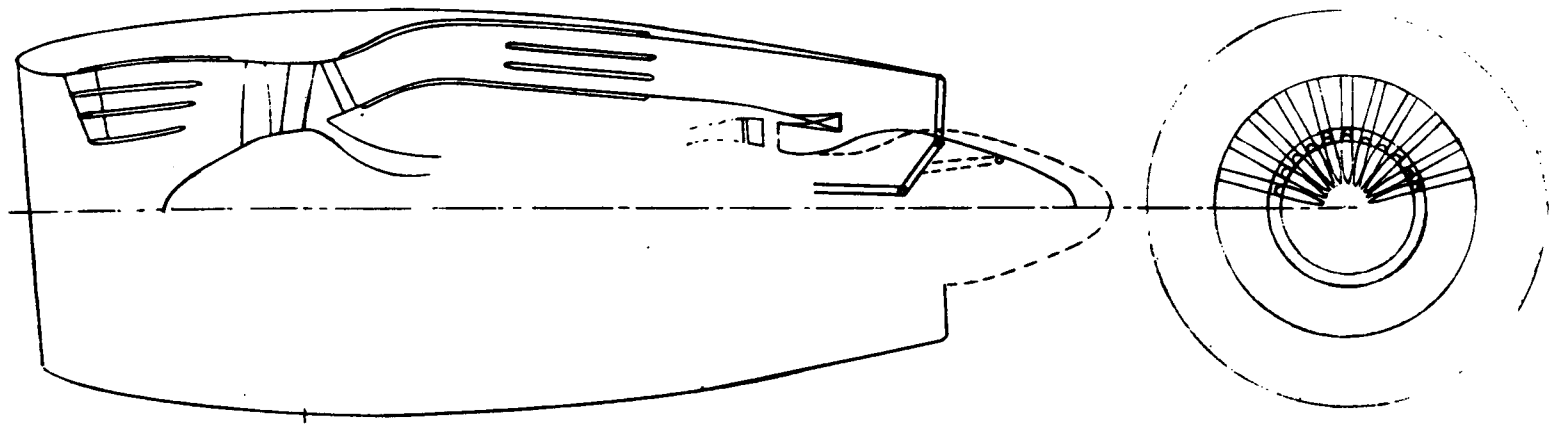

Evaluation

1.	Velocity decay characteristics	2.7
2.	Noise suppression characteristics	2.7
3.	Lift augmentation	1.7
4.	Cost and complexity	1.8
5.	Weight	1.8
6.	External drag	3.0
7.	Internal performance	2.3
8.	Risk/reliability/service life	1.6
9.	Maintainability	1.7
10.	Thrust reverser compatibility	2.4
11.	Overall installation	2.5
12.	Internal acoustics	2.7
		26.9

Comments

- Considered seriously for SST

Good = 3, Fair = 2, Poor = 1

Figure 21. Configuration 11 - Stowable Spoke System with Partial Mixer.

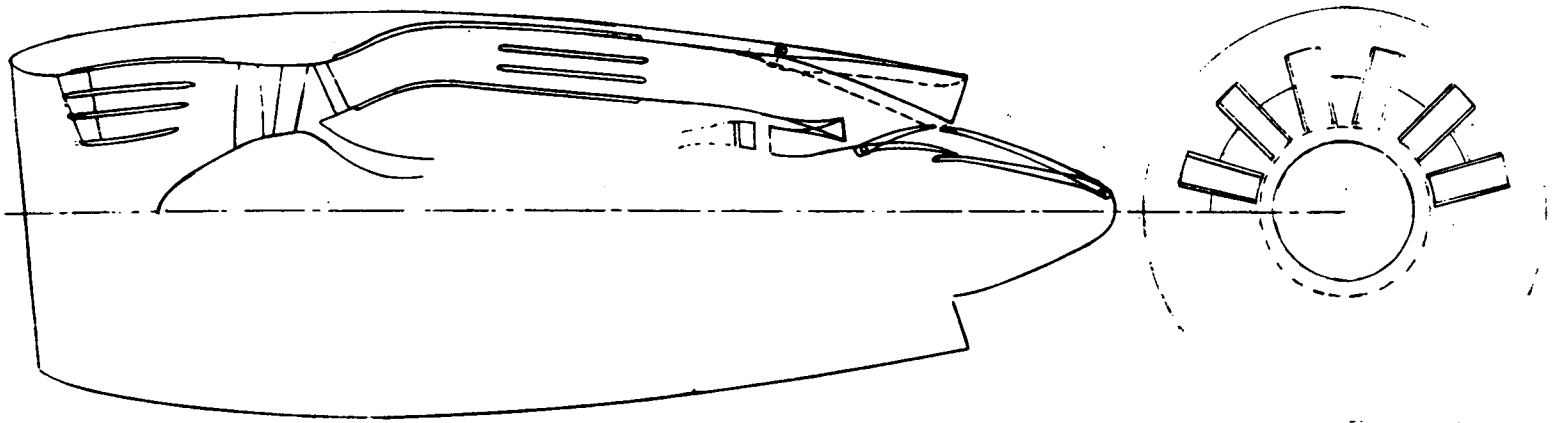

Evaluation

1.	Velocity decay characteristics	3.0
2.	Noise suppression characteristics	3.0
3.	Lift augmentation	2.0
4.	Cost and complexity	1.0
5.	Weight	1.0
6.	External drag	3.0
7.	Internal performance	3.0
8.	Risk/reliability/service life	1.5
9.	Maintainability	1.2
10.	Thrust reverser compatibility	2.4
11.	Overall installation	2.0
12.	Internal acoustics	2.7
		25.8

Good = 3, Fair = 2, Poor = 1

Figure 22. Configuration 12 - Moveable Tab Lobes with Partial Mixer.

(CONCEPTS)	(EVALUATION)
LOBED DAISY WITH PARTIAL MIXER: ELLIPTICAL	33.4
LOBED DAISY WITH PARTIAL MIXER: CIRCULAR	33.2
STOWABLE SPOKE SYSTEM WITH PARTIAL MIXER (SST TYPE)	28.8
RECTRACTABLE EJECTOR WITH LOBED DAISY & PARTIAL MIXER	28.6
LOBED DAISY: SEPARATE FLOW	27.2
MOVABLE TAB LOBES WITH PARTIAL MIXER	25.8
RETRACTABLE EJECTOR WITH PARTIAL MIXER	25.5
STOWABLE CHUTE SYSTEM WITH PARTIAL MIXER (SST TYPE)	25.4
FIXED TUBES WITH SEPARATE FLOW: RECTANGULAR	25.2
FIXED TUBES WITH PARTIAL MIXER: RECTANGULAR	25.0
RECTRACTABLE TUBES WITH PARTIAL MIXER: CIRCULAR (SST TYPE)	23.2
FIXED TUBES WITH SEPARATE FLOW	22.8

Figure 23. Initial Concepts and Evaluation.

N = NUMBER OF ELEMENTS

AR = ELEMENT ASPECT RATIO ~ h/W_0

SR = ELEMENT SPACING RATIO ~ s/W_0

A_{MAX} = MAX. ENVELOPE AREA ~ πR^2_{MAX}.

A_{MAX} / A_8 = AREA RATIO

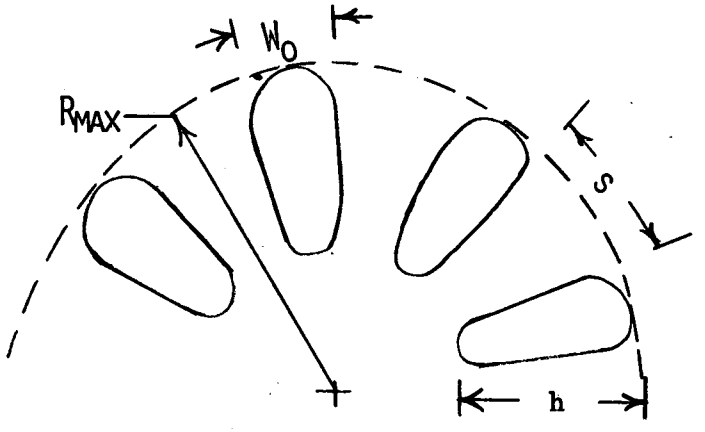

$$\frac{A_8}{A_{MAX}} = \left(\frac{1}{1+SR}\right)\left\{1 - \left[1 - \frac{2\pi AR}{N(1+SR)}\right]^2\right\}$$

Figure 24. Multi Element Nozzle Geometric Relationships.

(1) Mixer nozzle velocity decay characteristics for flap spacings from 2.15 - 4.3 m (85 to 170 inches).

(2) Studies to select minimum loss and weight mixer geometry.

(3) Definition of a procedure for estimating takeoff and cruise performance penalties of mixer nozzles - relative to a standard convergent reference nozzle.

(4) Studies to define exhaust flap interaction noise trends.

Velocity Decay Prediction Procedure

The objective of the velocity decay prediction trend studies was to formulate a procedure for rating velocity decay directly to nozzle geometry. The first step was to identify the mixer nozzle geometric features that most directly influence exhaust velocity decay. The following five parameters, describing mixer nozzle exit plane geometry, were chosen as being the key variables.

N	=	No. of Elements		
AR	=	Element Aspect Ratio	=	h/W_o
SR	=	Element Spacing Ratio	=	s/W_o
A_{max}	=	Maximum Envelope Area	=	πR^2_{max}
A_{max}/A_8	=	Area Ratio		

It was found that the interrelationships between these variables could be described by a relatively simple equation. This equation and these key geometric variable are illustrated in Figure 24.

The velocity decay data reported in References 27 and 33 was found to be sufficiently comprehensive that decay characteristics could be directly related to these five key mixer nozzle geometric variables by a series of semi-empirical equations developed by NASA.

For multi-element decayers, the variation of velocity ratio, V/V_{jet}, with distance was found to have three distinct segments, (see Figure 25).

The first part, or single element decay is described by

$$V/V_{jet} = \left\{ \frac{1}{1 + \left(.15X/C_e D_e \sqrt{1 + M_{jet}} \right)} \right\}^{1/A} \quad \text{where } A = \frac{4(2 - W_i/W_o)}{(1 + 8/3 \; D_e/D_h - 1)} \text{----(III-1)}$$

and C_e = flow coefficient

D_e = equivalent diameter of the area of 1 lobe

M_{jet} = jet Mach number

D_h = hydraulic diameter of 1 lobe

W_i = inner lobe width

W_o = outer lobe width

The point at which the multi-element flows begin to coalesce and the velocity decay becomes retarded has been defined as a design point, indicated as Point 1 in Figure 25. The distance parameter associated with Point 1 is -

$$X/C_eD_e \sqrt{1 + M_j}\Big|_{Pt.\ 1} = 11^{*} \left[1 + 1/4\ (SR)^{2/3}\right] (SR)^{1/3}\ \Gamma \text{----------(III-2)}$$

where $\Gamma = \left\{ 1 + 8/3\ (D_e/D_h - 1) \left[\frac{1}{1 + 5\ (1 - W_i/W_o)^8}\right] \right\}^{-1}$

and SR = spacing ratio - space between lobes divided by W_o

As can be seen, this is a strong function of spacing ratio (SR). Increasing the spacing delays the point of coalescence and has an insignificant effect on decay rate, while increasing the lobe aspect ratio (height/width), increases the decay rate with a minor effect on the location of the coalescence point.

In order to define the decay curve beyond Point 1, NASA has suggested the use of a constant slope of -.2. This means that:

$$\frac{LN\left[(V/V_{jet})_2 \ / \ (V/V_{jet})_1\right]}{LN\left[\left(\frac{X}{C_e D_e \sqrt{1 + M_j}}\right)_2 \Big/ \left(\frac{X}{C_e D_e \sqrt{1 + M_j}}\right)_1\right]} = -.2$$

* Equation 3 in Reference 33 uses a value of 12 rather than 11. This difference is considered to be insignificant for the purposes of this study.

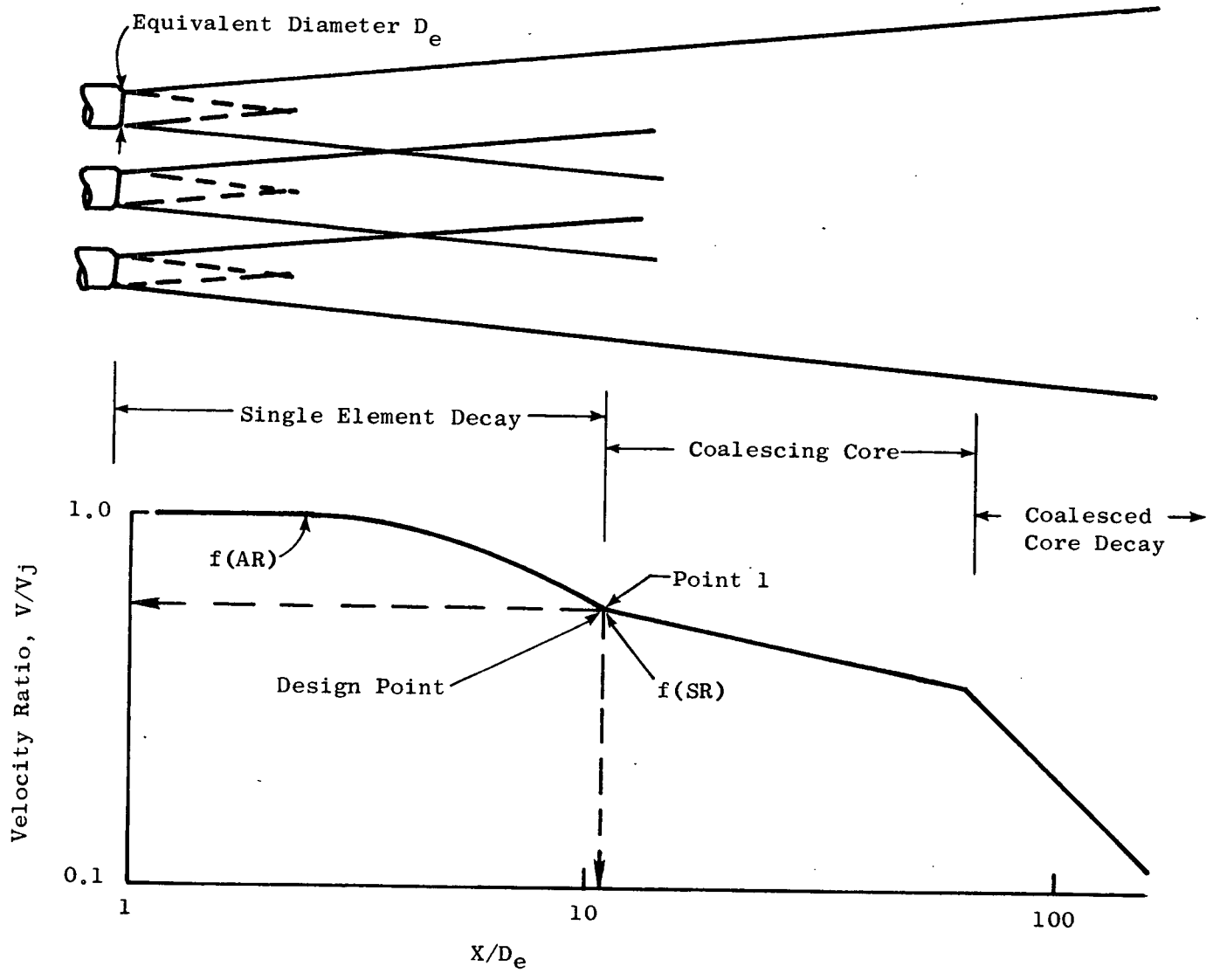

Figure 25. Multi-Element Nozzle Velocity Decay.

Or simplified for Cartesian coordinates:

$$\left.V/V_{jet}\right|_2 = \left.V/V_{jet}\right|_1 \left[\left. \frac{X}{C_e D_e} \frac{1}{\sqrt{1 + M_j}} \right|_1 \Big/ \left. \frac{X}{C_e D_e} \frac{1}{\sqrt{1 + M_j}} \right|_2 \right]^{.2} \text{-------(III-3}$$

The distance over which this slope is to apply, (the coalescing core region) is defined by F_X:

$$F_x = 1 + \left(\frac{D_{e,t}}{D_e} - 1 \right) \left[\frac{1}{1 + (SR) \left[\frac{1}{1 + 50 \, (D_e / D_h - 1)} \right]^{5/3}} \right]^{.8}$$

where $D_{e,t}$ = the equivalent diameter of the total nozzle flow area.

F_X is equal to the ratio of $X/C_eD_e \sqrt{1 + M_j}$ at the end of the coalescing core region to its value at Point 1.

At the end of the coalescing region, the velocity decay rate returns to what it was at Point 1, and is adjusted to maintain a consistent value thereafter.

These velocity decay equations were programmed for computer calculation. Sample calculations used to check the program are shown in Figure 26 for twelve (solid line) and six - (dashes line) element mixed nozzles. Similar comparisons with General Electric data are shown in Figure 27. In general the velocity decay calculations for the initial decay region are quite accurate. The calculations for the coalescent, fully-mixed regions appear to be somewhat conservative. Primary emphasis for this study has been given to velocity decay estimates on the velocity at the "Design Point".

Considerable attention was given to comparing General Electric velocity decay estimates with NASA estimates for TF34 multi-lobe mixer geometries that were significantly different from the NASA models tested. 16- and 32- lobe mixer nozzle decay estimates are compared in Figure 28. The velocity ratio at the 4.1 m (160 inch) distance corresponds to the NASA guideline on exhaust flap spacing. The increment between NASA and General Electric velocity decay estimates was considered to be satisfactory for this study.

An example of the velocity decay versus mixer nozzle geometry trend data is shown on Figure 29. All four mixer nozzles were designed to have a velocity ratio of 0.5 at their design point (the point at which the flow from all the individual lobes coalesces). The primary geometric variables controlling these decay characteristics were number of lobes and lobe aspect ratio. The large number of high aspect ratio mixer lobes greatly reduced the distance required to reduce maximum jet velocity to 0.5 of the exhaust velocity.

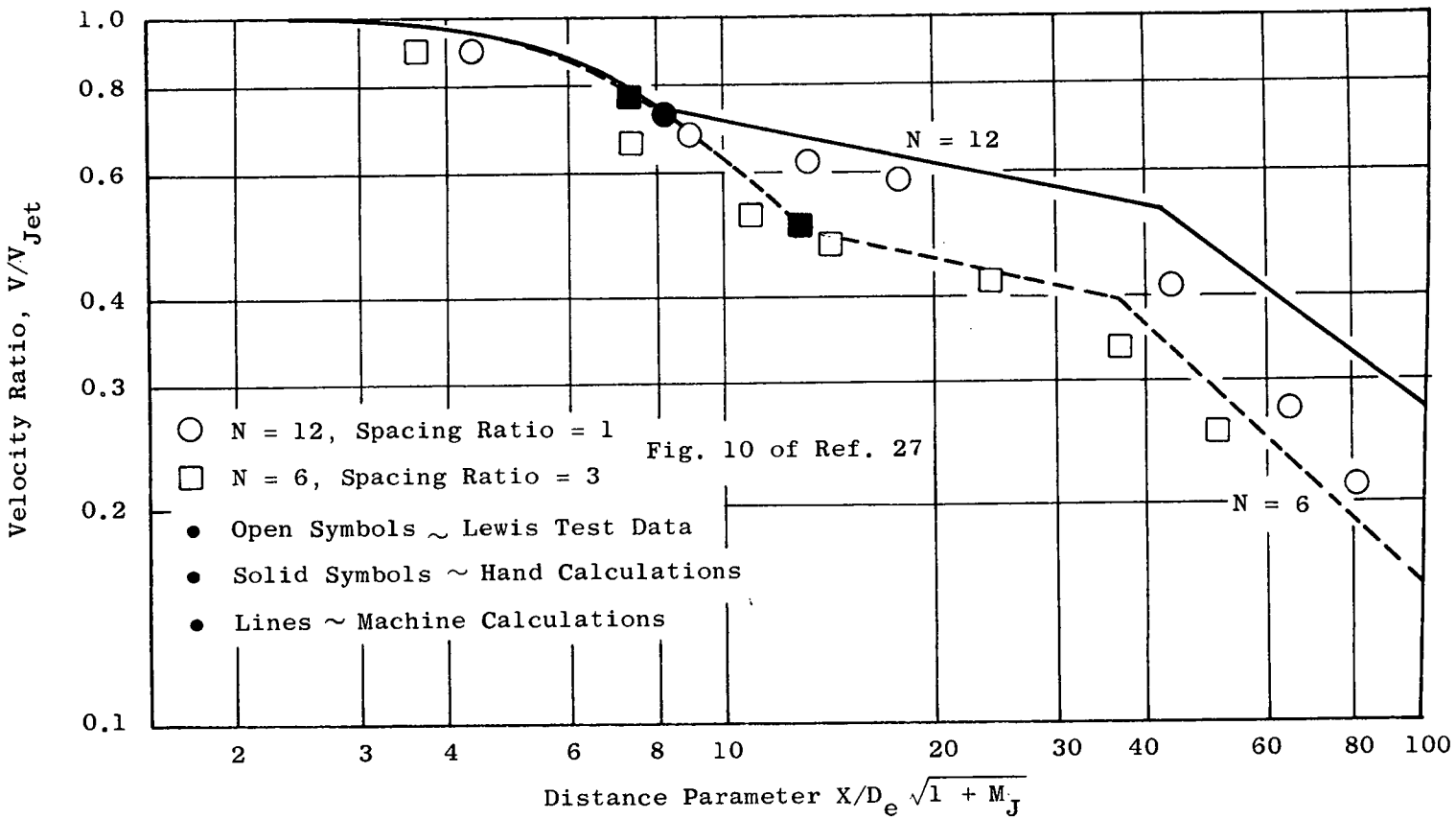

Figure 26. Comparison of Velocity Decay Calculations with NASA Lewis Test Data.

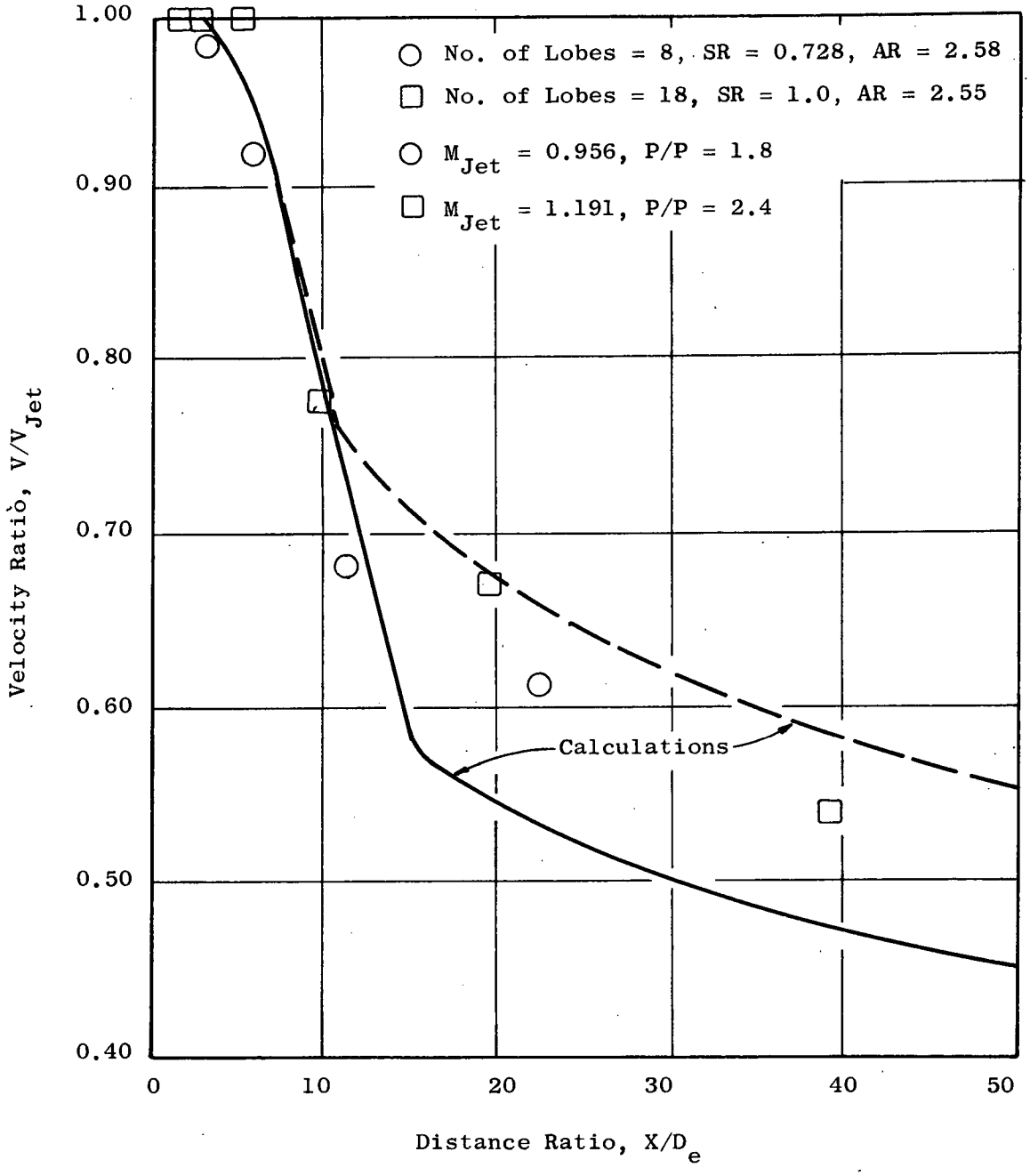

Figure 27. Comparison of Velocity Decay Calculations with GE Test Data.

Decay Parameters	16 Lobe Design		32 Lobe Design	
	NASA	GE	NASA	GE
$\left(\frac{V}{V_{jet}}\right)$ @ design point	0.79	0.74	0.81	0.74
$(X/D_e \sqrt{1 + M_j})$ @ design point	6.8	7.5	4.3	4.9
$\left(\frac{V}{V_{jet}}\right)$ @ x = 4.06 m (160 in.)	0.69	0.64	0.59	0.59

Figure 28. Comparison of NASA Lewis and GE Velocity Decay Estimates.

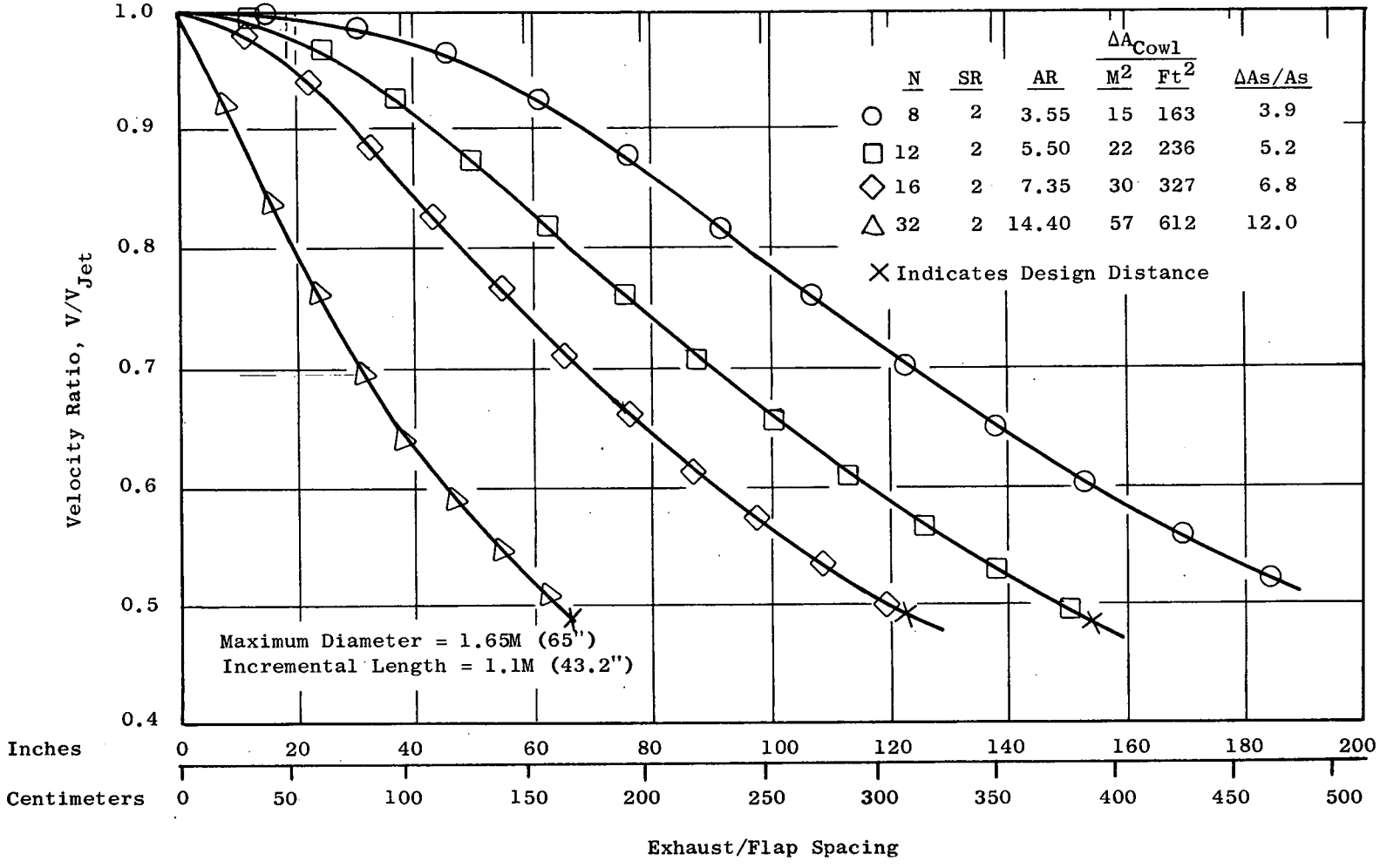

Figure 29. Velocity Decay for (V/V_{Jet}) Design ~ 0.5.

All four of these designs required an increase in nacelle length of 1.1 m (43 inches) in order to satisfy external nozzle conical boattail angle design constraints. In order to avoid boattail separation and increased pressure (or profile) drag the maximum boattail angle was limited to .35 rad (20^{o}).

An important design consideration for these mixer nozzles was the surface area of the lobes and the centerbody plug. A convergent nozzle configuration was used as reference base. The additional surface area and the ratio of this additional area to total nacelle surface area were computed for each mixer nozzle installation. These parameters were considered to be useful indicators of the increase duct and external friction drag performance losses and additional weight.

Multi-Lobe Geometry Optimization

The increased cowl surface areas required for the four mixer nozzle designs described in Figure 29 are very large. These velocity decay relationships indicated that a specified level of velocity decay could be accomplished with a variety of lobe shapes. Studies were initiated to explore how mixer surface area could be minimized by varying lobe aspect ratio and spacing ratio without sacrificing velocity decay. The basic approach used in this study was to:

- Select number of lobes (N) - dominant design variable
- Select lobe aspect ratio (AR), spacing ratio (SR) that give minimum increase in wetted surface area (minimum performance loss)
- Consider a range of jet exhaust flap spacing 2.15 - 4.3 m (85 - 170 inches)

The details of this geometry analysis procedure are reviewed in the following paragraphs.

The geometric relationships describing the mixer design shape, in terms of the key geometric variable influencing velocity decayer, were developed in the following manner:

Exhaust Plane Geometric Relationships

Spacing ratio, $SR = S/W_o$

Aspect ratio, $AR = H/W_o$

Area Ratio $= A_8/A_{max}$

Number of lobes $= N$

$A_e = \pi (R_{max}^2 - R_{in.}^2)\ \varphi/2\pi$; $A_8 = N\ A_e$

$N\varphi + N\theta = 2\pi$; $SR = R_{max}\theta / R_{max}\varphi = \theta/\varphi$

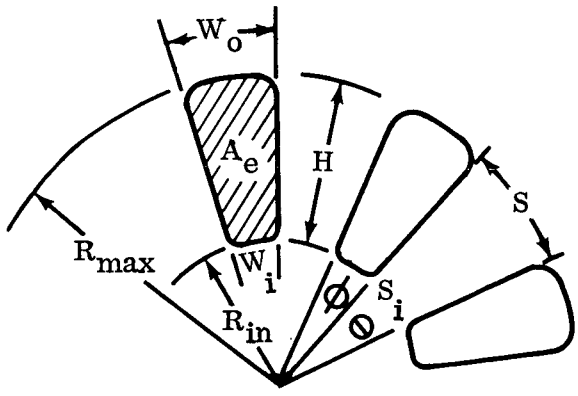

$$\therefore \varphi = 2\pi/N(1 + SR) \quad \text{and} \quad A_8 = \pi/1 + SR\,(R_{max}^2 - R_{in}^2)$$

$$A_8/A_{max} = 1/(1 + SR)\left[1 - \left(\frac{Rin}{Rmax}\right)^2\right] \quad ; \quad AR = (R_{max} - R_{in})/\varphi R_{max}$$

$$\varphi AR = 1 - Rin/Rmax \rightarrow \left(Rin/Rmax\right)^2 = (1 - \varphi AR)^2$$

$$A_8/A_{max} = \left(\frac{1}{1 + SR}\right)\left[1 - (1 - \varphi AR)^2\right], \quad \text{but} \quad \varphi = 2\pi/N(1 + SR)$$

$$\therefore A_8/A_{max} = \left(\frac{1}{1 + SR}\right)\left[1 - \left(1 - \frac{2\pi AR}{N(1 + SR)}\right)^2\right] \quad \text{where} \quad A_{max} = \pi R_{max}^2$$

The assumptions used to develop these relationships are:

- The lobe side is a radial line to the center of the exhaust plane.
- The lobe is trapezoidal with minimum rounding of the corners.
- The elements (lobes) are all identical.

With the exhaust plane geometry defined in this manner, it was a simple matter to parametrically vary the geometry. Naturally, a configuration selected from the analysis must be designed compatible with the above-stated assumptions.

A vast amount of calculations were necessary to complete the design analysis. This was possible only through use of the GE Time Sharing Facility. One of the simple programs, DAISY 3, was written to provide the performance definition curves. Specifically, the program was used to calculate the following:

1. the Area Ratio = A_8/A_{max}
2. the Wetted Area Ratio = Ratio of the wetted area of the daisy (decayer) to the clean cowl wetted area aft of the interface plane. The interface plane could be defined as the most forward station at which the decayer can interface with the "clean" nacelle. For the TF34 this is just aft of the acoustic treatment area and splitters in the bypass duct.
3. the Length Ratio = Ratio of the total nacelle length with the daisy installed to the "clean" nacelle length.
4. Perimeter Ratio = Ratio of the perimeter of the decayer at the exhaust plane to the standard convergent nozzle perimeter.

5. the Plug Wetted Area Ratio = Ratio of the wetted area of the daisy's plug to the clean cowl plug - internal only.

6. External Plug Wetted Area = wetted area of external part of plug.

The schematic below indicates some of the important geometry, either input, or calculated by the program.

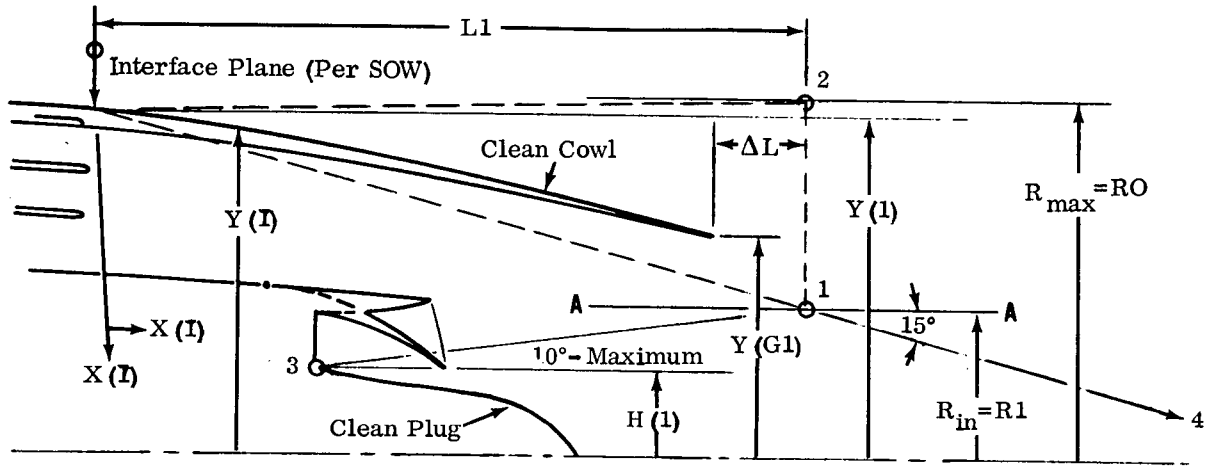

The assumptions and simplifications made in writing the program are listed below:

1. Maximum chordal angle between lobes is held at a constant stipulated value (.26 rad (15°)) for the TF34 studies. This is part of the criteria which set the exhaust plane location.

2. The perimeter around the decayer varies linearly between the exhaust plane and the clean cowl intersection station.

3. The new plug that goes with the decayer can be described by straight lines between points 3 - 1 - 4 for the purpose of calculating its wetted area.

4. The maximum angle between points 3 and 1 is set at some stipulated value (.175 rad (10°) for the TF34 based on sketches defining a reasonable limit)). This is the second part of the criteria which set the exhaust plane location.

The longest decayer length, L1, which results from items 1 and 4 above, is the one used in the calculations.

Very briefly, the stepwise procedure followed in the program is described below:

1. The "clean" cowl and plug wetted areas are calculated by numerical integration.

2. The area ratio, A_8/A_{max}, and the values of R_{max} (RO) and R_{in} (R1) are calculated using the equations listed above.

3. If $R_{max} \geq Y(1)$ then the point 0 becomes the intersection point of the decayer with the clean cowl.

4. If $Y(G2) \leq R_{max} < Y(1)$ then the exact value of X at the point of intersection with the clean cowl is interpolated for using the X (I) and Y (I) input data.

5. If $R_{max} < Y(G2)$ then a message is printed out and the next calculation is started; i.e., no answers are printed.

6. The maximum chordal angle limit is used to locate point 1.

7. The angle between points 1 and 3 is calculated.

8. If the angle is greater than the limit, point 1 is moved aft along line A-A to the point where the angle becomes the limit value. This reduces the chordal angle between lobes accordingly and determines a new and larger value for L1.

9. The perimeter of the decayer at the exhaust plane is calculated using

$$P_3 = \left[2H + W_o + S_i \right] N$$

10. If $R_{max} > Y(1)$ then the perimeter at point 0 is calculated ($= 2\pi Y(1)$), averaged with P3 and multiplied times L1 to get the wetted area.

11. If $Y(G2) \leq R_{max} < Y(1)$ then the perimeter, $2\pi R_{max}$, is averaged with P3 to get the wetted area. The additional wetted area of the clean cowl between Y (1) and R_{max} is calculated and added on.

12. The internal wetted area of the plug is calculated by assuming a straight line plug contour between points 1 and 3.

13. The external wetted area of the plug is calculated by assuming the plug is a .26 rad (15°) cone.

14. Once a calculation is complete, aspect ratio, and then spacing ratio are incremented according to input values. The maximum value of spacing ratio is also input. Aspect ratio is limited to its maximum possible value of:

$$N\ (1 + SR)\ 2\pi \text{ (i.e., } R_{in} = 0 \text{) less } 0.5$$

15. Once a complete set of calculations has been done, a new value of number of lobes, N, is read, and the whole procedure, except for step 1, is repeated.

The DAISY 4 program was written to provide the design distance and associated velocity decay ratio for all possible combinations of spacing and aspect ratio for a given number of lobes. This information, when combined with that supplied by DAISY 3 provides most of the information required to do the design selection and analysis. The equations used are the NASA Lewis developed equations with the geometry as defined previously. No other assumptions or simplifications are necessary. The program is very simple and prints out the following:

1. Spacing ratio
2. Aspect ratio
3. Area ratio
4. Velocity ratio
5. Distance ratio - $X/D_e \sqrt{1 + M_j}$ ($C_e = 1$) @ point 1 (design point)
6. Design distance - X in inches at design point
7. X/D - $X/D_{e,t}$ where X is in inches and $D_{e,t}$ is the equivalent diameter of a circle with an area - A_8 in inches^2.

DAISY 5 calculates velocity decay ratio versus length for any specific design. The equations used are, again, those developed empirically by NASA Lewis and presented earlier. The program prints out two groups of information. The first group is primarily for reference.

Ideally, for a velocity decayer design, the nozzle location relative to the flap and the required velocity decay ratio needed to meet the noise requirements would be known. The design analysis would then be a matter of looking at all possible decayer configurations which would meet these criteria and the one with the least penalty would be selected. In our case, however, the velocity ratio and design distance were essentially unknowns, so the approach was to determine these parameters as a function of penalty and select a design which provided a reasonable balance of the objectives, i.e., high decay, short distance, and low penalty.

Following is a brief synopsis of the design analysis performed using the Time-Sharing Computer programs described above. The working curves shown in simplified form with the various steps below are included in complete form in the Appendix.

Step 1 involved running the DAISY 4 time-sharing program which yields the three curves shown for one value of number of lobes. A complete set of these curves was generated for 8, 12, 16 and 32 lobes in order to parameterize the analysis in terms of number of lobes. The spacing and aspect ratios corresponding to various levels of decay at the design distance point were superimposed on cuve C yielding contour lines of constant decay ratio. Where these lines intersected the minimal loss line (from step 2), defined the minimum loss for that respective decay ratio.

Step 2 (DAISY 3) A complete set of the curves (D, E, F, & G) depicted was generated for each of 8, 12, 16 and 32 lobe decayers. These might be considered the "performance definition curves". Superimposed on the wetted area ratio plot (D) were, again, lines of constant V/V_j at the design distance point, from curve A. These contour lines have a "bucket" if not limited by area ratio. Therefore, the "bucket" or area ratio limit points defined the design value of spacing and aspect ratio in each case. The curve E defined the nacelle length increase associated with each design. Curves F and G were used later to calculate the total additional performance loss associated with each design.

Multi-Lobe Nozzle Performance

The review of available design data indicated that there was insufficient mixer nozzle performance data to permit the type of correlations used to compute velocity decay. As a result, previous design and test experience was used to formulate an approximate performance loss calculation procedure.

The sources of performance loss and the assumptions used in formulating these predictions are outlined in Figure 30. The assumptions on external pressure drag at cruise were based on wind tunnel test experience on the CJ-805-23 8-lobe daisy mixer nozzle. This data indicated that by limiting the maximum conical boattail angle (in the trough of a mixer lobe) to .26 rad (15°), no significant increase in pressure drag was experienced up through 0.8 flight Mach number.

- The internal (% change in C_V) loss was determined using flat plate friction/pressure drop calculation techniques. The pressure drop was then equated to an equivalent loss in thrust (change in C_V). At takeoff, the percent loss in C_V was equal to the percent loss in net thrust (F_N); but at cruise the loss was:

  $\% F_N = \frac{F_g}{F_N}$ (percent loss in C_V cruise condition). so the gross (F_g) to net thrust ratio at the cruise condition was an important number.

- The plug scrubbing drag was calculated using flat plate equations and the wetted area from curve G. This was a very small number compared to the other external friction loss.

- External friction loss at cruise was determined using the clean cowl wetted area aft of the interface plane, the wetted area ratio, and the flat plate friction equation. The characteristic length was determined using the entire cowl length (used to compute Reynolds number). The drag simplifies to the following equation:

  ΔF_N = Clean Cowl Drag (wetted area ratio - 1)

Mixer nozzle takeoff and cruise performance losses were computed for three classes of mixer designs:

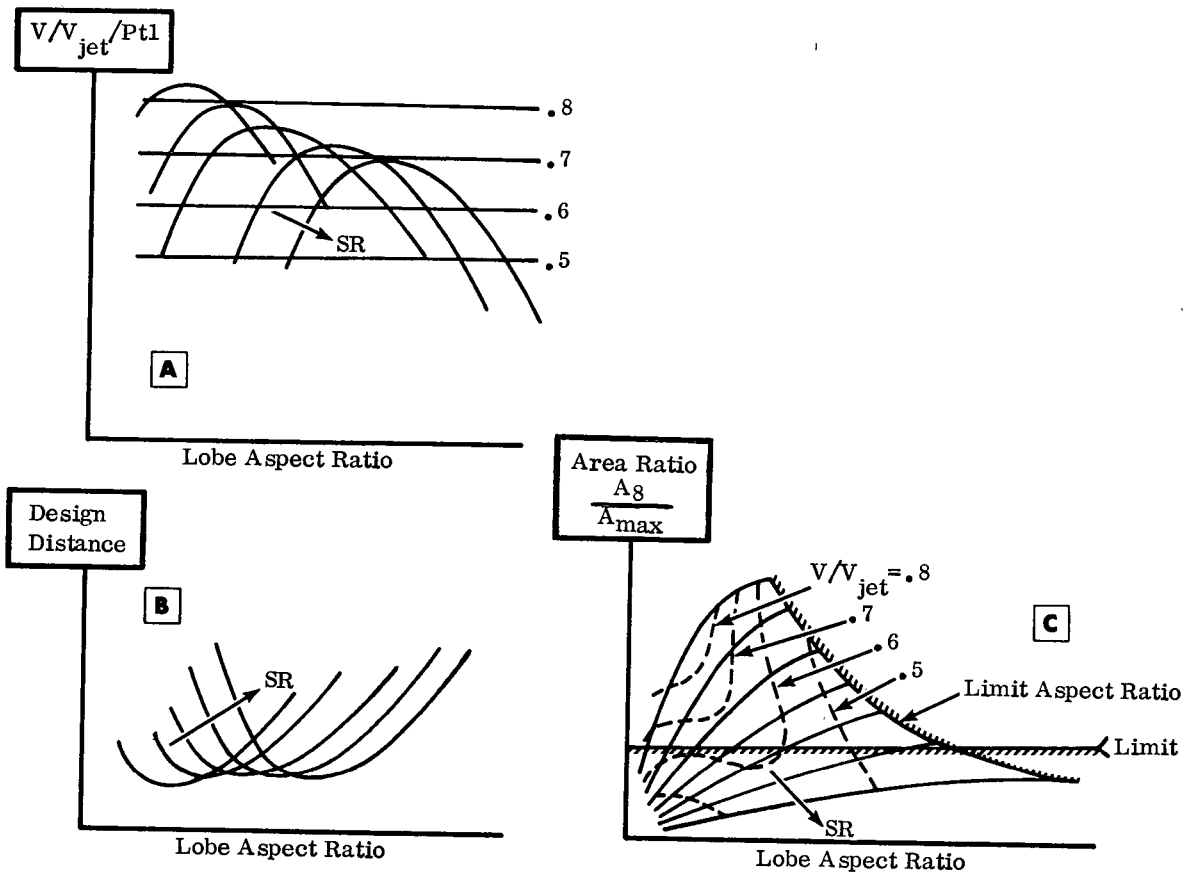

The point of maximum velocity decay with minimal loss was defined by the intersection of the minimal loss line with the area ratio limit line.

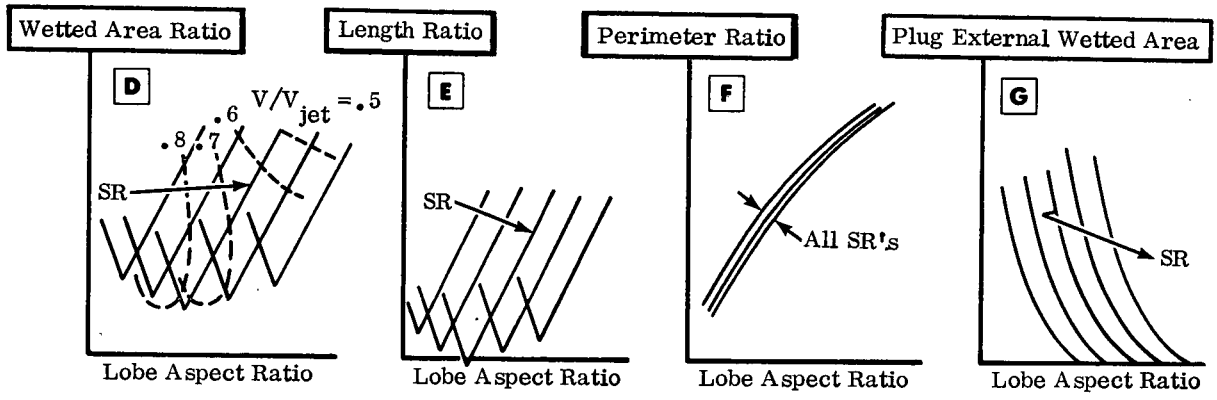

(SOURCE OF LOSS)	(APPROXIMATION)
• INTERNAL DUCT PRESSURE LOSS	f ($\Delta A_{\text{wetted surface}}$)
• JET SCRUBBING DRAG	f ($\Delta A_{\text{scrubbed surface}}$)
• COWL DRAG	
- FRICTION DRAG	f ($\Delta A_{\text{cowl surface}}$)
- PRESSURE DRAG	Small
• EXHAUST ANGULARITY LOSS	Small *
• BASE DRAG	Small

PERFORMANCE LOSS $\sim \Delta A_{\text{surface}}$ AREA

* (CJ 805 Daisy Design Technology)

Figure 30. Simplified Performance Loss Approximations.

1. Mixer nozzles with a design velocity decay ratio of 0.5.

2. Mixer nozzles with a design velocity decay ratio of 0.6.

3. Minimum surface (maximum performance) mixer nozzles with velocity decay ratio of 0.59 and 0.65 at their design point as shown in Figure 31.

The takeoff performance trends shown in Figure 32 show the large increases in performance loss that come with increasing number of lobes. Minimizing the mixer nozzle surface gives large improvements in performance.

Similar cruise performance penalty trend curves are shown in Figure 33. The cruise losses include both the internal losses experienced during cruise and the increased nacelle conical drag due to the additional external friction drag or the mixer nozzle surfaces. The influence of these losses on cruise net thrust is multiplied by the fact that the ratio of gross to net thrust is from 2 to 3 times the takeoff value.

Flap Interaction Noise Prediction Procedure

Estimates of the total jet noise (jet + EBF) have been made, for the case of a STOL aircraft equipped with four mixed flow TF34 engines with velocity decayers. Figures 34 and 35 are presentations of these estimates for takeoff and approach, respectively; the noise levels are plotted as a function of jet exhaust velocity.

The term "V_{Flap}/V_{Jet}" refers to the ratio of decayed flap impingement velocity to jet exhaust velocity and is a "figure of merit" for the performance of the velocity decayer. The jet noise goal (92 PNdB) is presented for comparison. As an example on takeoff, with a jet exhaust velocity of 250 m/s (813 ft/sec), the decayer must reduce the flap impingement velocity to a value somewhat less than 60% of the exhaust velocity, to meet the noise goals. 250 m/s is a typical velocity for a suppressed engine cycle.

The basic jet noise from the engine exhaust is assumed to be unaffected by the presence of the decayer. This simply means that the exhaust from the decayer would cause the same jet noise level as the exhaust from a conical nozzle having the same effective area and jet velocity. It is possible that the basic jet noise will be lowered (dependent on final decayer design), but for the purposes of this study it provides a "noise floor", below which total jet noise cannot be lowered.

The use of 60 M (200 ft) altitude on takeoff and 150 m (500 ft) altitude on approach represents a "best judgement" estimate made to define the points of maximum total engine noise. The basic jet noise, along with the fan and turbomachinery noise, of course diminishes with increasing altitude. However, the EBF noise adder to basic jet noise increases with altitude, due to the pronounced downward directional effects of EBF noise.

The detailed information uncovered during the data review and the specific calculating procedures used to generate Figures 34 and 35 are discussed in the following paragraphs.

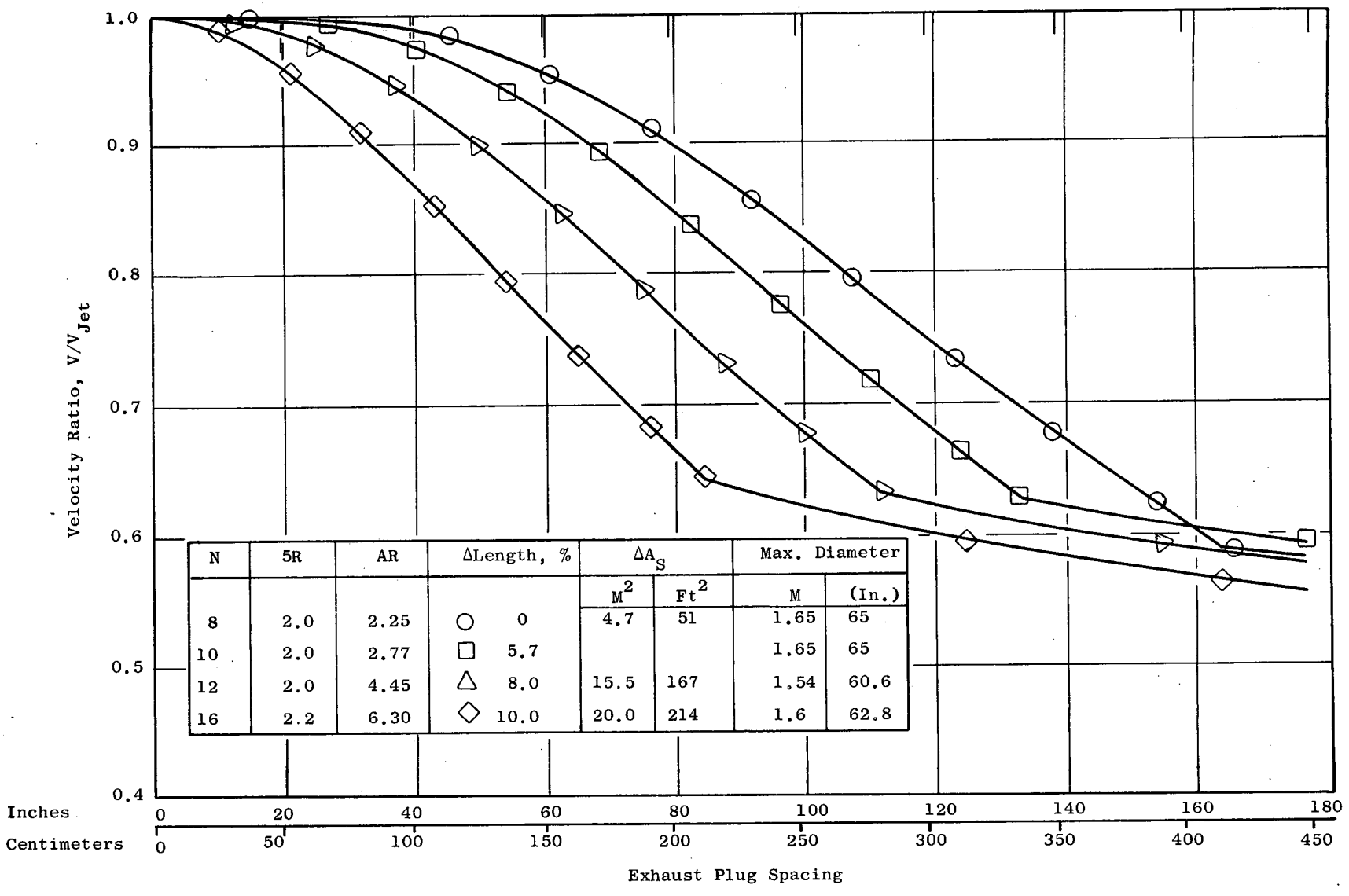

N	5R	AR	ΔLength, %	ΔA_S		Max. Diameter	
				M^2	Ft^2	M	(In.)
8	2.0	2.25	○ 0	4.7	51	1.65	65
10	2.0	2.77	□ 5.7			1.65	65
12	2.0	4.45	△ 8.0	15.5	167	1.54	60.6
16	2.2	6.30	◇ 10.0	20.0	214	1.6	62.8

Figure 31. Velocity Decay for Minimum $\Delta A_{Surface}$ Designs.

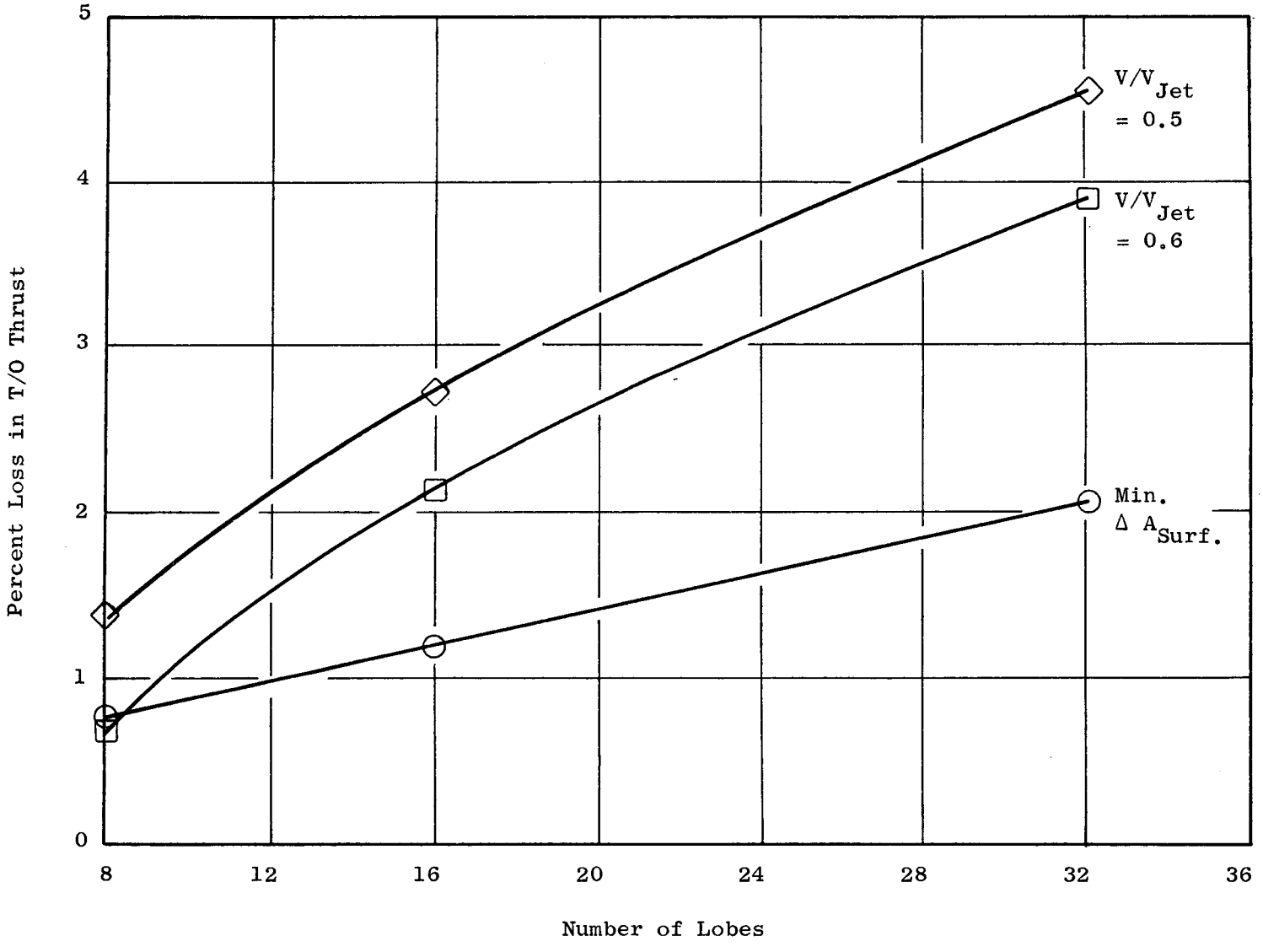

Figure 32. Influence of Number of Lobes on Takeoff Thrust.

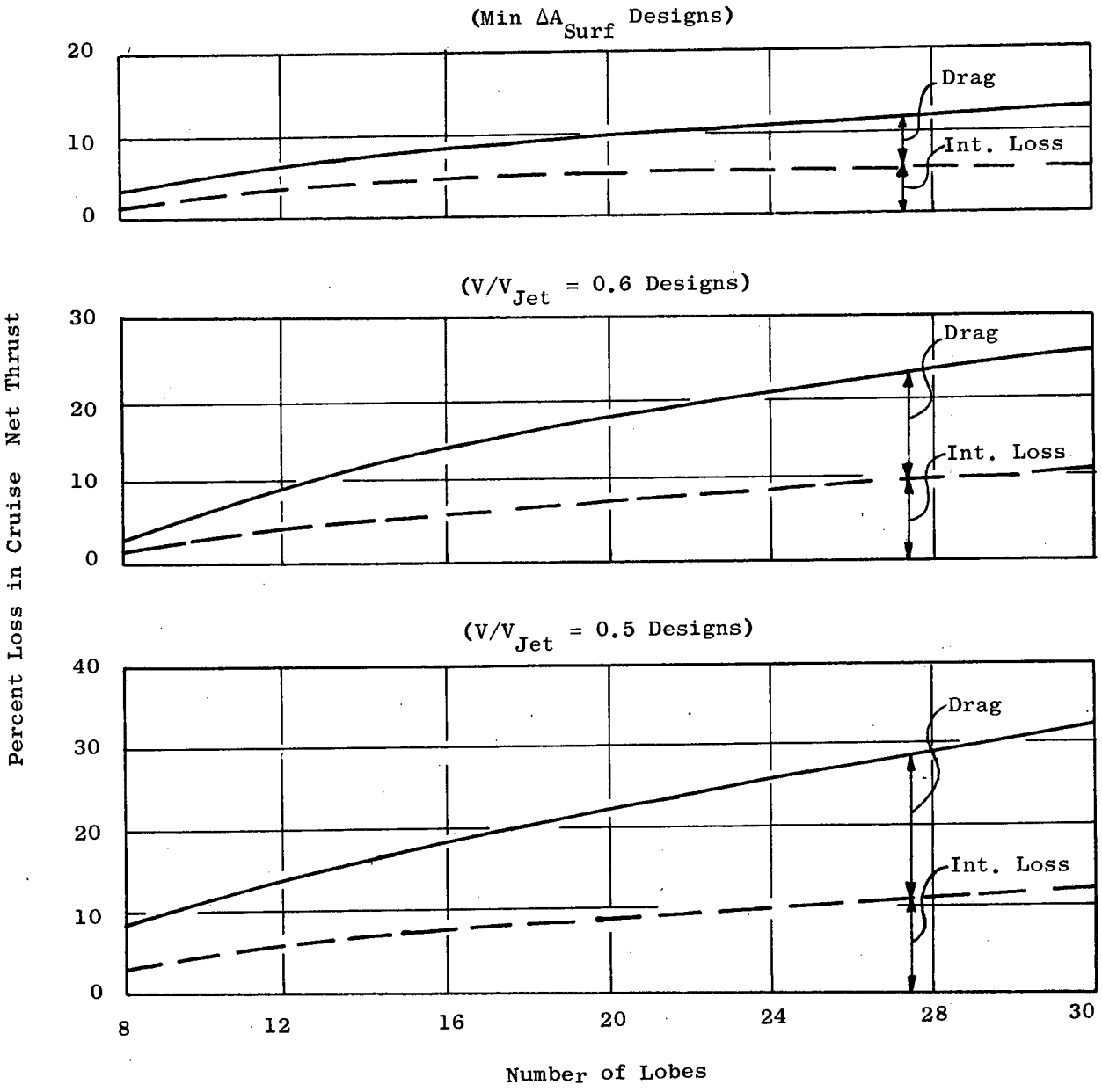

Figure 33. Influence of Number of Lobes on Cruise Thrust.

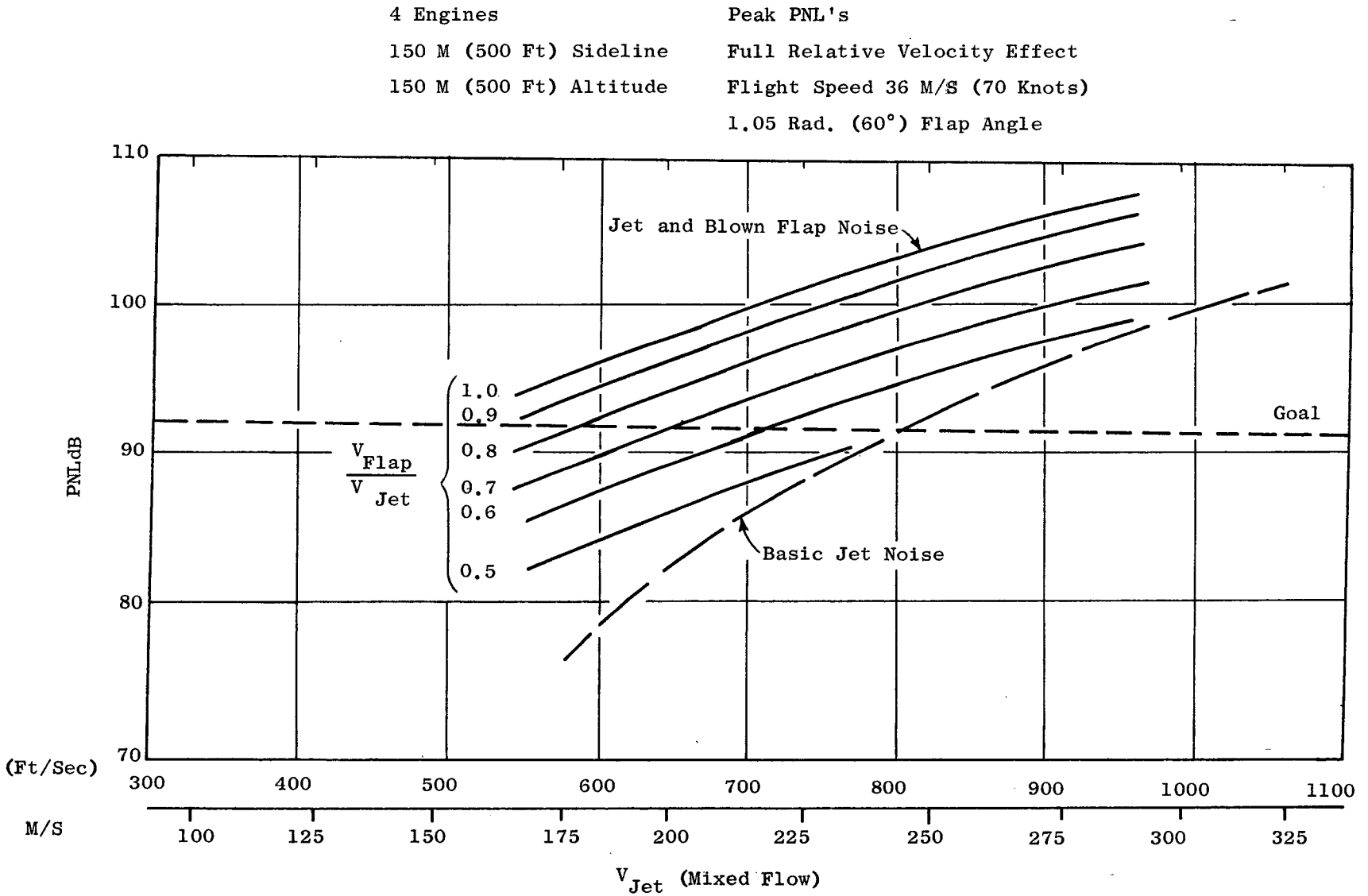

Figure 34. Approach Flap Impingement Noise Trends.

4 Engines
150 M (500 Ft) Sideline
60 M (200 Ft) Altitude

Peak PNL's
Full Relative Velocity Effect
Flight Speed 50 M/S (100 Knots)
.52 Rad. (30°) Flap Angle

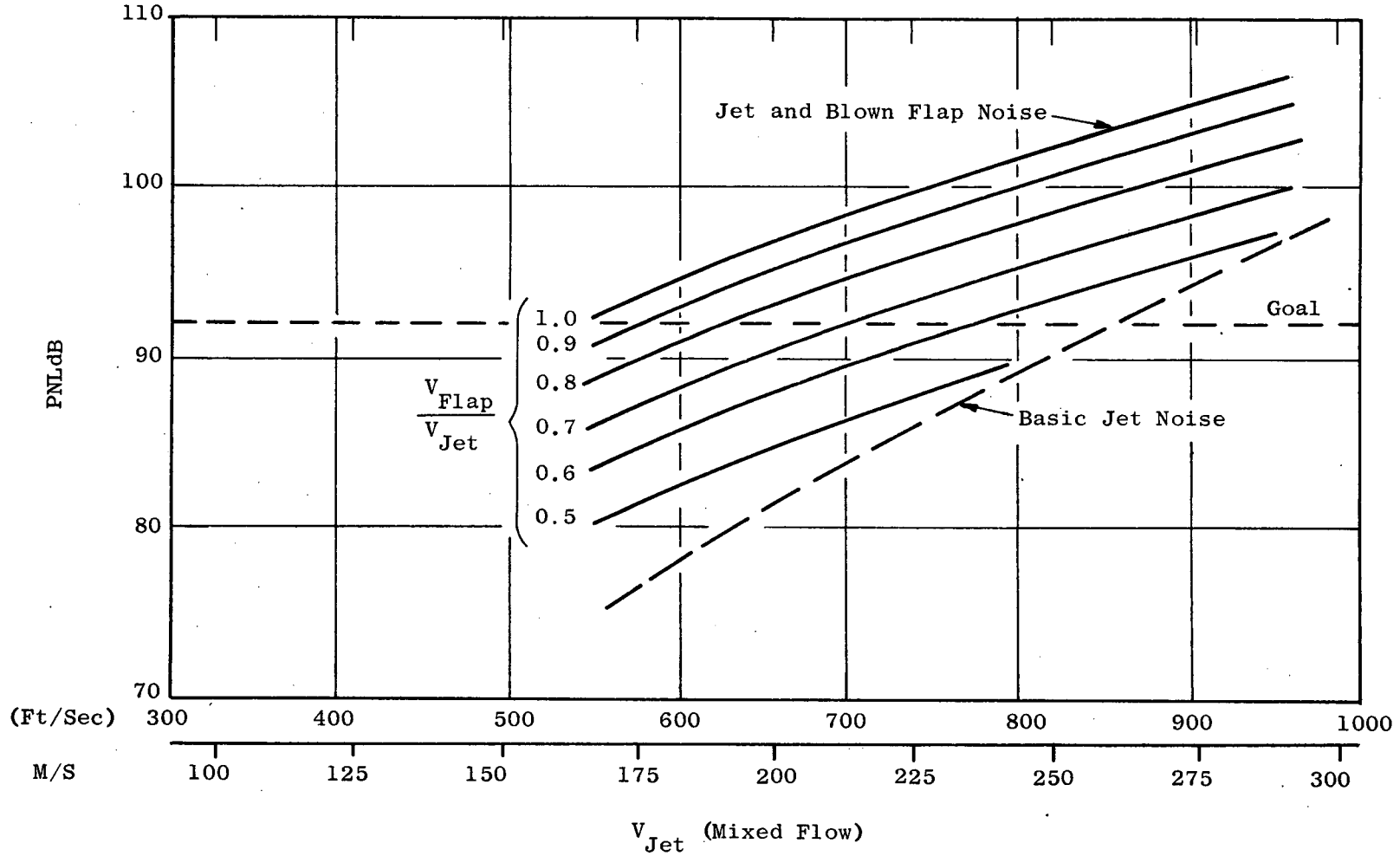

Figure 35. Takeoff Flap Impingement Noise Trends.

A survey of existing literature on external blown flap noise (Reference 7, 8, 28) revealed these salient conclusions:

1) External blown flap noise adds 8 - 12 dB (Overall Sound Pressure Level) to the static jet noise, measured at a point directly underneath the wing, with the increase in general across the spectrum.

2) External blown flap noise varies directly as the sixth power of the flap impingement velocity.

The following procedures were adopted to make use of these conclusions:

Predictions of the basic jet noise, as a function of jet velocity, were made for the TF34 mixed flow engine with a conical nozzle. These predictions were based on scale model data from the tests of a 1/16 scale model mixer nozzle. The in-flight jet noise was derived through the application of the SAE relative velocity correction (Reference 34). The basic in-flight jet noise was assumed to provide a floor beneath which the total system jet noise could not be lowered. Since the TF34-2 (S3A configuration) jet velocity on takeoff is approximately 280 m/s (920 ft/sec), this jet velocity was chosen as the base point for the development of the prediction procedure. The increase in the nozzle/flap system noise due to EBF noise at 920 ft/sec was estimated to be 10 PNdB directly below the wing at a distance of 500 feet for a 1.05 rad (60°) flap angle.

This estimate of the EBF adder is based on a survey of existing test data in References 7, 8, and 28. These references present EBF increase in terms of OASPL or PWL. The assumption was made that the increase in OASPL or OAPWL would result in a similar increase in PNdB. The 10 PNdB increase due to the wing/flap interaction noise should be applied to the "basic jet noise" before the correction due to the relative velocity effect has been applied. For example, the basic static jet noise at 280 m/s (920 ft/sec) is 101.8 PNdB. To this level the 10 PNdB EBF adder would be applied for a 1.05 rad (60°) flap setting yielding a new level of 111.8. However, Figure 19 of Reference 7 indicates that a view factor correction should be applied to the EBF noise as the measurement point moves from directly underneath the flight path to a specified sideline. The view angle is defined on Figure 36. For the specific example the view angle is 0.78 rad (45°). Applying the view angle correction as specified by Figure 19, Reference 7, the (EBF + jet) system noise is lowered by 5 PNdB for this view angle. This increase is only 5 PNdB higher than the basic static jet noise. However, the basic in-flight jet noise is 4.8 PNdB less than the basic static jet noise because of the relative velocity effect. Therefore, the increase in total system noise (EBF + jet) for the in-flight case is 9.8 PNdB. This procedure was used to establish a point on the curve for the total jet and blown flap noise with no decayer (Vdecayed/Vflap = 1.0) at 920 ft/sec (280 m/sec jet velocity (Figures 34 and 35). The sixth-power dependency on impingement velocity was then employed to generate the rest of the upper curve by the use of the relationship:

$$\Delta \text{ PNL} = 60 \text{ Log}_{10} (V_1/V_2)$$

2

TAKEOFF:

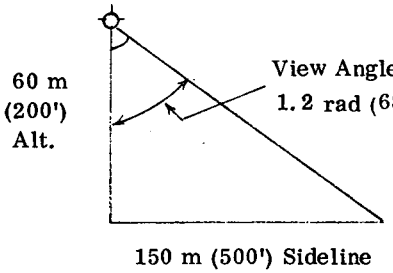

- TOTAL JET NOISE (0 VIEWING ANGLE) = STATIC JET NOISE + 10 PNdB
- CORRECTION FOR S. L. (1.2 RAD (68°) VIEWING ANGLE) = - 8 PNdB
- TOTAL JET NOISE (1.2 RAD (68°) VIEWING ANGLE) = STATIC JET NOISE + 2 PNdB

APPROACH:

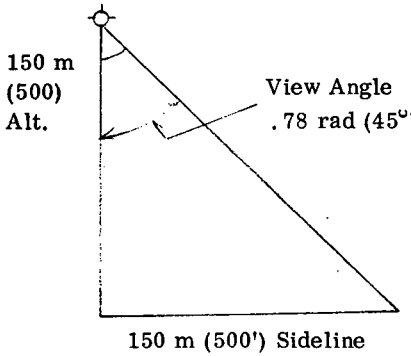

- TOTAL JET NOISE (0 VIEWING ANGLE) = STATIC JET NOISE + 10 PNdB
- CORRECTION FOR S. L. (.78 RAD (45°) VIEWING ANGLE) = - 5 PNdB
- TOTAL JET NOISE (.78 RAD (45°) VIEWING ANGLE) = STATIC JET NOISE + 5 PNdB

EGA & ATMOSPHERIC ATTENUATION EFFECTS
ARE INCLUDED IN THE + 10 PNdB ADDER.

Figure 36. Impingement Noise Estimation Guidelines.

FIGURE 37 - MULTI-LOBE VELOCITY DECAY DESIGN REQUIREMENTS

	(V_{jet})	(V_{flap}/V_{jet}) 92 PNdB	(Δ PNdB)
• APPROACH	198-213 m/s (650-700 ft/sec)	0.7 ---> 0.63	6 ---> 8
• T/O	250-259 m/s (820-850 ft/sec)	0.55 --> 0.5	12

To obtain the rest of the family of curves, for the configurations with decayer nozzles of varying effectiveness, the following equation was used.

$$\Delta \text{ PNL} = 60 \text{ Log}_{10} (V_{Flap}/V_{Jet}) + 10 \text{ Log}_{10} (A_{Decayed}/A_{Conical})$$

This relationship takes into account the fact that the flap impingement area of the jet, as well as the velocity, is changed by the decayer nozzle. Since limited test data on these areas were available, some simplifications were necessary. Assuming that the momentum of the jet impinging on the flaps is unchanged by the addition of the velocity decayer, it is then apparent that:

$$\frac{(\rho V^2 \text{ A}) \text{ Flap}}{(\rho V^2 \text{ A}) \text{ Jet}} = 1$$

If density changes are neglected, this becomes:

$$\frac{(V^2 \text{ A}) \text{ Flap}}{(V^2 \text{ A}) \text{ Jet}} = 1$$

and, therefore:

$$(A_{Decayed}/A_{Conical} = (V_{Flap}/V_{Jet})^{-2}$$

substituting this into the original equation:

$$\Delta \text{ PNL} = 60 \text{ Log}_{10} (V_{Flap}/V_{Jet}) - 20 \text{ Log}_{10} (V_{Flap}/V_{Jet})$$

therefore: Δ PNL = $40 \text{ Log}_{10} (V_{Flap}/V_{Jet})$

The Δ PNL's from the above relationship were then applied as constant increments to the total jet noise curve for the convergent nozzle, to arrive at the curves for decayer nozzles of varying effectivity.

The mixer nozzle velocity decay requirements for the takeoff and approach jet and flap interaction noise goal are summarized in Figure 37. Takeoff noise requirements are clearly the most difficult, requiring exhaust velocity decay in the 0.5 to 0.55 region. Since multi-lobe nozzle decay is relatively insensitive to exhaust velocity level (higher exhaust velocity jets do decay slightly faster than low velocity jets), a design that satisfies takeoff requirements will over-suppress approach noise.

Recommended Design Concepts

The results of the initial Task I concept selection studies led to the following four conclusions:

- Mixed flow cycle offers lowest noise potential.
- Fixed multi-lobe nozzle design approach offers most potential.
- Simple axisymmetric design recommended for ground test nacelle.
- Non-symmetric, multi-lobe design recommended for flight nacelle.

The multi-lobe nozzle design performance and noise trend data and analysis techniques were used to identify six potentially promising designs. Two types of 8, 12, and 16-lobe designs were selected. One of each was necessary to have a velocity decay ratio of 0.5 at the design point. The velocity ratio of 0.5 ensured that the takeoff flap interaction noise level might be met. However, the design distance required ranged from 5 m (200 inches) for the 8-lobe design to 3 M (120 inches) for the 16-lobe design. The NASA guide-lines indicated 4.1 m (160 inches). The corresponding cruise performance losses ranged from 9% of net thrust for the 8-lobe design to 18% for the 16-lobe design.

Flap exhaust spacings ranging from 2.5 m to 4.1 m (100 to 160 inches) were selected as being the most probable range of interest. For this spacing range, the 8-lobe design produced velocity decay ratios from 0.78 to 0.58.

A second series of 8-, 12- and 16-lobe mixer nozzles with minimum surface area were refined. As expected, these optimized designs cut the takeoff and cruise thrust loss approximately in half. This was done at a relatively small increase in velocity decay ratio.

The geometric, velocity decay and performance characteristics of these six multi-lobe nozzles are compared in Figure 38. The three designs considered to be most likely candidates are noted in this Figure.

The 12-lobe minimum surface design is recommended as offering the best balance between performance, weight and noise considerations. A more detailed tabulation of the geometric velocity decay and performance characteristics of this recommended design is presented in Figure 39.

Task II Study

The recommended 12-lobe mixer nozzle design concept was selected for more detailed design and analysis during Task II.

GEOMETRY								V_{flap} / V_{jet}		Thrust Loss, %		
No. of Lobes	Design	Aspect Ratio	Maximum Diameter		Length, ΔL		Surface Area, ΔA	A	B	T/O	Cruise	
			m	(in.)	m	(in.)	m^2 (ft^2)					
8	Min. Surf. Area	2.25	1.65	65	0	0	.06 50.7	0.83	0.6	0.8%	4%	
	$(V/V_j)_d$ = .5	3.6	1.5	59.2	1.1	43.2	.2 163.3	0.78	0.58	1.4%	9%	← (3)
12	Min. Surf. Area	3.3	1.65	65	0	0	.08 67.6	0.68	0.58	1%	8%	← (1)
	$(V/V_j)_d$ = .5	5.5	1.54	60.5	1.1	43.2	.3 236.5	0.66	0.48	2.2%	14%	
16	Min. Surf. Area	4.5	1.65	65	0	0	.12 101	0.63	0.56	1.2%	9%	← (2)
	$(V/V_j)_d$ = .5	7.4	1.5	60.8	1.1	43.2	.4 326.5	0.56	0.48	2.7%	18%	

	Nozzle-Flap Distance m	(in.)
A	2.54	100
B	4.06	160

Figure 38. Comparison of Multi-Lobe Mixer Concepts.

- DESIGN FEATURES

- NO. OF LOBES		= 12
- LOBE SPACING RATIO (SR)		= 2.0
- LOBE ASPECT RATIO (AR)		= 4.45
- MAX ENVELOPE DIAMETER	m(in.)	= 1.65 (65)
- CENTERBODY PLUG DIAMETER	cm (in.)	= 34.3 (13.5)
- ADDITIONAL NACELLE LENGTH	cm (in.)	= 29.2 (11.5)
- INCREASED SURFACE AREA	m^2 (ft^2)	= 15.8 (170)

- VELOCITY DECAY

- (V/V_{jet}) design point		= 0.634
- DESIGN DISTANCE	m (in.)	= 2.84 (112)
- (V/V_{jet}) at 4.06 m (160 in.)		= 0.59

- PERFORMANCE LOSS

- LOSS IN T/O THRUST	1%
- LOSS IN CRUISE THRUST	7.8%

Figure 39. Recommended Design Concepts.

Ground Test Mixer Nozzle Design

The ground test version of this mixer nozzle had to be designed to be installed and tested on the acoustically-treated ground test nacelle designed under modification 1 of this TF34 Turbofan Quiet Engine Program. Since the Task I design was primarily conceptual and more of a flight concept, revisions were needed to convert to practical ground test hardware.

In anticipating future test program requirements it became clear that the acoustic and performance characteristics of this 12-lobe mixer nozzle could not be evaluated unless there were a good basis of comparison. The exhaust nozzle design formulated in the Ground Test nacelle Design Study was a separate flow system. In order to get a more direct evaluation of the acoustic and performance characteristics of the 12-lobe design, the reference nozzles were included in the ground test nozzle design studies:

1. Reference configuration - Conical nozzle with the internal fan turbine stream mixer.

2. Alternate performance configuration - Conical nozzle with confluent or free mixing fan and turbine streams.

The reference design provides a more direct comparison of the flap interaction noise reduction capability of the external 12-lobe mixer nozzle. The alternate design, with the non-uniform exit profile will permit evaluation of the flap interaction noise reduction due to the internal mixer. Schematic sketches of all three mixer nozzles mounted on the ground test nacelle design are shown in Figure 40.

Engine Nacelle Nozzle Systems Studies

A first step in this design refinement was to revise the TF34 engine cycle data using the more exact results of the ground test nacelle design and performance study. Mixer nozzle jet area was sized at a minimum value of .68m^2 (1000 $in.^2$) to avoid significantly changing the takeoff fan operating line.

It was anticipated that changes to the acoustic treatment during the course of the test program would result in changes in ducting pressure losses. To account for these changes and to account for uncertainties in nozzle flow coefficient, nozzle area trim capability had to be designed into this hardware. The studies to define the range of this trim capability consisted of estimating minimum and maximum ducting loss values around the nominal, and permitting the resulting area change needed to hold the fan operating point. The ducting, nozzle and other loss values used in the study are tabulated in Figure 41. Estimates for a flight installation have been included for purposes of comparison. A significant difference between flight and ground test conditions will be the flight installation requirements for bleed and horsepower extraction. The influence of these effects is readily accounted for.

The input of these loss estimates on the important engine and mixer nozzle parameters is shown in Figure 42. These results indicate that consideration has been given to reducing mixer nozzle velocity decay requirements by reducing exhaust velocity by increasing nozzle area. A system study was conducted to explore this possibility. Nozzle areas 10, 20, 40 and 60 percent greater than the nominal value were considered. The resulting reductions in exhaust velocity are shown in Figure 43. The two limiting conditions shown were set by fan operating constraints. At sea level, maximum power, where nozzle area might be increased by 25%, gives approximately a 15% reduction in exhaust velocity before running into overly difficult fan operating conditions. Cruise operating conditions will not permit more than a 10% increase before running into the same problems. A variable area nozzle would be required to use more than a 10% increase in jet area. Cruise thrust drops off very quickly with increasing nozzle jet area. The trend data shown in Figure 44 indicates that a 4% increase in cruise nozzle area would provide the same amount of thrust loss as the external mixer.

The area trim capability required for variations in acoustic treatment and uncertainties in predicting nozzle discharge coefficients, is approximately the same as the area changes considered practical for reducing exhaust velocity. These systems studies led to the conclusion that trimming nozzle area (A_8), and fan duct area at the internal mixer exhaust, A_{27}, 850 and 450 cm^2 (130 and 70 square inches) respectively, should satisfy a practical range of test conditions.

Mixer Nozzle Flowpath and Performance

The locations at which the test nozzle flowpaths started were specified as a flange on the fan case at station 232.3, and a flange on the turbine exhaust duct at station 256.9. Special care was taken in selecting flowpath contours that would permit maximum interchangeability of common parts for all four exhaust systems:

1. The separate flow nozzles (nacelle design study).
2. The 12-lobe mixer nozzle.
3. The reference convergent nozzle.
4. The alternate reference convergent nozzle.

The schematic sketches in Figures 45 and 46 illustrate how the parts of the 12-lobe mixer nozzle, a single conical external cowl duct, and a simple internal splitter can be interchanged to give four different test configurations. The combination of an external mixer with no internal mixer is considered to be a potentially interesting configuration. There is a possibility that the external mixer may stimulate sufficient mixing between the fan and the turbine exhausts that an internal mixer may not be necessary. The flexibility to readily test this configuration has been designed into this test hardware.

The distance of 68 cm (26.7 inches) from the internal mixer exhaust plane to the nozzle exit plane (for all three designs) was selected to give a 60% mixing effectiveness for the reference convergent nozzle. This amount of mixing has been found to give a good balance between the performance gains, and the length and weight of mixers for STOL engine installations.

BASE CONFIGURATION

- EXTERNAL MIXER
- INTERNAL MIXER

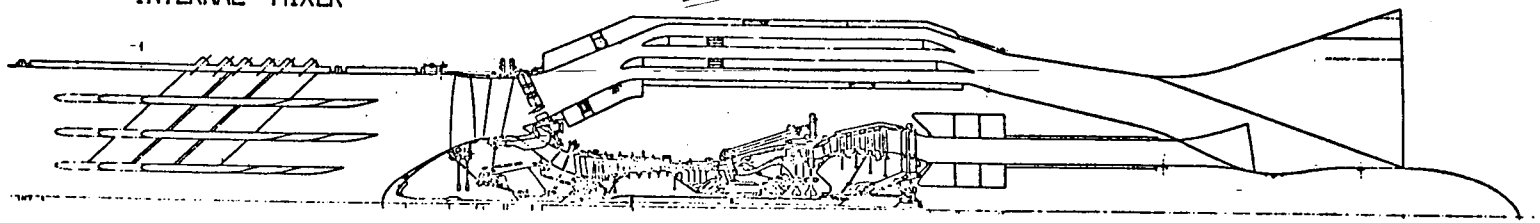

REF. CONFIGURATION

- CONVERGENT NOZZLE
- INTERNAL MIXER

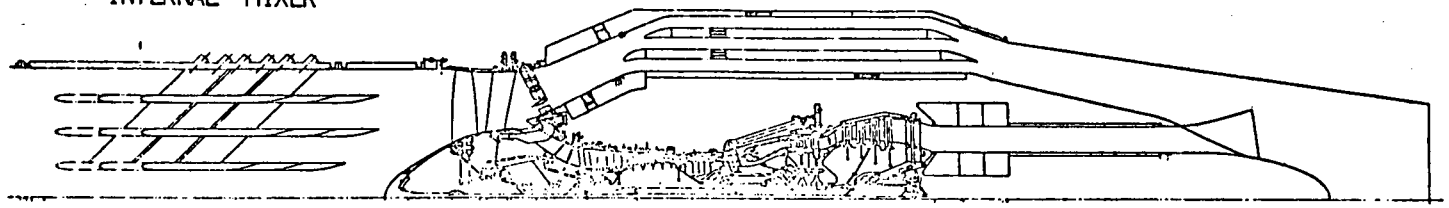

ALT. REF. CONFIGURATION

- CONVERGENT NOZZLE
- INTERNAL "FREE MIXER"

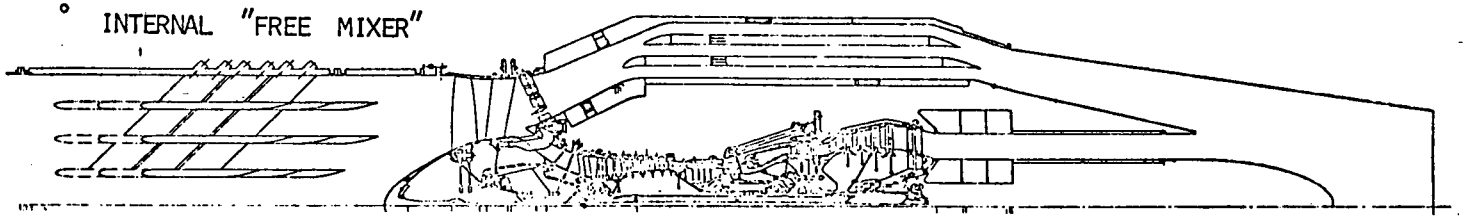

Figure 40. Ground Test Mixer Configurations.

Pressure Loss, ΔP/P	GROUND TEST CONFIGURATIONS						FLIGHT CONFIGURATION
	Base Internal Mixer External Mixer		Reference Internal Mixer Convergent Nozzle		Alternate Reference Free Mixer Convergent Nozzle		Base Internal Mixer External Mixer
	Nom.	+/-	Nom.	+/-	Nom.	+/-	Nom.
Inlet	0.02	0.03/0.015	0.02	0.03/0.015	0.02	0.03/0.015	0.02
Fan Exhaust	0.05	0.08/0.04	0.05	0.08/0.04	0.05	0.08/0.04	0.042
Fan Internal Mixer	0.065	0.10/0.05	0.065	0.10/0.05	-	-	0.065
External Mixer	0.01	0.008/0.02	-	-	-	-	0.010
Turbine Exhaust	0.009	0.023/0.005	0.009	0.023/0.005	0.009	0.023/0.005	0.007
Turbine Internal Mixer	0.014	0.023/0.009	0.014	0.023/0.009	-	-	0.014
Nozzle Velocity Coefficient, C_v	0.995	-	0.995	-	0.995	-	0.993
Extraction: Bleed Kg/s (lb/s)	-	-	-	-	-	-	0.227 (0.5)
Power Watts (HP)	-	-	-	-	-	-	18650 (25)
Mixing Effectiveness, %	60	60+	60	60	12.5	12.5	60

Figure 41. Duct Loss Estimates.

	Base Internal Mixer External Mixer Nom	+/-	Reference Internal Mixer Convergent Nozzle Nom	+/-	Alternate Mixer Free Mixer Convergent Nozzle Nom	+/-
Static thrust, F_n, lb	7 990	8550/7750	8028	8590/7787	8028	8590/7787
Airflow, lb/sec	330	353/320	330	353/320	330	353/320
Jet velocity 100% F_n, ft/sec	810	866/785	813	870/788	766.7 (1) 1142 (2)	820/744 1222/1107
Jet velocity 60% F_n, ft/sec	606.3	648/588	609	652/590.8	601.7 (1) 794 (1)	634/584 849/770
Areas						
Exhaust, ft^2	7.05	7.26/6.55	6.98	7.2/6.5	6.68	6.87/6.21
Mixer hot side, ft^2	1.77	-	1.77	-	1.77	-
Mixer cold side, ft^2	6.14	6.3/5.7	6.14	6.3/5.7	6.14	6.3/5.7

(1) Undiluted cold stream

(2) Undiluted hot stream

Figure 42. Ground Test Configurations (FPS Units).

	Base Internal Mixer External Mixer		Reference Internal Mixer Convergent Nozzle		Alternate Mixer Free Mixer Convergent Nozzle	
	Nom	+/-	Nom	+/-	Nom	+/-
Static thrust, F_n, N	35541	38029/34475	35710	38210/34639	35710	38210/34639
Airflow, Kg/s	149.6	160.1/145.1	149.6	160.1/145.1	149.6	160.1/145.1
Jet velocity 100% F_n, m/s	246.7	263.9/239.3	247.9	265.2/240.4	233.7(1) 348.1(2)	250.0/226.8 372.4/337.6
Jet velocity 60% F_n, m/s	184.8	197.7/179.2	185.7	198.7/180.1	183.4(1) 241.9(2)	196.2/178.0 258.8/234.6
Areas						
Exhaust, m^2	.655	.675/.609	.649	.669/604	.621	.639/.577
Mixer hot side, m^2	.165	-	.165	-	.165	-
Mixer cold side, m^2	.570	.586/.530	.570	.586/.530	.570	.586/.530

(1) Undiluted cold stream

(2) Undiluted hot stream

Figure 42. Ground Test Configurations, S.I. Units (Concluded).

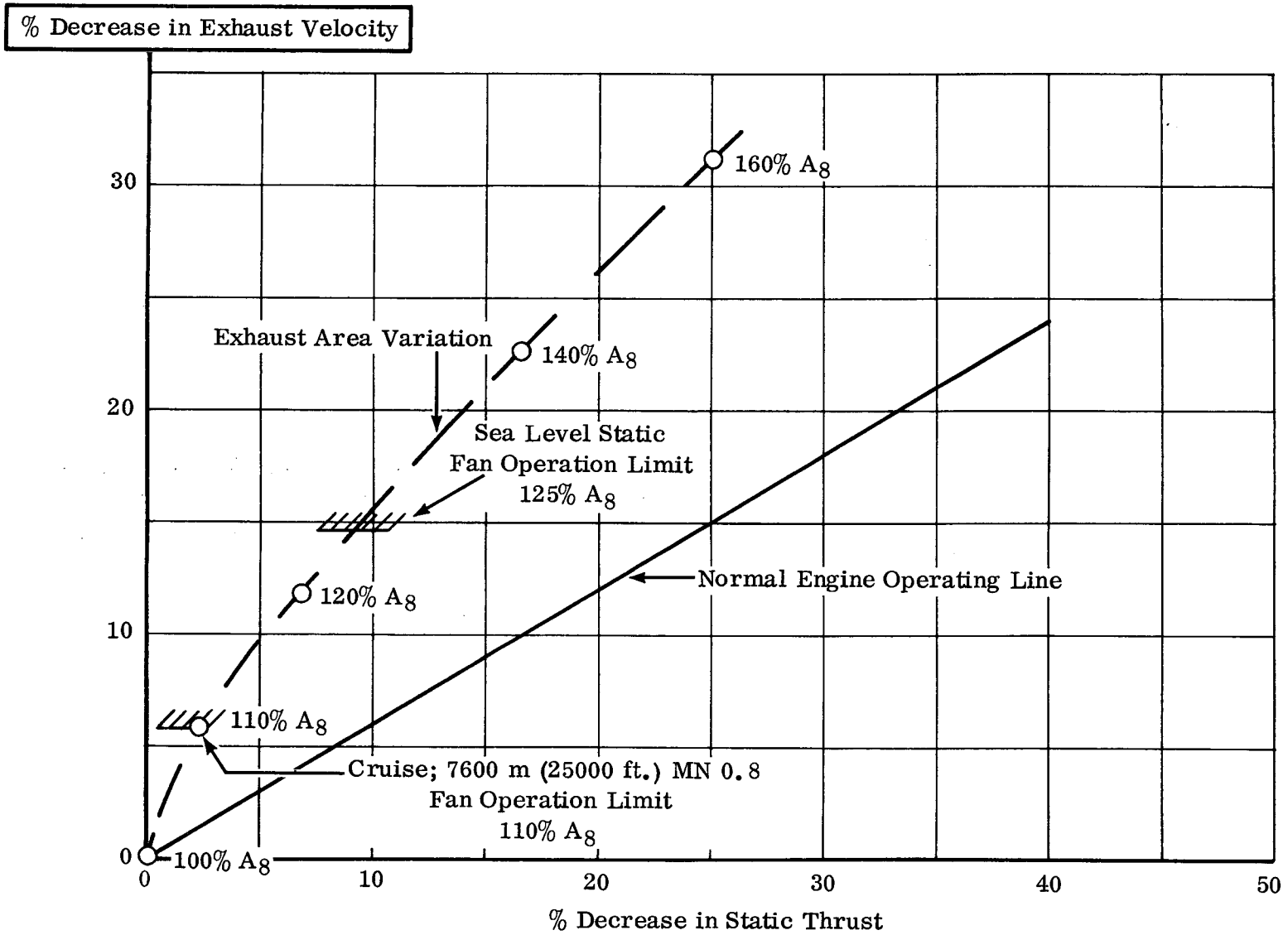

Figure 43. Influence of Increased Nozzle Area, A_{8_f} on Exhaust Velocity & Thrust.

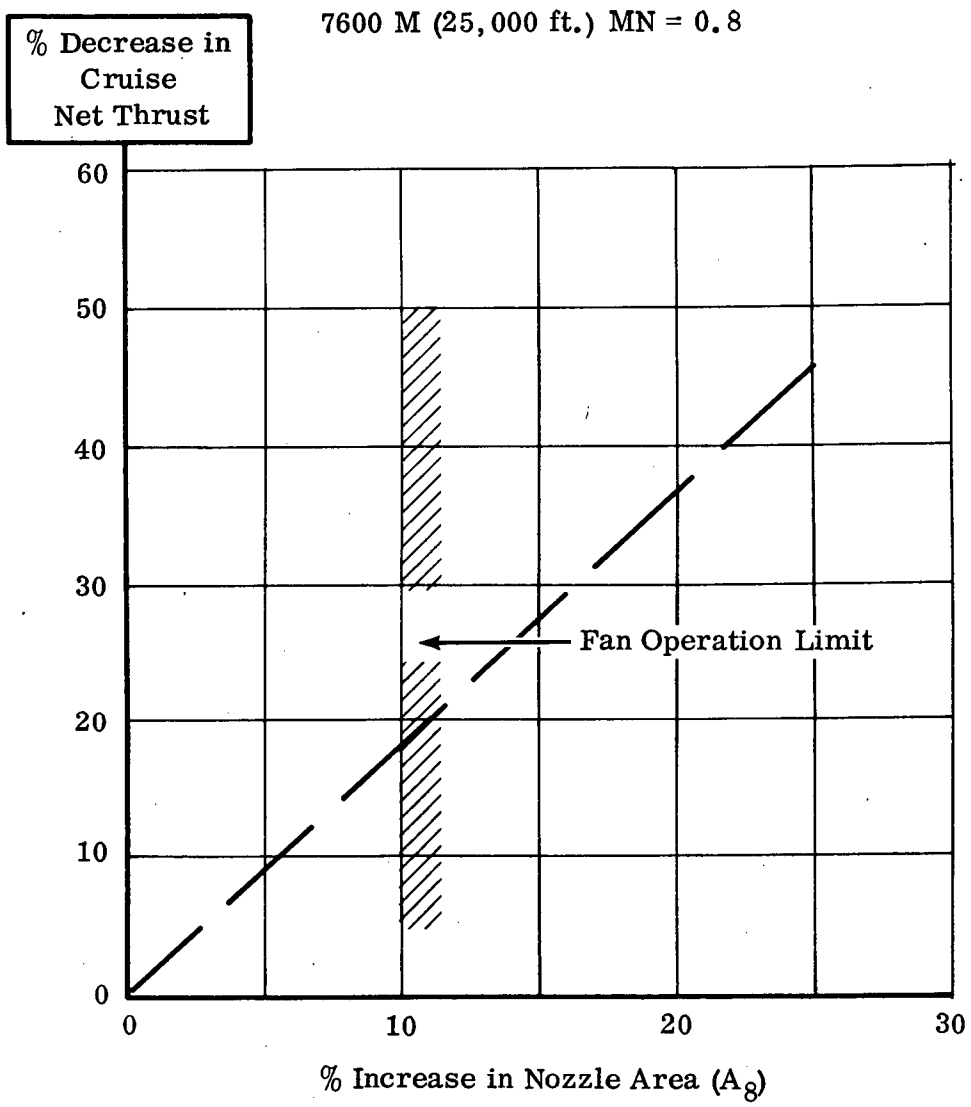

Figure 44. Influence of Increased Nozzle Area, A_8, on Cruise Net Thrust.

The mixing effectiveness parameter K_4^1 used in this study is defined as follows:

$$K_4^1 = \frac{T_P - T_U}{T_F - T_U} \times 100 \quad \text{where} \quad K_4^1 = K_4 (1 + \sin \theta) \quad \text{(See Figure 4}$$

T_P = partially mixed thrust

T_U = unmixed thrust = sum of the thrusts of the separate core stream and fan stream

T_F = 100% mixed thrust

θ = injection angle of core stream flow

The terms of the interface area function, PL/D^2, are defined as follows:

P = the perimeter of the mixer at the mixing plane

L = the mixing length = distance from mixing plane to exhaust plane

D = equivalent diameter of a circle of area equal to the total flow area at the mixing plane

The presence of the large 12-lobe external mixer is expected to influence internal mixing effectiveness. The magnitude of this influence is not known at this point.

The flowpath and performance guidelines used in defining the internal mixer were based on a broad background of model test experience and mixed flow STOL engine design study experience.

The more important of these guidelines include:

- Core stream entrance Mach $\approx$ .4 (design = .43)
- Flow area from mixer entrance to exit should converge
- Plug radius should be constant through the mixer
- The locus of points describing the lobe troughs should be a straight line not exceeding an angle of .35 rad (20°), (design = .27 rad (15.4°))
- The locus of points describing the outer lobe contour should not exceed an angle of .3 rad (17°) (design .25 rad (14.0))
- The fan stream entrance station Mach number should $\approx$ .43 - .46 (design = .45)
- There should be a slight convergence from the entrance station to the mixing plane on the fan stream side of the mixer.

The area distribution through the internal mixer is shown in Figure 47.

Partial Mixer With External Mixer

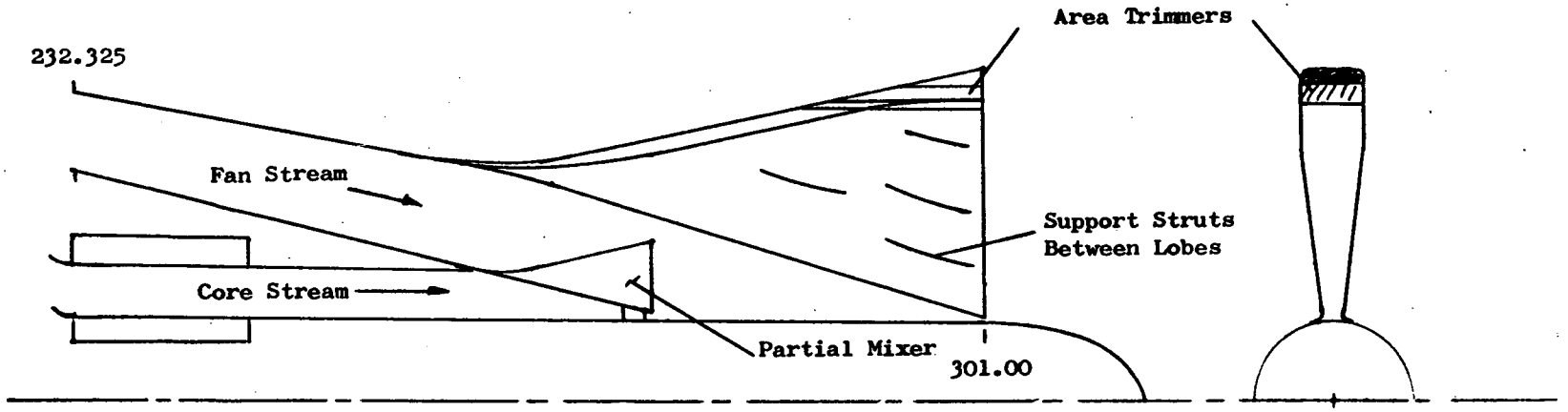

Partial Mixer With Standard Nozzle

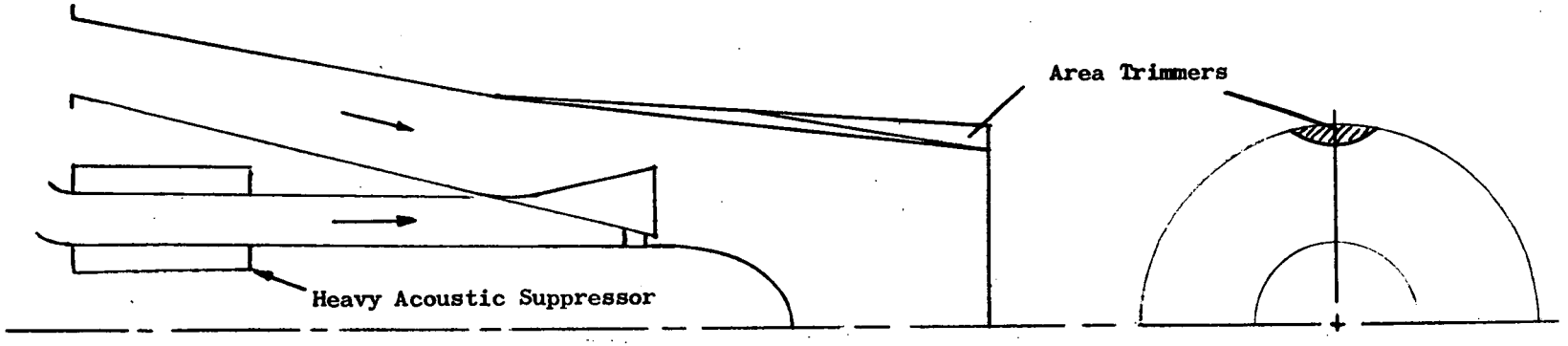

Figure 45. Partial Mixer Schematic Sketches.

Free Mixer With External Mixer

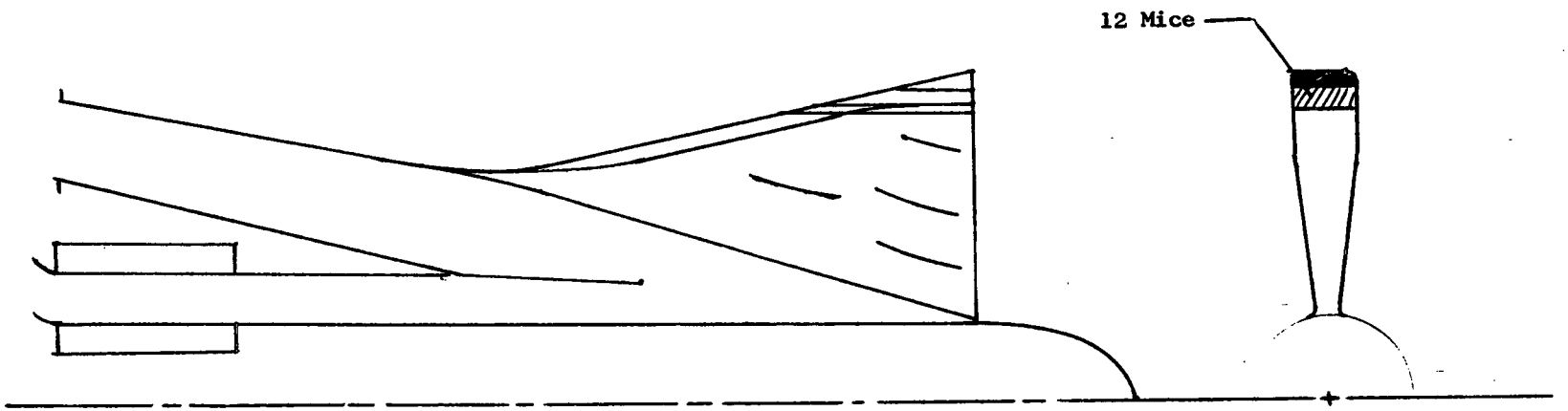

Free Mixer With Standard Nozzle

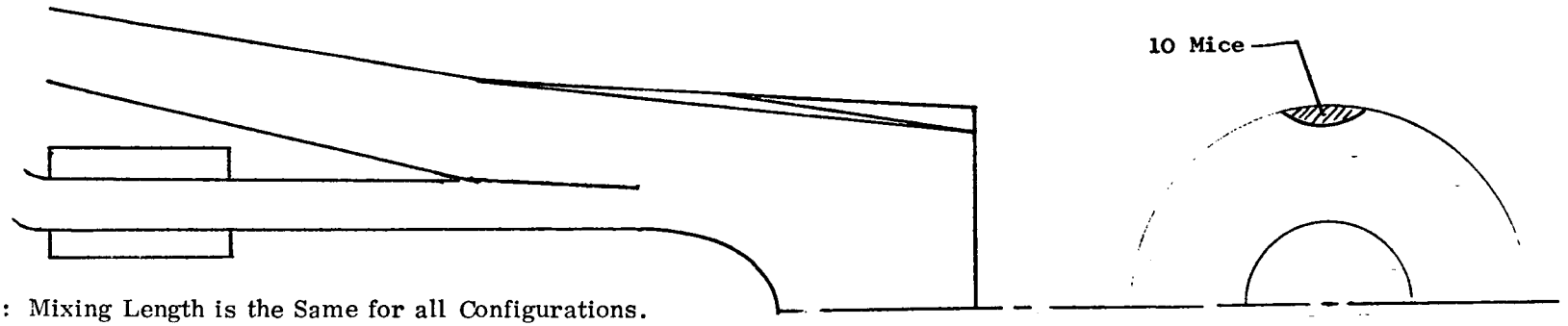

NOTE: Mixing Length is the Same for all Configurations.

Figure 46. Free Mixer Schematic Sketches.

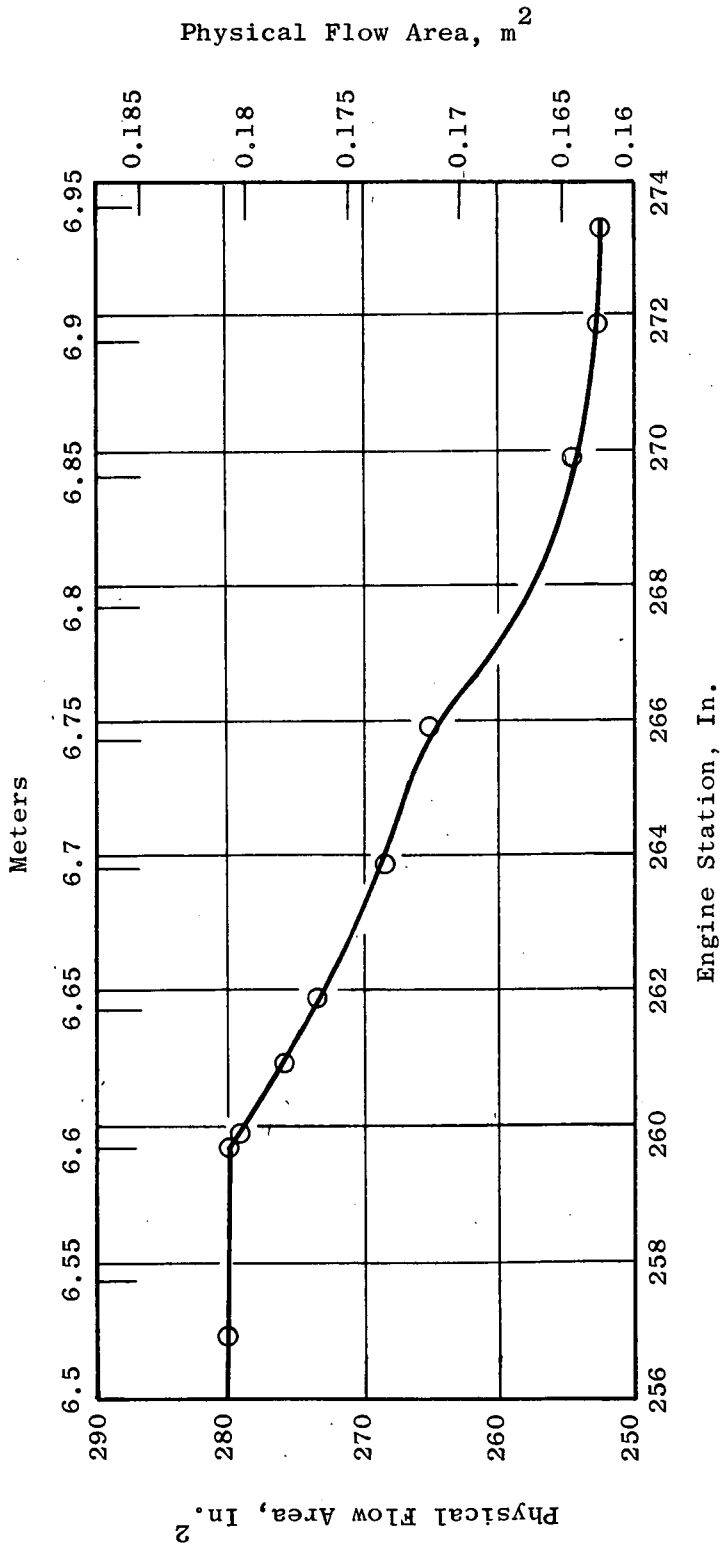

Figure 47. TF34 Internal Mixer Flow Area Distribution.

The flowpath design guidelines used for the external mixer included the following:

- Proper maximum flow areas at mixing and exhaust plane
- Convergence in the tailpipe
- Minimal steps and gaps
- Gradual turning to avoid separation
- Mild diffusers, if necessary
- Reasonable flow area distributions

Early in this design it was thought that turning vanes might be required in the lobes flowpath at the outer corner where the lobes begin to develop. However, a simple boundary layer analysis verified that there was no chance of separation mainly because of the flow area convergence through that section. Figure 48 shows the flow area distribution for the mixer.

The pressure drops for the exhaust system configurations were estimated using the flat plate friction equation corrected for compressibility as listed below:

$$C_f\Big|_{m=o} = \frac{.455}{(\text{Log RN})^{2.58}} \qquad \text{(Turbulent, Prandtl-Schlichting)}$$

$$C_f/C_f\Big|_{m=o} = \left(1 + \frac{\gamma - 1}{2} M^2\right)^{-.467} \qquad \text{(Frankl-Voishel)}$$

Drag was converted to pressure drop using:

$$\Delta P_T/P_T = \frac{\text{Drag}}{P_T A_{flow}} = \frac{C_f \; q \; A_{wetted}}{P_T \quad A_{flow}}$$

where the values of flow area and dynamic pressure used were the averages for the duct section under consideration. All losses calculated aft of station 256.9 were increased 10% to account for turning, steps, gaps, roughness, and any diffusion. Mixing effectiveness was determined using T.H. Frost's correlation shown in Figure 49. A summary of the calculated losses and a sketch showing the sectional breakdown of the exhaust system is provided in Figure 50.

Mixer Nozzle Exhaust Velocity Profiles

To serve as an additional guide in estimating flap interaction noise, the exhaust velocity profile at a 2.85 m (112") flap spacing was estimated. This estimate was based primarily on General Electric exhaust flow field profile data measured on 8- and 18- lobe mixer nozzles. The small islands of velocity equal to 0.67 rather than 0.63 of the exhaust velocity are considered to be an item of concern but are not large enough to warrant a change in flap noise or velocity decay predictions. (See Figure 51).

There is no applicable test data nor analysis procedure available at this point on which to base a reliable estimate of the velocity profiles. However, it is anticipated that exhaust velocity profiles should be relatively uniform.

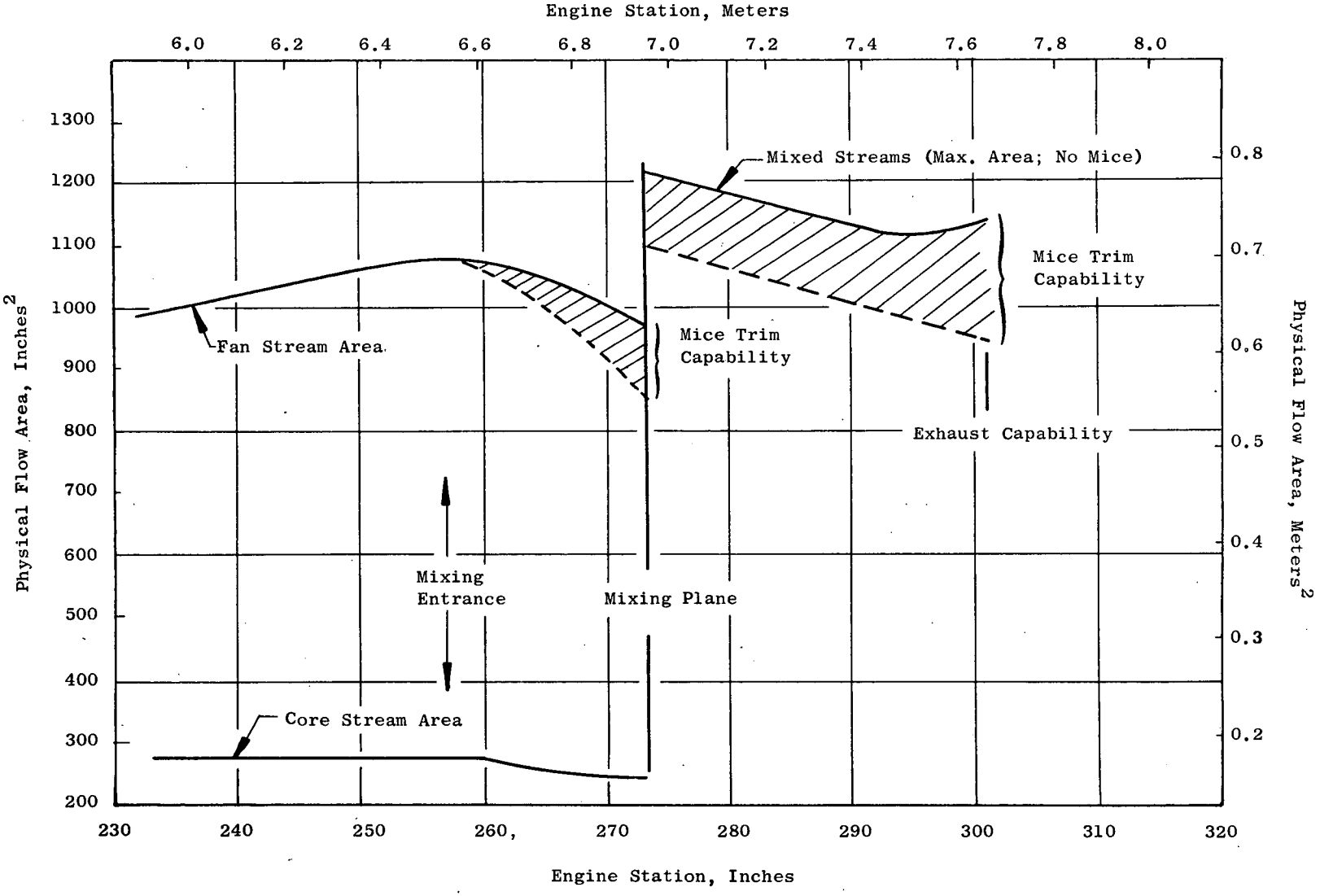

Figure 48. TF34 Ground Test Mixer/Decayer Flow Area Distribution.

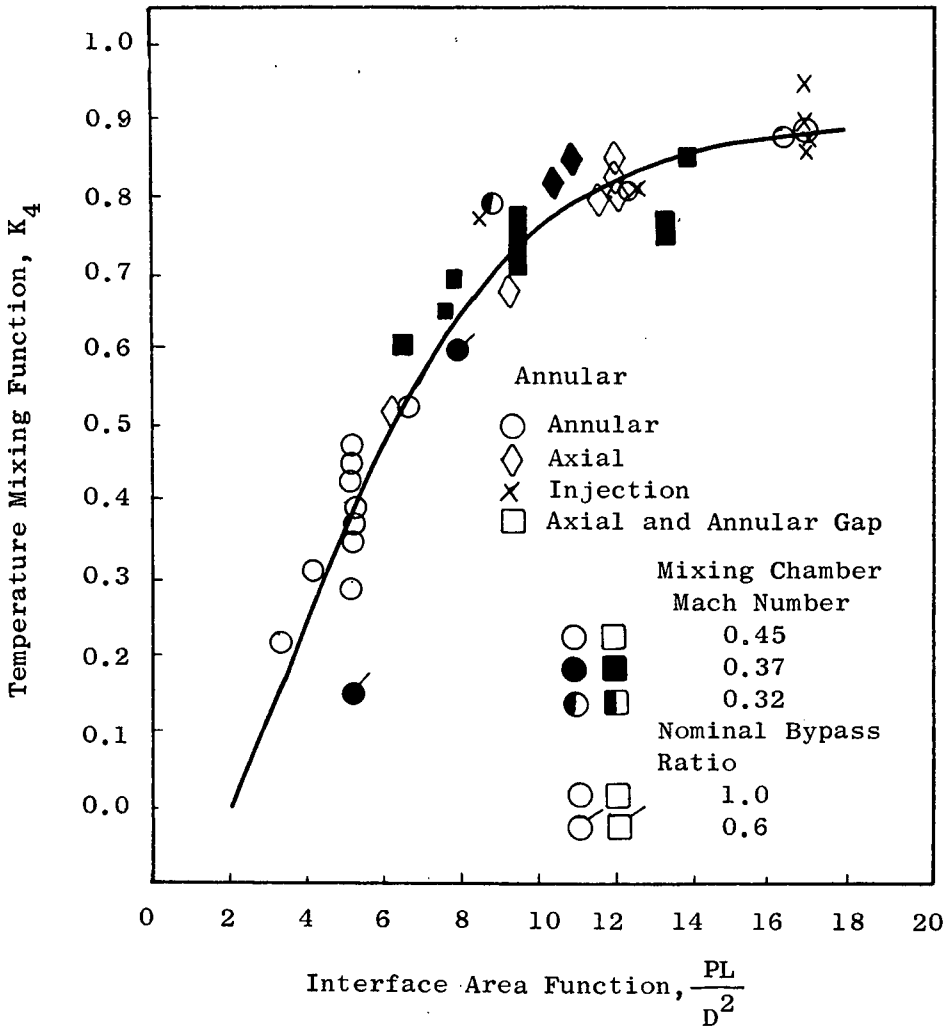

Figure 49. Mixing Effectiveness T.H. Frost Curve and Test Data.

Section	Stations		N/m^2 q ref. (psi)		With Decayer $\Delta P_T/q$	A_{wet} m^2 (ft^2)	With Standard Nozzle $\Delta P_T/q$	A_{wet} m^2 (ft^2)
1F	232.3	256.9	16962	(2.46)	.017	4.25 (45.7)	.017	4.25 (45.7)
2F	256.9	273.3	15169	(2.2)	.030	4.20 (45.3)	.0188	2.63 (28.3)
M	273.3	301.0	23443	(3.4)	.058	9.88 (106.4)	.013	2.55 (27.5)
1C	-	256.9		-	.036		.036	
2C	256.9	273.3	15403	(2.234	.040		.040	

- External plug drag for decayer configuration = 3.0 kg (6.7 lb) (A_{wet} = .3m^2 (3.2 ft^2))
- Partial mixer effectiveness = 60%
- Free mixer effectiveness = 12.5%

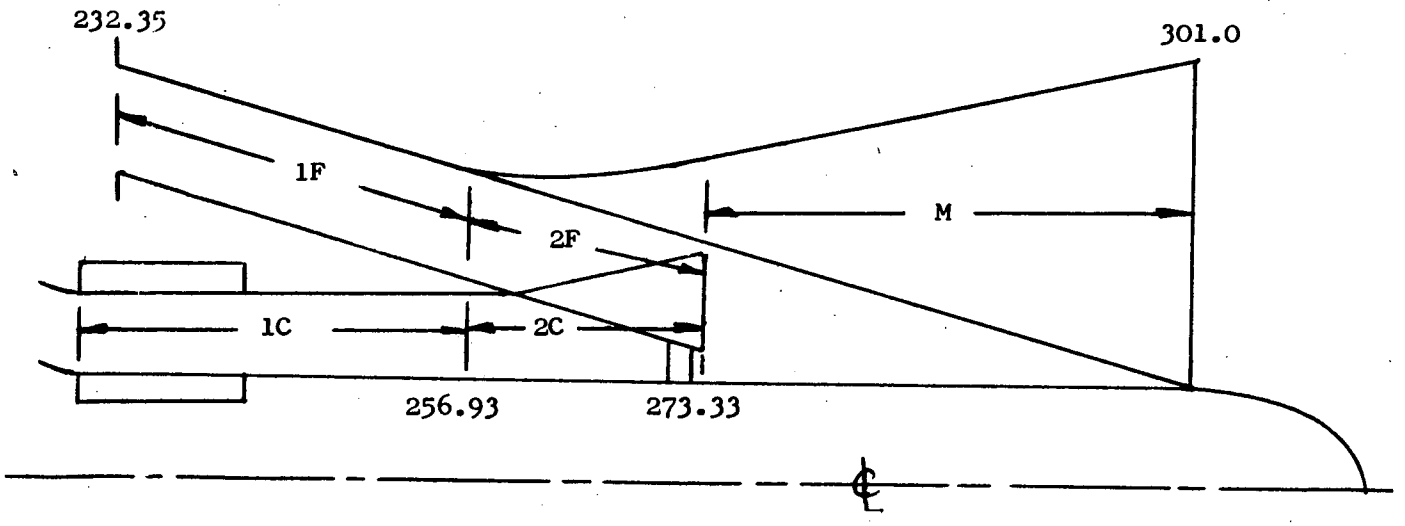

Figure 50. Summary - Nozzle Losses.

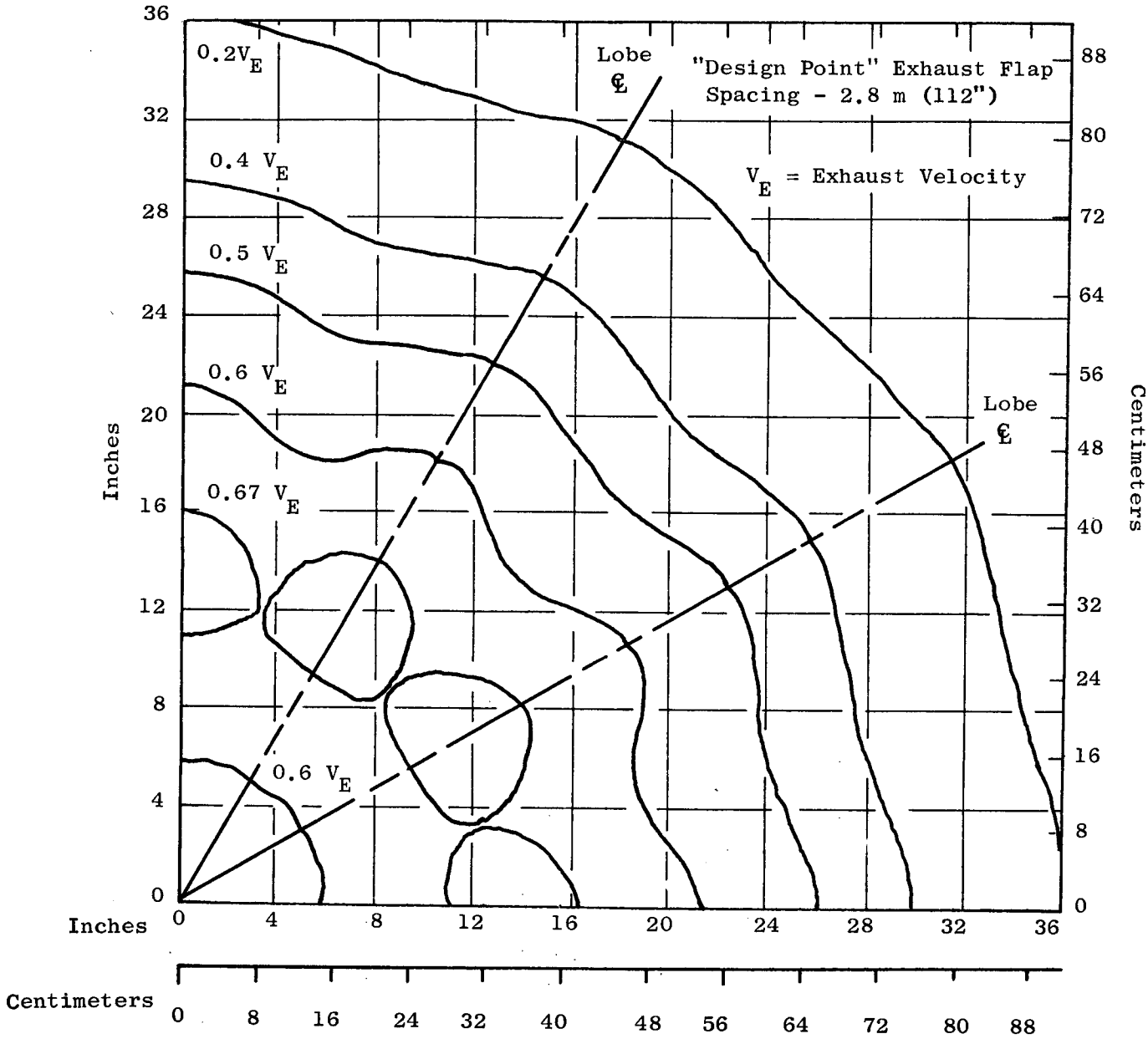

Figure 51. Ground Test Flap Impingement Flow Velocity Profiles (Base Configuration).

In-Flight Effects on Velocity Decay

The influence of flight velocities on velocity decay is another area in which there is very little applicable information. A simplified calculation procedure, based on the reduced relative velocity of the exhaust jet to the surrounding flow, has been formulated. Using this approach, a correlation faction was applied to the static velocity decay estimates made for the 12-lob mixer nozzle. The results shown in Figure 52 point toward a significant reduction in velocity decay at a typical takeoff flight Mach number of 0.15.

The impact of reduced in-flight velocity decay on flap interaction noise is not at all clear.

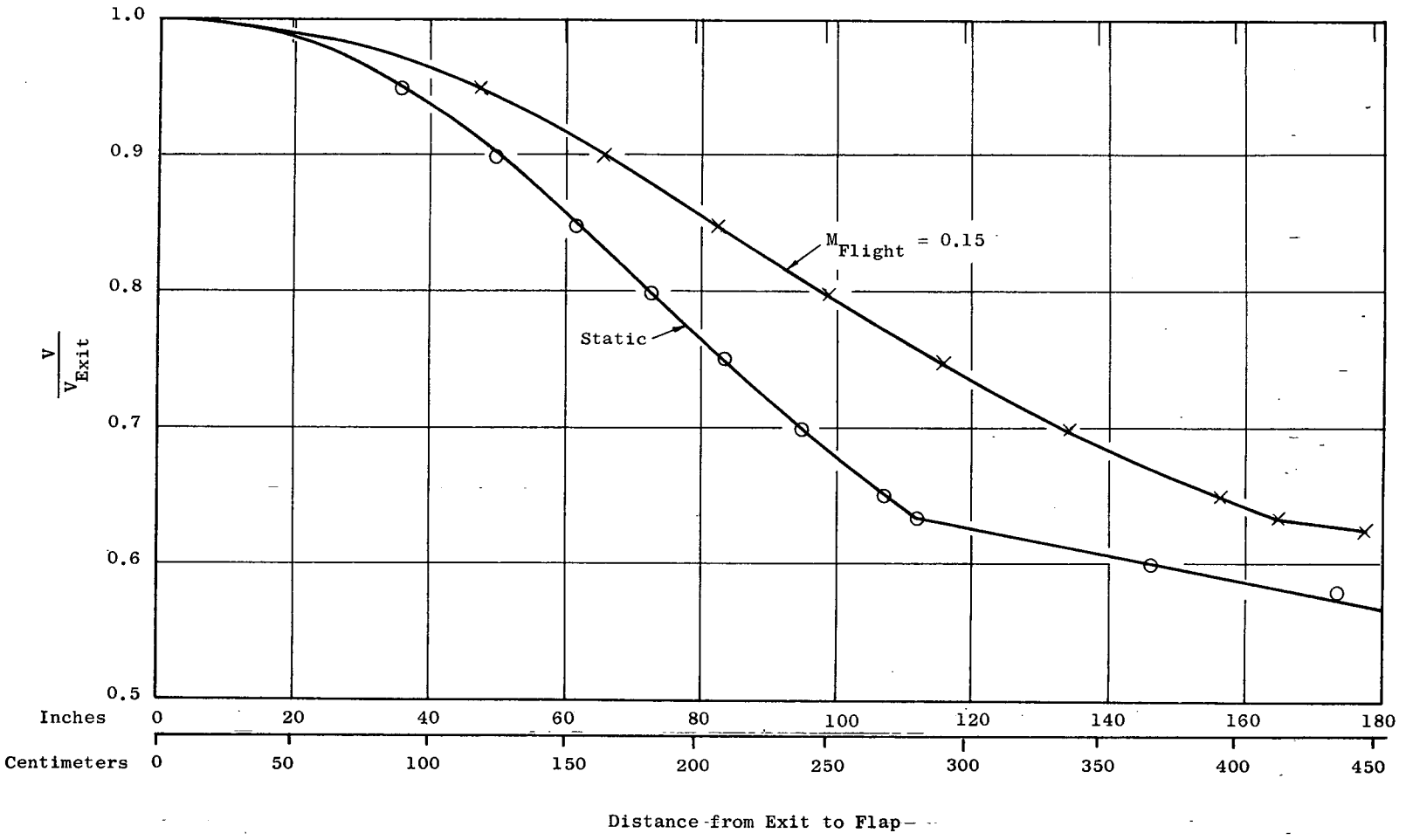

Figure 52. Flight Concept, Potential Inflight Effects on Flap Impingement Velocity.

Flap and Jet Noise Prediction

The flap interaction and jet noise prediction procedure developed during Task I was thoroughly reviewed for possible refinement during Task II. This review, based on scale model and full-scale engine preliminary test results, produced new insight into the sources of flap interaction noise. A tentative list of the four most important noise sources is shown in Figure 53. If EBF noise reduction is to be achieved by decaying the exhaust velocity at the flap impingement point, then proper attention must be paid to each of the other sources listed on Figure 53. For example, the "free jet noise" is produced by the undeflected portion of the flow. Scale model tests have shown that multi-lobe nozzles which are good "decayers" can produce more free jet noise than a conical nozzle. This phenomenon is especially important at exit velocities less than 300 m/s (1000 ft/sec.) Similarly the noise produced by the high velocity flow scrubbing the wing surface can be increased with the decayer, if the scrubbed area is increased substantially without attendant reductions in the scrubbing gas velocity.

There may be other identifiable sources which will be discovered with additional tests and analyses, but the review conducted for Task II came to the conclusion that if care is taken to minimize these "other sources" by proper design then the noise trend curves developed during Task I should still be applicable, within an uncertainty band of +3, -2 PNdB.

These trend curves for takeoff and approach noise are shown in Figures 54 and 55.

These figures show the revised exhaust velocity values for both mixer and reference nozzle designs. At takeoff power conditions, the selected 12-lobe mixer nozzle design will produce approximately 94 PNdB, 2 dB more than the design goal. However, at approach this design will generate approximately 2 dB less than the design goal.

Additional detailed information on this flap interaction noise prediction procedure plus three sample calculations are included. A table presenting a comparison between the static and flight jet noise levels at takeoff is shown on Figure 56. These parameters and the methods for determining the effects of each are as follows:

1. Extra Ground Attenuation Effects (EGA) - Were calculated for the static case using the SAE relationships for a 59°F, 70% relative humidity day. However, the EGA effects for the flight case were calculated assuming that this extra amount of ground attenuation would occur only in the 30 m (100 ft) layer next to the ground plane (Reference 35).

2. Number of Engines - ΔPNdB = 10 Log N
   Where N is the number of engines (Reference 34).

3. External Blown Flap Noise - The effect of this contribution was determined from a survey of existing literature (References 7, 8, and 21).

4. View Factor - Determined using the results presented in Reference 7.

5. Engine Shielding Effects - Calculated using the recommended SAE procedure.

   $$\Delta PNdB = 5 \text{ Log } N$$

   Where N is the number of engines (Reference 34).

- FREE JET NOISE - INCREASE CAN BE MINIMIZED BY PROPER LOBE DESIGN & NUMBER
- WING SCRUBBING NOISE - CAN BE MINIMIZED BY TAILORING EXHAUST SHAPE AND LOCATION TO MINIMIZE SCRUBBED SURFACE AREA
- FLAP IMPINGEMENT NOISE - PRIMARILY LOW FREQUENCY, HIGHLY DIRECTIONAL. SIGNIFICANT REDUCTIONS EXPECTED WITH EXTERNAL MIXER
- DEFLECTED JET NOISE - SIGNIFICANT REDUCTIONS EXPECTED WITH EXTERNAL MIXER

Figure 53. Current Thinking on Design Guides to Minimize 4 Sources of Exhaust/Wing - Flap Noise.

4 Engines

150 M (500 Ft) Sideline

60 M (200 Ft) Altitude

Peak PNL's

Full Relative Velocity Effect

Flight Speed 50 M/S (100 Knots)

.52 Rad. (30°) Flap Angle

No EGA Included

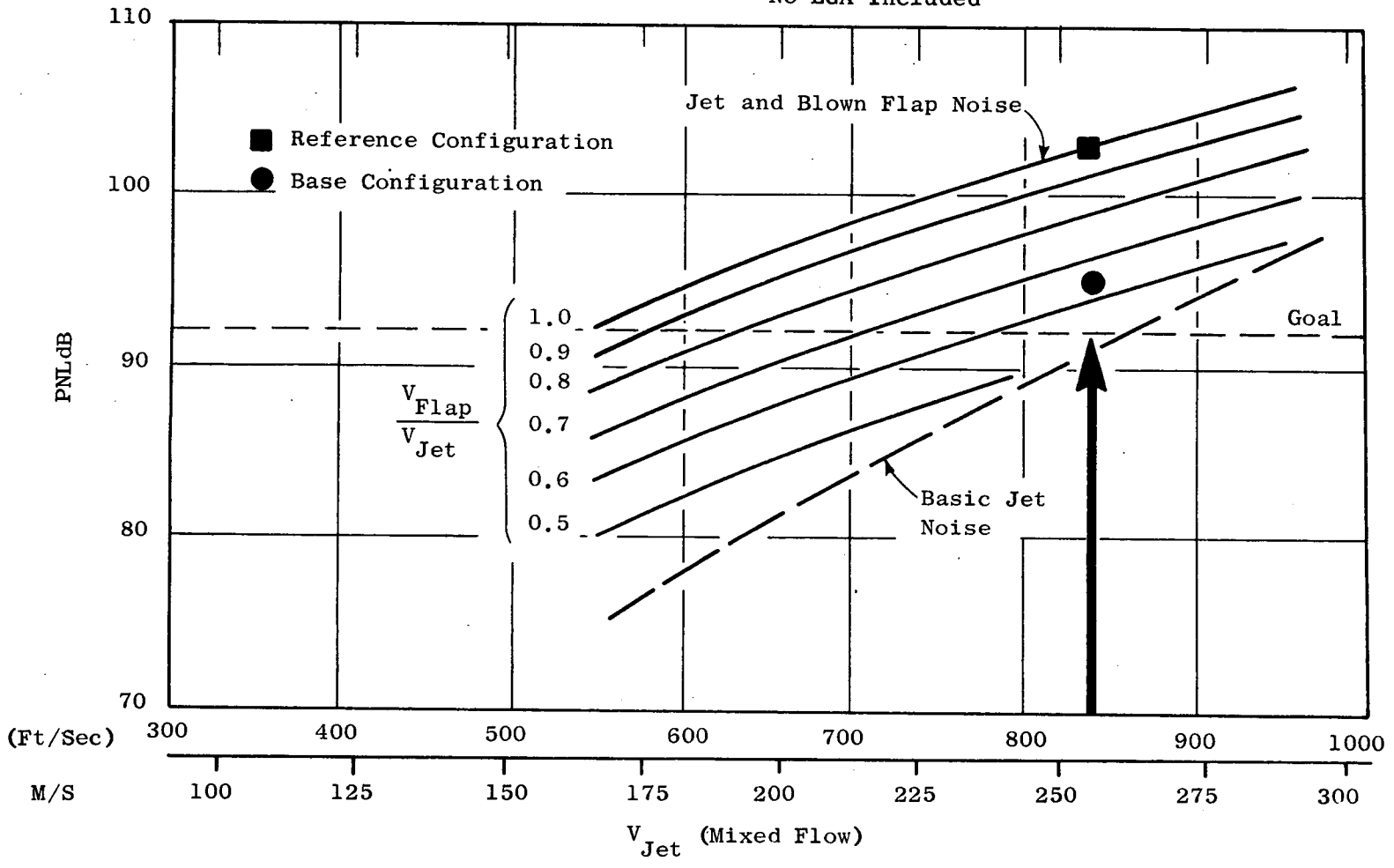

Figure 54. Takeoff Flap Impingment Noise Trends.

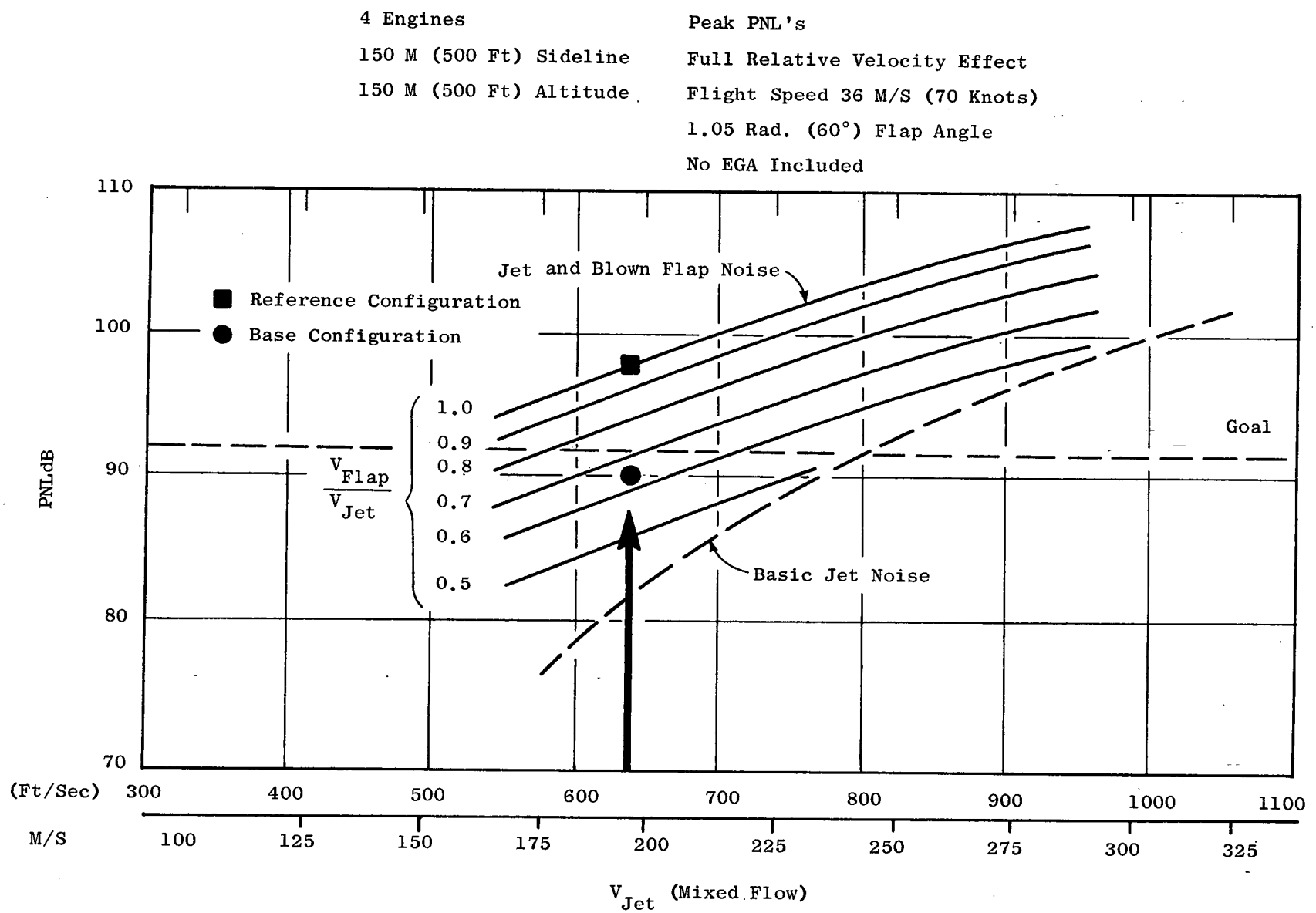

Figure 55. Approach Flap Impingement Noise Trends.

- Takeoff Power Setting
- 288 °K (59 °F) 70% Relative Humidity - Standard Day
- $V_{flap}/V_{jet} = 1.0$

STATIC NOISE LEVELS

Mixed Flow Velocity	150m (500') Sideline Single Engine Peak PNdB with EGA	4 Engines	EBF Contribution	View Factor Correction to EBF Noise	Shielding Effects	Relative Velocity Effects	Final Level
250 m/s (813 Ft/Sec)[3]	91.5	+6 dB	+10 dB	-9 dB	[1] -3 dB	(2)	95.5 PNdB

FLIGHT NOISE LEVELS

V_o = 50 m/s (100 knots)

Mixed Flow Velocity	150m (500') Sideline 60m (200') Altitude Single Engine Peak PNdB with EGA	4 Engines	EBF Contribution	View Factor Correction to EBF Noise	Shielding Effects	Relative Velocity Effects	Final Level
250 m/s (813 Ft/Sec)[3]	92.0	+6 dB	+10 dB	-8 dB	0	-8 dB	100.0 PNdB

(1) Assume this shielding effect applies to baseline and EBF noise.

(2) V_R effect applies to baseline noise only, not EBF noise.

(3) Typical jet velocity for a suppressed engine including the effects of inlet and exhaust losses from acoustic treatment. The effect of the ram pressure at 50 m/s is very small.

Figure 56. Summary of TF34 In-Flight and Static Jet Noise Levels.

6. Relative Velocity Effects -
(Reference 34)

$$80 \text{ Log } \frac{V_J - V_O}{V_J}$$

where V_J - fully expanded Jet Velocity

V_O - Flight Velocity

The problem now is to calculate the peak PNdB levels accounting for the effects of these six parameters. To explain the mechanics and assumptions of this procedure, three examples are presented.

Example 1 - Calculation of static noise levels

Conditions: V_J = 250 m/s (813 ft/sec)
.52 rad (30°) flap angle
150 m (500 ft) sideline

Peak PNdB without EGA	94.7	
with EGA	91.5	EGA effect 3.2 PNdB
4 engines	+6.0	
	97.5	
EBF Contribution	+10.0	
	107.5	
View Factor	-9.0	
	98.5	
Shielding Effects	-3.0	
Static Peak PNdB 150m (500 ft) sideline	95.5	

Example 2 - Calculation of flight noise levels

Conditions: V_j = 150 m/s (813 ft/sec)
.52 rad (30°) flap angle
150 m (500 ft) sideline - 60 m (200 ft) altitude
V_O = 50 m/s (100 knots)

Peak PNdB without EGA	93.9	
with EGA	92.0	EGA effect 1.9 PNdB
4 engines	+6.0	
Baseline Noise Level	98.0	

Assumption - relative velocity (V_R) effect applies only to baseline noise level not EBF noise.

Baseline Noise Level	98.0
V_R effect	-8.0
Baseline Noise level with relative velocity	90.0

Assumption - EBF contribution should be added to baseline noise level before relative velocity effect is taken into account.

Baseline Noise Level	98.0
EBF contribution	+10.0
	108.0
View Factor	-8.0
	100.0

This breakdown indicates that the EBF noise dominates.

The inflight peak PNdB on a 150 m (500 ft) sideline, 60 m (200 ft) altitude would be 100 PNdB

Example 3 - Presented on Figure 54 is the method recommended to predict the effect of EBF noise for the takeoff power setting. The objective of this example is to compare the results of this method with those of example 2 and explain where the differences occur.

Figure 54 - Peak PNdB = 101.9 includes - No EGA
at 250 m/s (813 ft/sec)
View Factor -8 dB
EBF Adder +10 dB

From example 2, the Peak PNdB = 100 Includes - EGA -1.9 dB
View Factor -8.0 dB
EBF Adder +10.0 dB

The conclusion of this exercise is that maximum takeoff noise may be reduced by 1.9 dB due to EGA effects. The noise trend curves used to design this external mixer may be somewhat conservative as they do not include this favorable EGA correction. It will be necessary to account for EGA effects in projecting ground test noise measurements to takeoff and approach flight conditions.

Mechanical Design Considerations

The internal and external mixer designs have been conceived to expand the use of the TF34 quiet engine separated flow ground test configuration. Figure 57, to include the following:

- Figure 58 - Engine with internal and external mixer
- Figure 59 - Engine with internal mixer and convergent nozzle
- Figure 60 - Engine with confluent internal flow and convergent nozzle

These engine configurations are designed for maximum use of common parts as indicated in Figure 65 . The major common items are listed below:

Items common to all configurations included in Figures 57 through 60.

- Acoustically-treated inlet
- Acoustically-treated fan exhaust
- Basic TF34 engine
- Inlet-engine and nacelle mounting in test stand
- Acoustically-treated core exhaust
- Exhaust centerbody
- Core exhaust duct vibration damper and attached inner fan exhaust duct forward
- of snubber.

Items common to the external mixer configuration, Figure 58 and convergent nozzle with mixer, Figure 59 .

- Internal mixer
- Inner fan flow duct

Items common to external mixer configuration, Figure 58, and confluent configuration, Figure 60 .

- Frame aft of core exhaust treatment

Items common between confluent flow configuration with mixer, Figure 57 and confluent flow without mixer, Figure 60 .

- Mixed flow exhaust nozzle

External Mixer Nozzle Mounting

The external mixer, being a ground test design is heavy, weighing in the order of 273 kg (600 lb), and is, therefore, mounted to the aft end of the quiet nacelle with additional supports to the test cell rail, Figure 61 , designed to provide axial expansion, thus minimizing the loading to the nacelle.

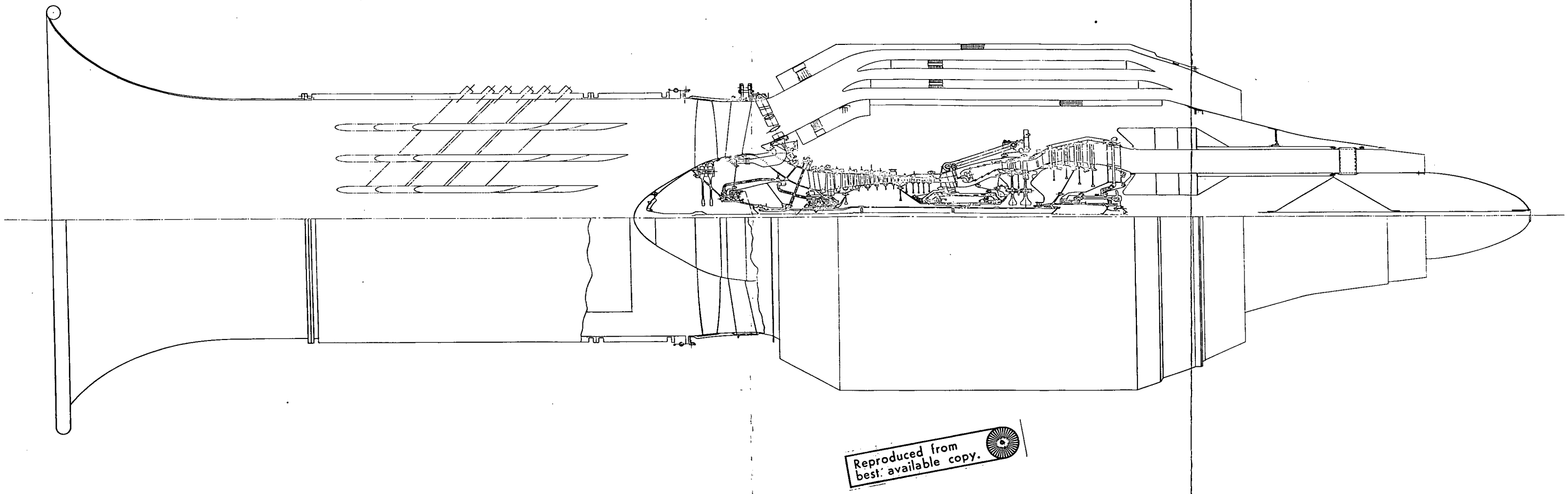

Figure 57. TF34 Engine - Separated Exhaust with NASA Acoustic Treated Inlet, Fan Exhaust and Core Exhaust.

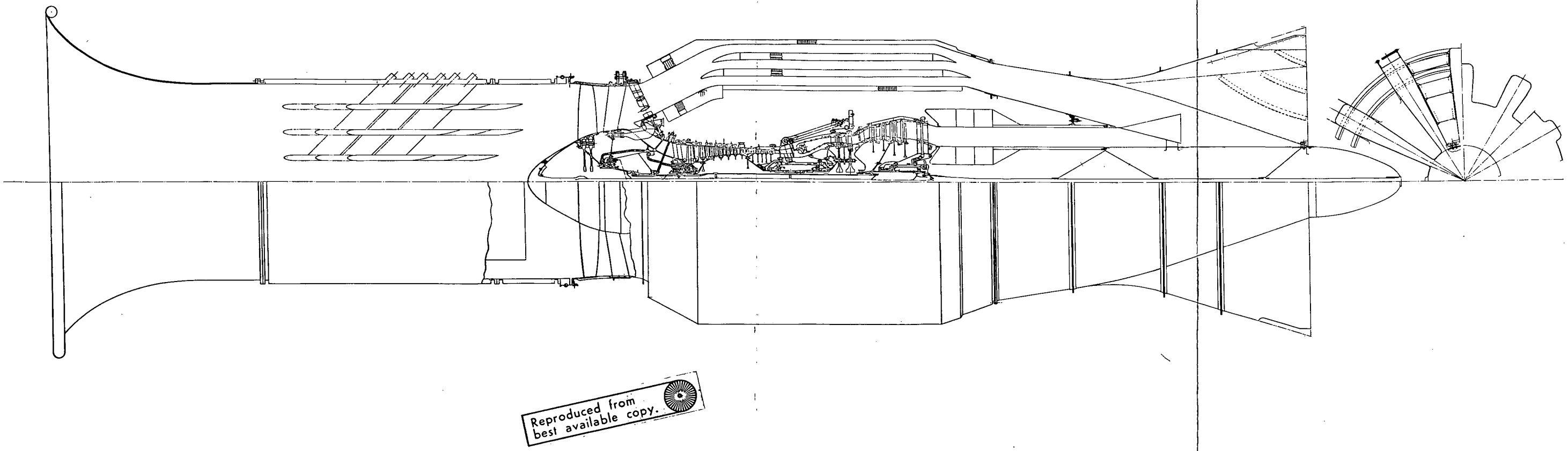

Figure 58. TF34 Engine - Mixed Exhaust with Internal and External Mixer, NASA Acoustic Treated Inlet, Fan Exhaust and Core Exhaust.

PRECEDING PAGE BLANK NOT FILMED

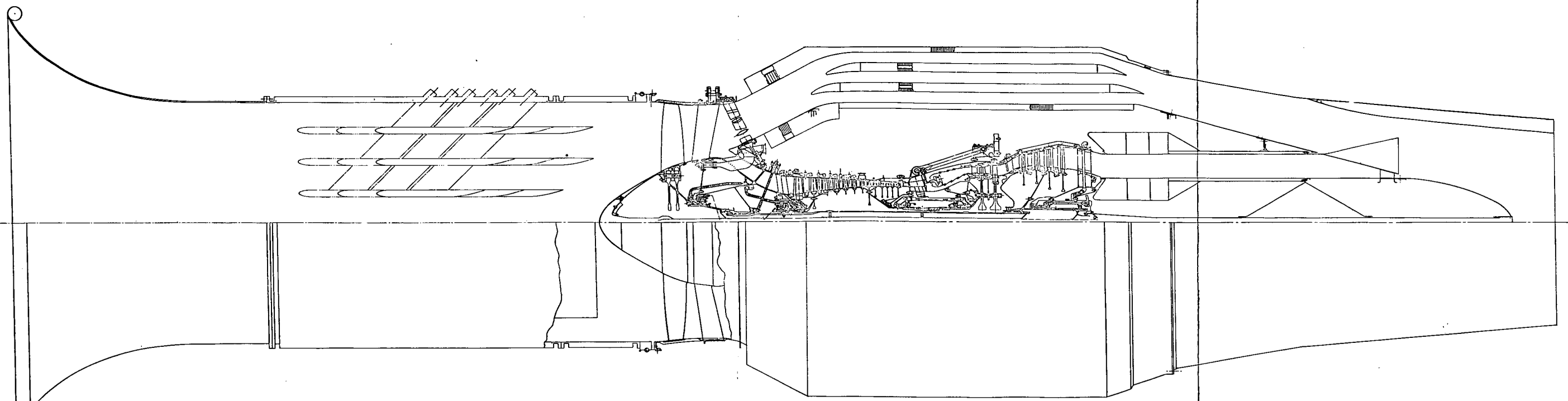

Figure 59. TF34 Engine - Mixed Exhaust with NASA Acoustic Treated Inlet, Fan Exhaust and Core Exhaust.

FOLDOUT FRAME 1

FOLDOUT FRAME 2

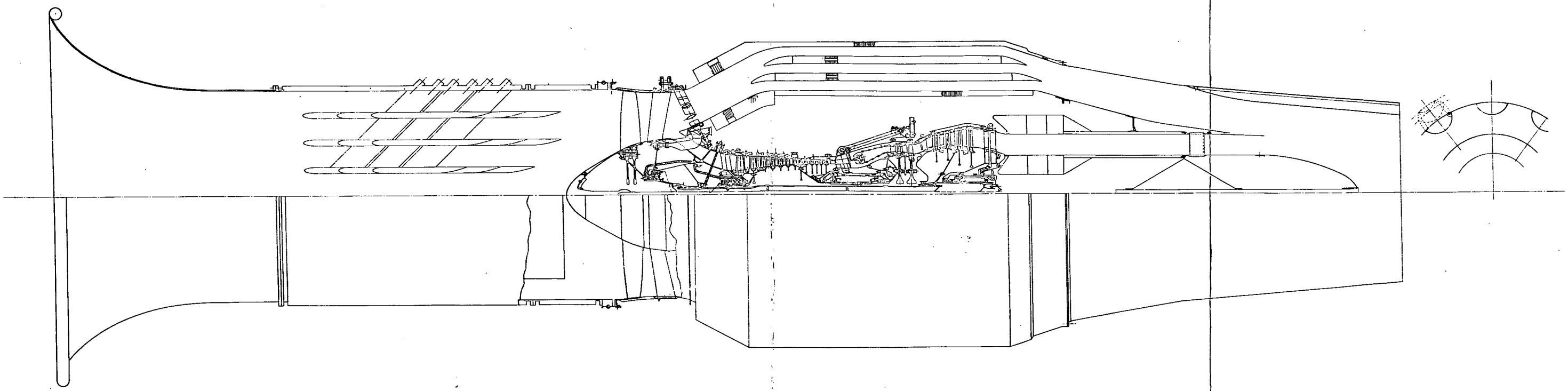

Figure 60. TF34 Engine - Confluent Exhaust with NASA Acoustic Inlet, Fan Exhaust and Core Exhaust.

Engine - Wing Test Cell Mounting

The engine mounting in the test stand with the mixer-nozzle configuration is shown in Figure 61. Special precautions have been taken to limit the loadings introduced to the TF34 engine by the heavy test items by mounting the basic engine separately. The relative position of the engine exhaust to the wing is adjustable in all required directions as shown in Figure 61 .

External Mixer

The external mixer, Figures 62 - 64, is designed to mount on the TF34 ground test nacelle at the aft flange forming a smooth flowpath to the twelve-lobe mixer nozzle. The external mixer is a carbon steel welded fabrication. An inner ring at the discharge and two outer rings maintain the mixer "round". The sides of the lobes are flat 2 mm (0.080 in.) thick sheet metal with three supports between the sides of the opposing lobes reducing the deflections and adding stability to the lobes. The flowpath is designed to accept trimmers which are used to change the flow area and to alter the circumferential flow distribution within the requirements. The lobe at 3 o'clock is radially shorter in order to allow placing the jet centerline closer to the wing.

The temperatures, velocities, maximum stress and deflection in the decayer are shown in Figure 65 . The maximum stress is 2.97×10^7 N/m^2 (4300 lb/in.^{2}) and deflection of 0.15 mm (0.006 in.) at the trailing edge with 6895 N/m^2 (1 lb/in.^{2}) Δ P. The stress and deflections are within the requirements. The natural frequency of the lobe sides was a major consideration in regard to engine resonance and vortex excitation. The decayer lobe sides will be instrumented during initial engine testing to assure the vibrations are within limits.

Internal Mixer

The internal mixer, Figure 66, is designed to mount on the aft flange of the TF34 ground test core acoustic suppressor. The decayer is a daisy type with twelve lobes fabricated from 1.3 mm (0.05") thick Inco 625 material. The 24 bolt holes in the attachment flange allows assembly of the mixer lobes in line with the external mixer lobes, or oriented 1/2 pitch, thus giving flexibility for testing two circumferential orientations of the mixer with respect to the external mixer. There is practically no pressure differential between the cold and hot sides of the lobes to produce bending stress in the lobes. The velocity and temperatures through the mixer are given in Figure 65.

Exhaust Nozzle

The exhaust nozzle, Figure 67 and 68 , is designed to replace the external mixer for either confluent flow or mixed flow by the removal of the external mixer using the same exhaust centerbody, using maximum common parts.

PRECEDING PAGE BLANK NOT FILMED

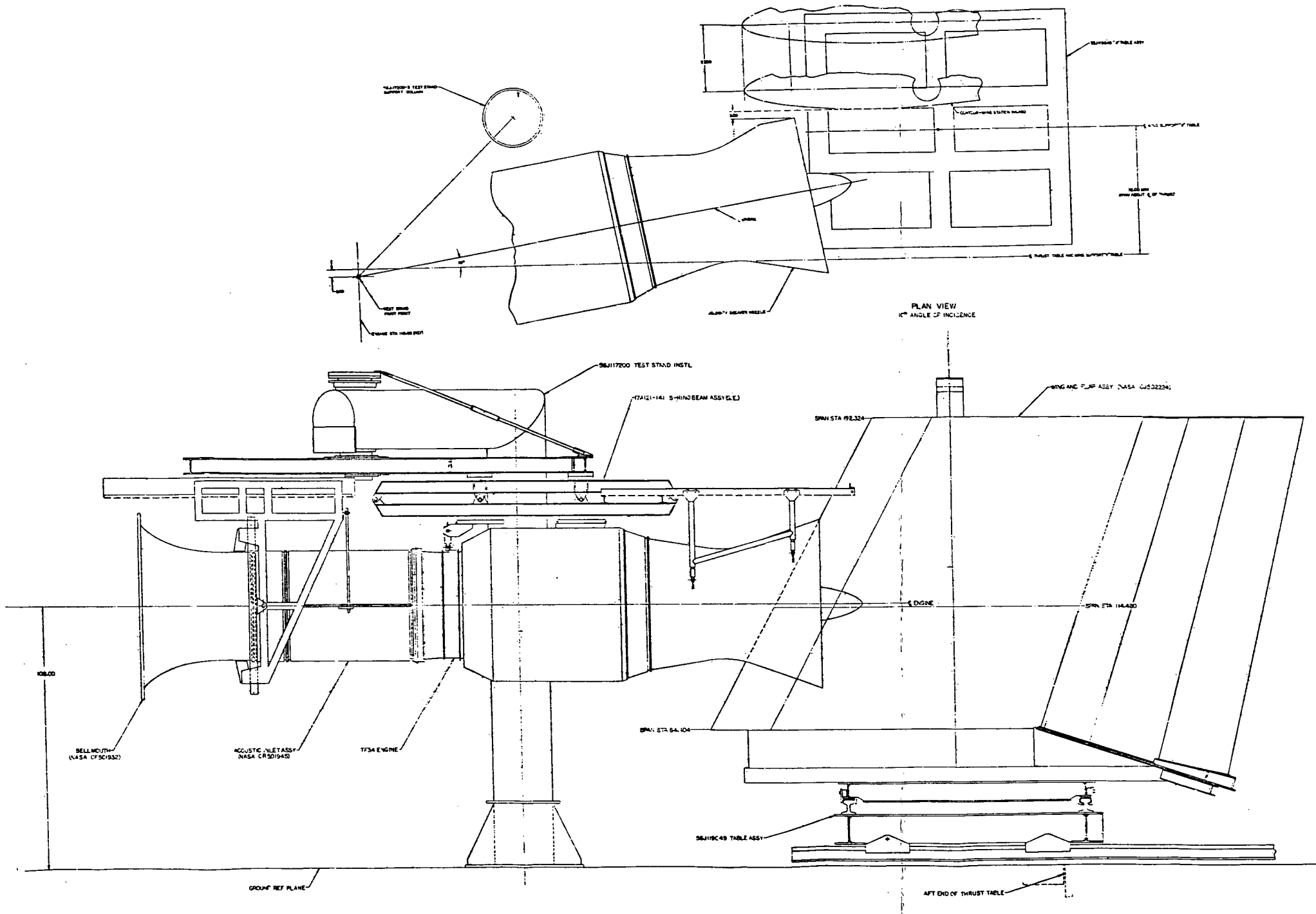

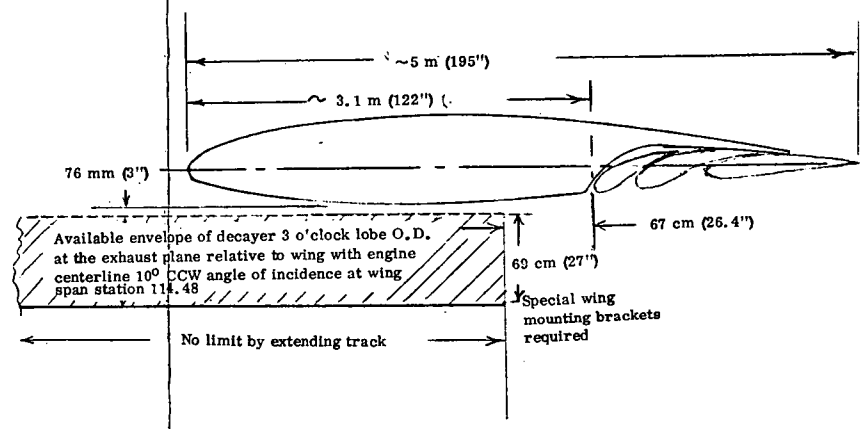

NOTE: With engine at 0° incidence, the side movement is larger than 69 cm (27")

Figure 61. TF34 Engine - Acoustically Treated with Exhaust External Mixer, Mounted for Wing Flap Impingement Noise Test.

FOLDOUT FRAME 1

FOLDOUT FRAME 2

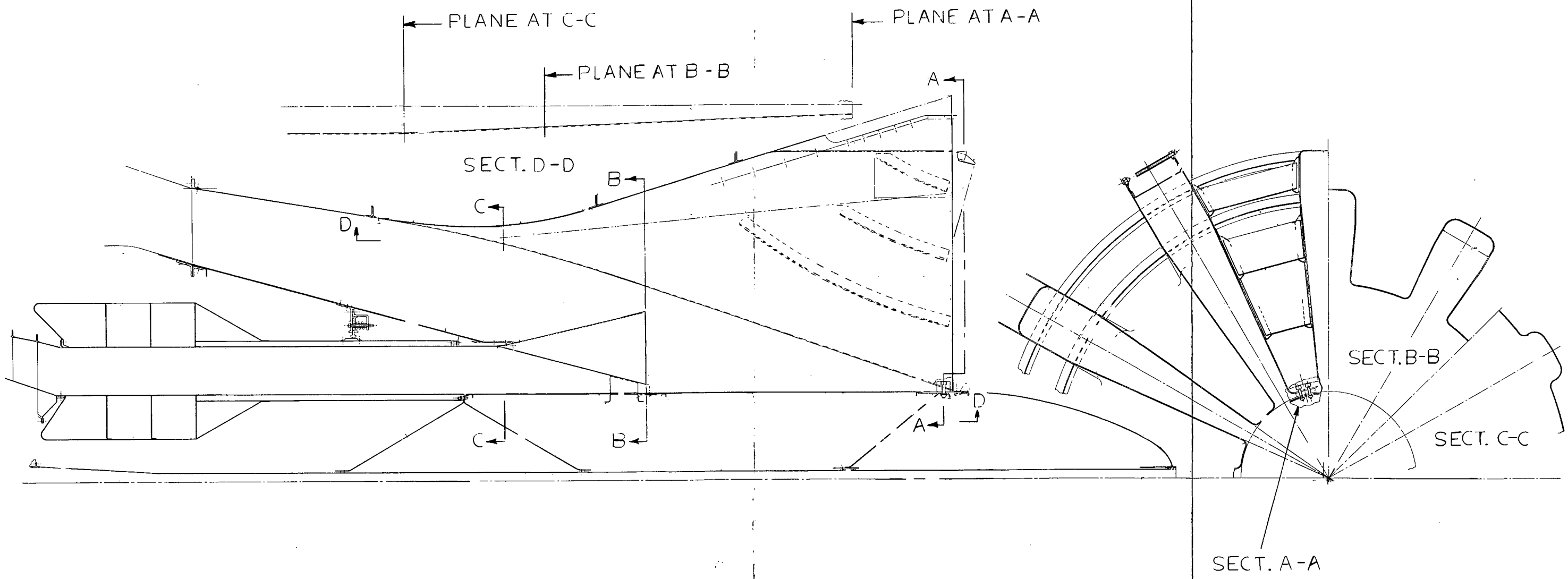

Figure 62. Ground Test Internal and External Mixer.

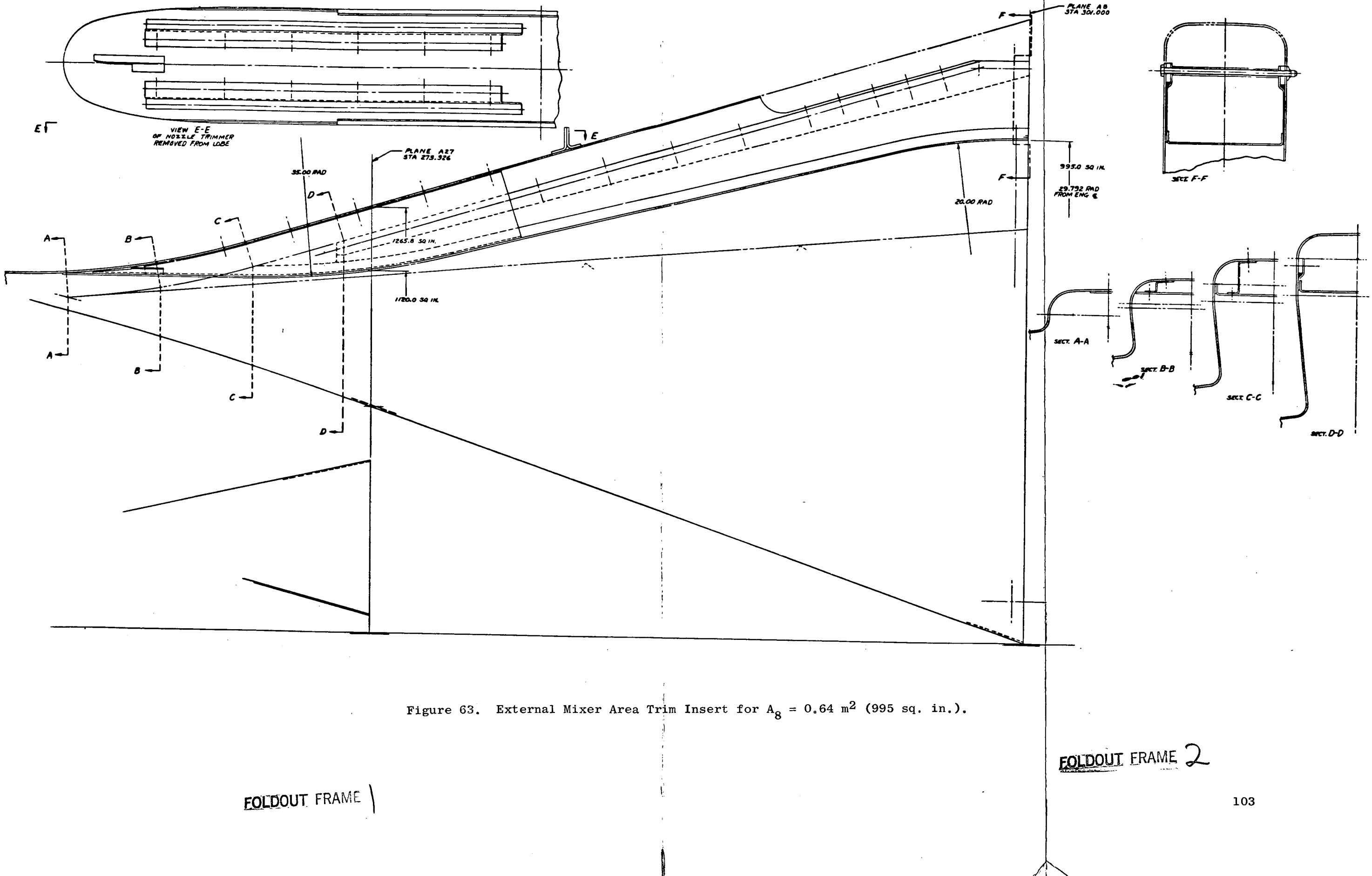

Figure 63. External Mixer Area Trim Insert for A_8 = 0.64 m^2 (995 sq. in.).

FOLDOUT FRAME 1

FOLDOUT FRAME 2

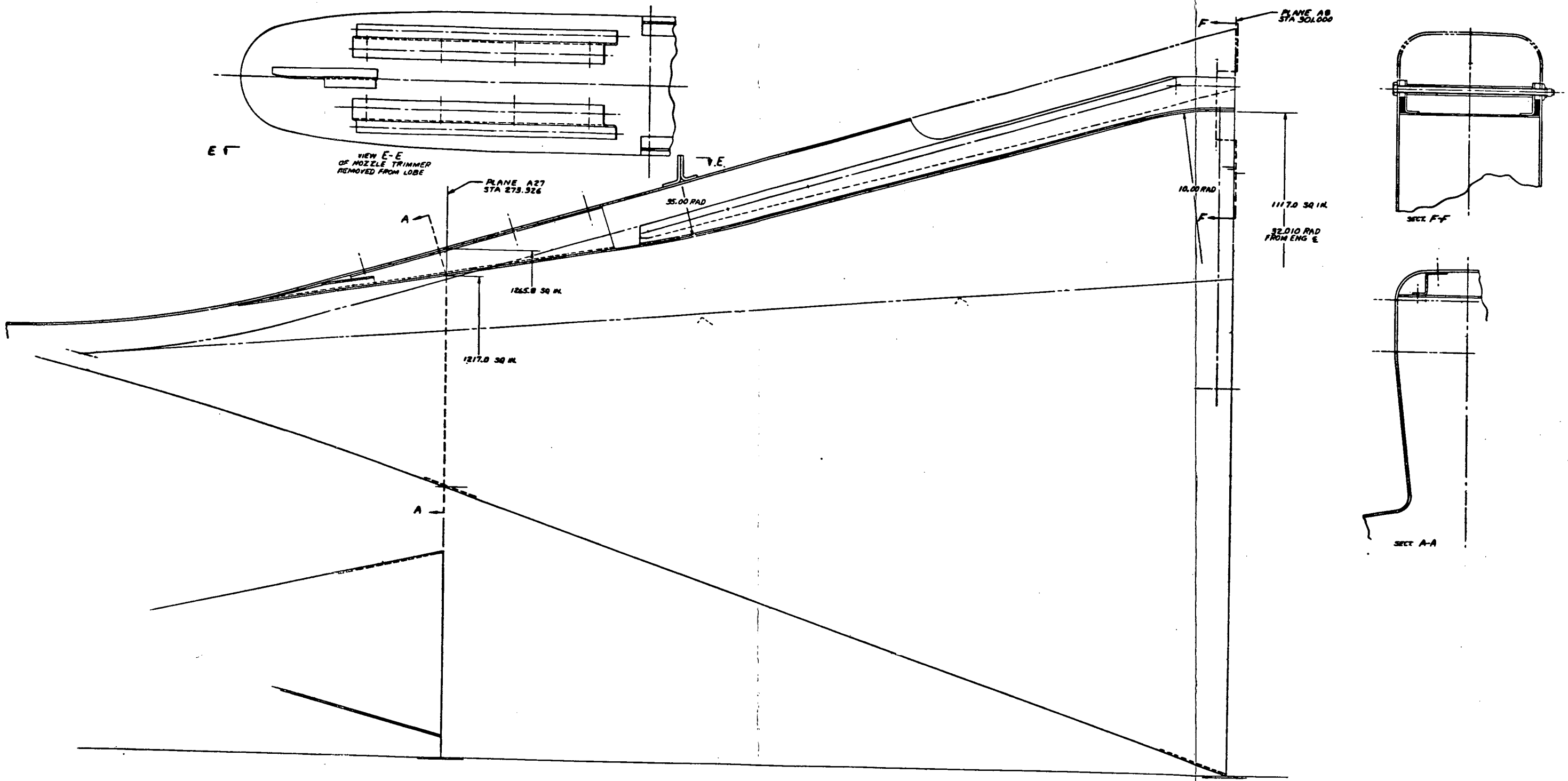

Figure 64. External Mixer Area Trim Insert for $A_8 = 0.72\ m^2$ (1117 sq. in.).

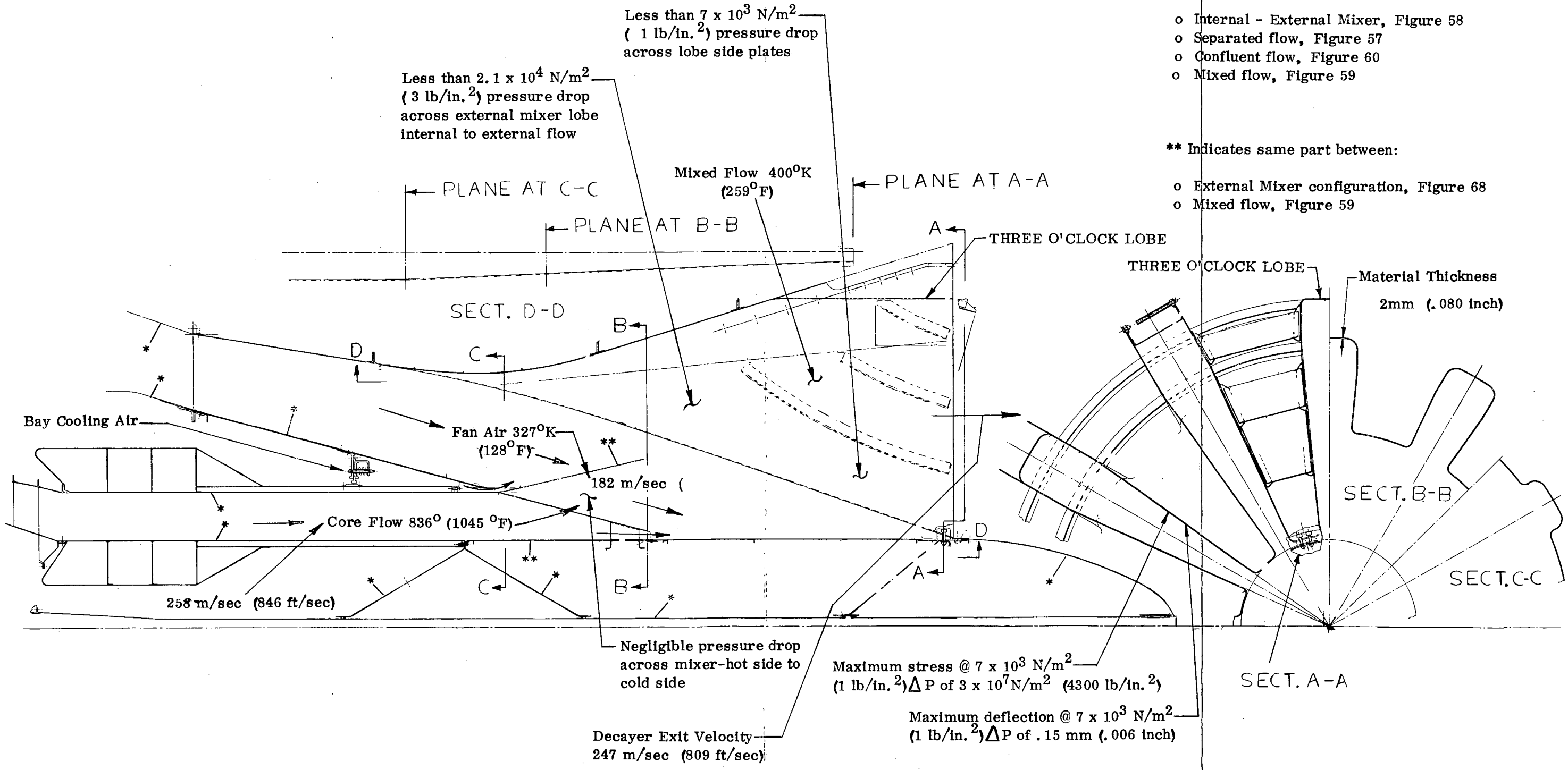

* Indicates same parts for the following configurations:

- o Internal - External Mixer, Figure 58
- o Separated flow, Figure 57
- o Confluent flow, Figure 60
- o Mixed flow, Figure 59

** Indicates same part between:

- o External Mixer configuration, Figure 68
- o Mixed flow, Figure 59

Figure 65. NASA TF34 Quiet Nacelle Ground Test Internal - External Mixer Information Drawing.

FOLDOUT FRAME 1

FOLDOUT FRAME 2

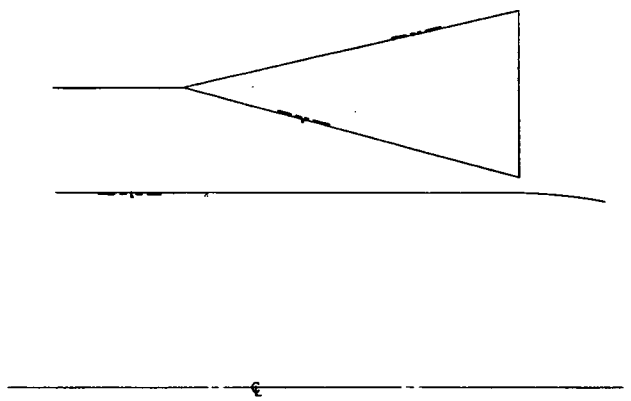

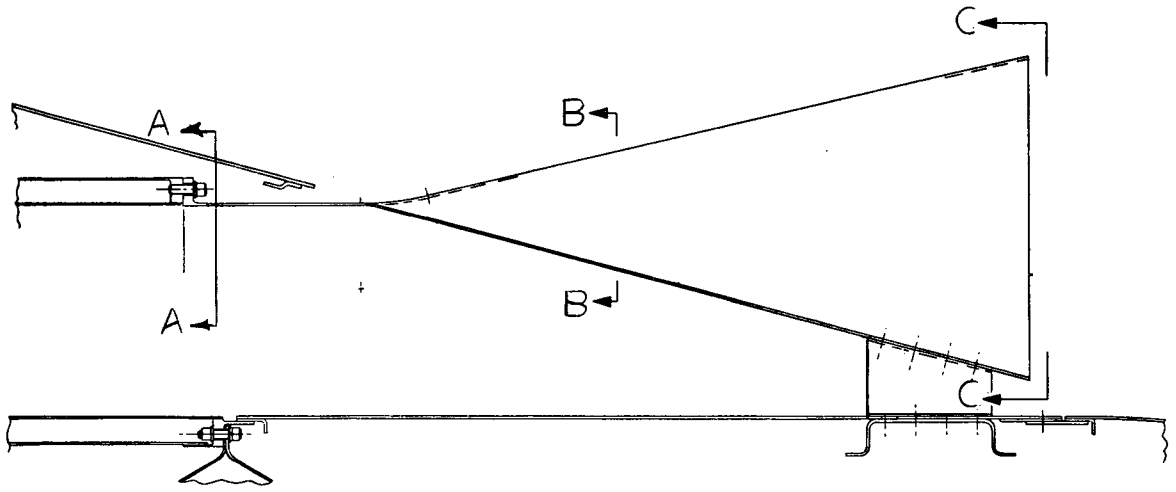

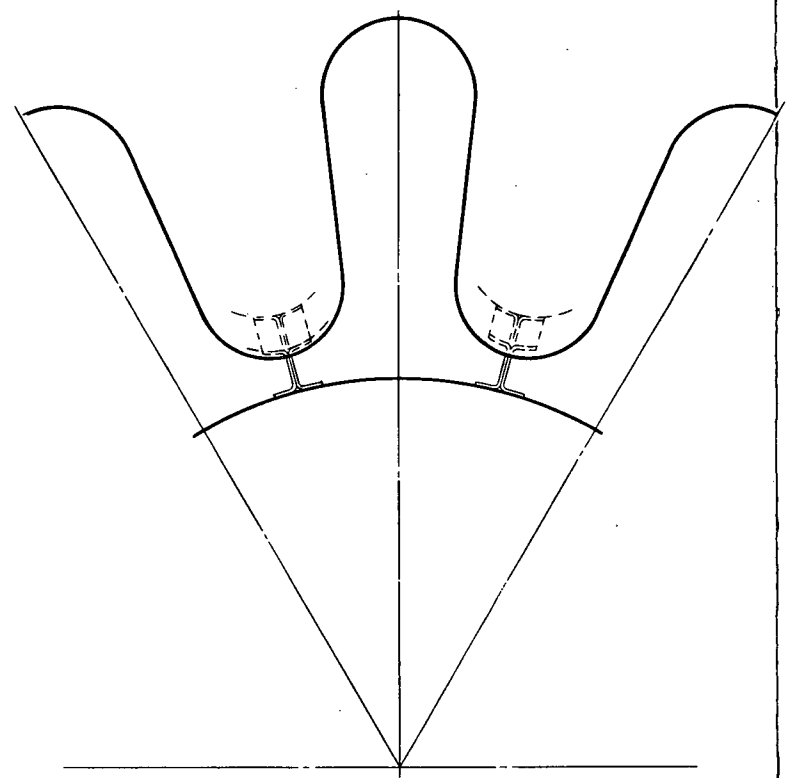

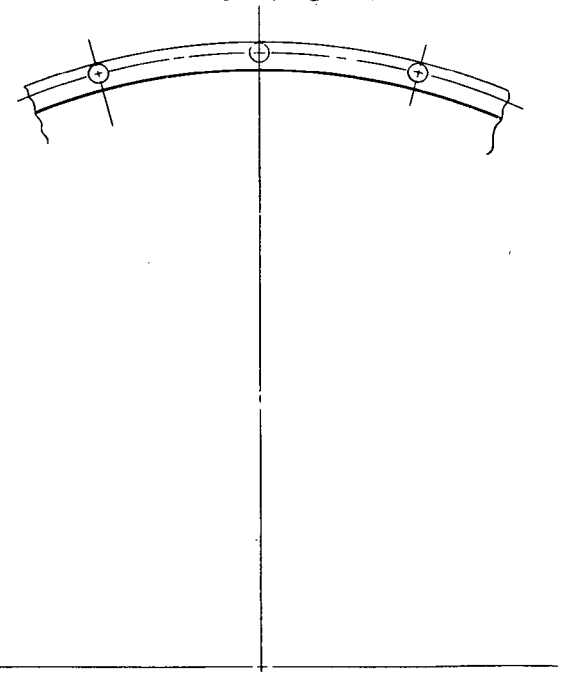

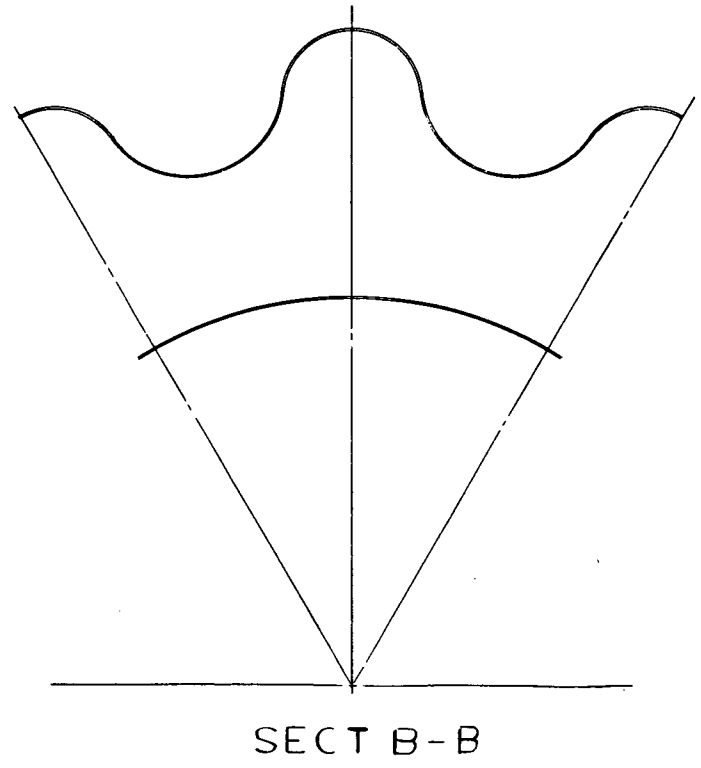

Figure 66. Internal Mixer Working Layout.

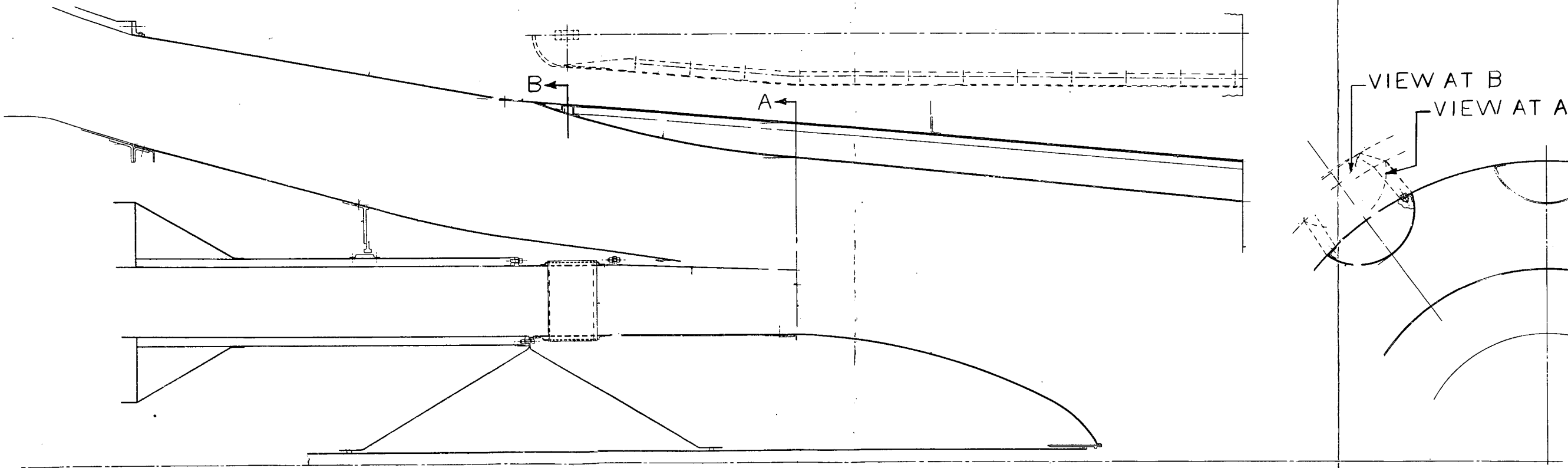

Figure 67. TF34 Ground Test Confluent Exhaust.

PRECEDING PAGE BLANK NOT FILMED

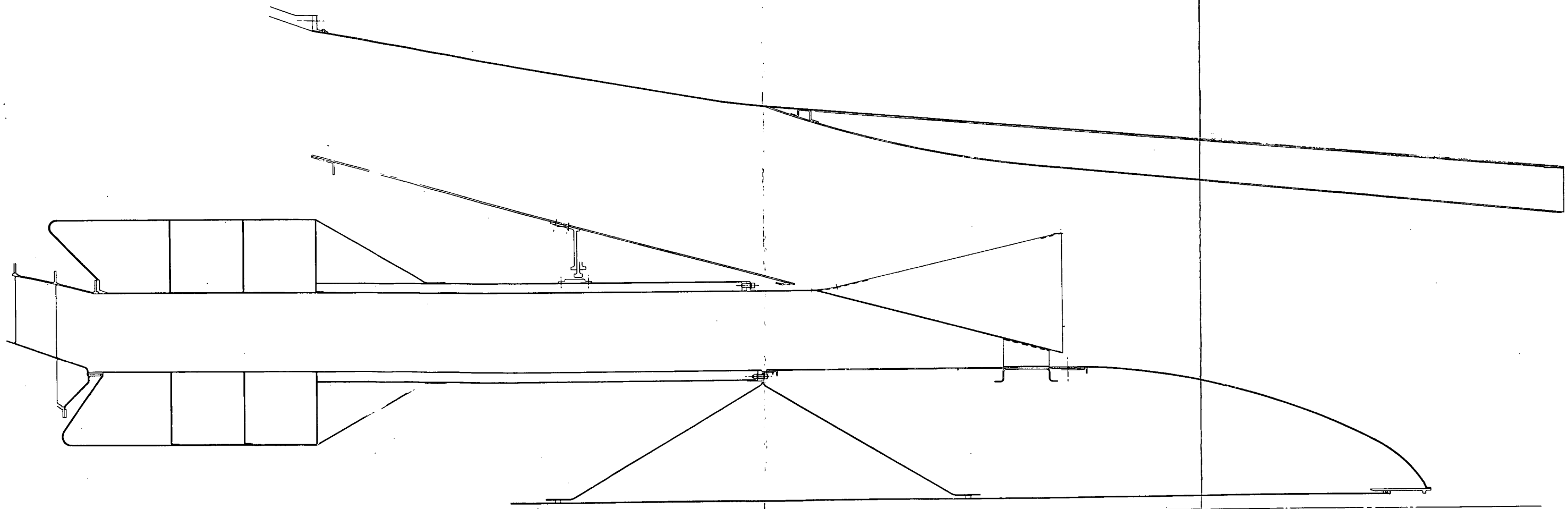

Figure 68. TF34 Ground Test Mixed Exhaust.

FOLDOUT FRAME 1

FOLDOUT FRAME 2

Flight Mixer Nozzle Design Study

The flight version of this 12 lobe internal external mixer design concept includes some modifications made to satisfy anticipated EBF engine and nacelle installation considerations. These modifications shown in Figure 69 include:

1) Eliminating the top lobe, to avoid aerodynamic interference with the large pylon anticipated for an EBF engine installation.

2) Tailoring lobe size (aspect ratio) to avoid premature impingement of engine exhaust on the wing, and to spread the flow laterally to get better distribution of the exhaust flow over the wing flaps.

3) A single aerodynamically shaped structural support strut located between external lobe surfaces.

Performance and Noise Considerations

These modifications are not expected to have an appreciable influence on either the velocity decay characteristics or the performance of the basic 12-lobe design.

The velocity decay ratio of 0.63 at the design point distance of 2.8m (112 inches) has been retained by selecting combinations of lobe aspect and spacing ratio that results in the flow from each lobe coalescing at the same point, (2.8m (112 inches)).

The internal performance and external drag of this flight design are expected to be essentially equal to the estimates made for an asymmetric design. The increased surface areas in the larger lobes at the 3 and 9 o'clock locations should be cancelled out by the decreased surface areas at the 12 and 6 o'clock locations. Eliminating the top lobe will give a small increase in performance due to the decreased losses that go with fewer lobes; however, it is expected that this will be practically cancelled out by the upstream redistribution of flow entering the different shape lobes and the flow angularity losses in the 3 and 9 o'clock lobes. The external drag is not expected to be changed. The maximum boattail angle constraint needed to avoid an increase in pressure drag has been met. The afterbody fineness ratio, based on cross-sectional area distribution has not been significantly changed.

Mechanical Design and Weight Considerations

The flight concept is a modification of the ground test design incorporating lightweight construction and configuration changes for the pylon interface, Figure 69 . The fabrication technique and materials for a flight type design have not been frozen; however, the following are being considered:

- Aluminum sheet welded fabrication with supports between the lobes in the cool region riveted to a titanium inner aft hotter section.
- Titanium welded fabrication with supports between the lobes.

The estimated incremental weights for each of these fabrications compared with a nozzle with no mixer are:

- Aluminium titanium composite fabrication 91 kg (200 lb)
- Titanium welded construction 132 kg (290 lb)

The aft inner section of the external mixer nozzle is subjected to temperature at the upper limit for aluminum thus eliminating this material for this section. The temperature distribution measured in the ground test nozzle will provide information for a flight type design in the region of the hot section.

Titanium honeycomb and steel honeycomb were studied and considered impractical at this time because of cost and fabrication difficulties.

The ground test internal mixer, Figure 66, is essentially the same design as would be used for a flight design, Figure 69.

3

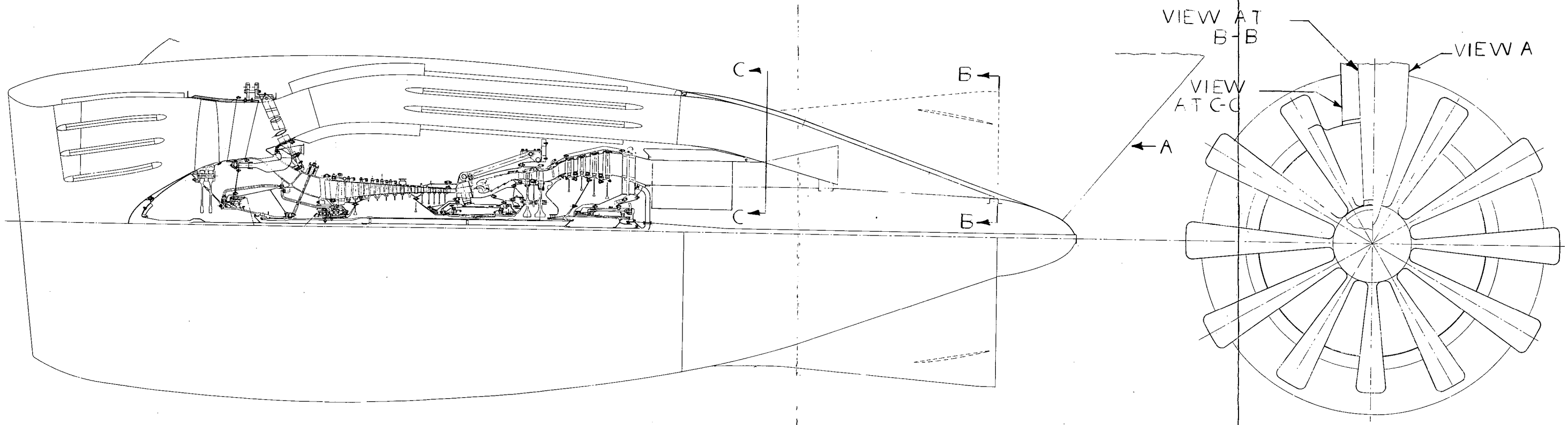

Figure 69. TF34 with Conceptual Flight Type Design of Acoustically Treated Fan Inlet, Fan Exhaust, Core Exhaust with Internal Mixer and External Mixer.

FOLDOUT FRAME 1

FOLDOUT FRAME 2

CONCLUSIONS

1. The recent NASA Lewis Research Center data on EBF engine exhaust wing flap interaction noise and multi-element nozzle exhaust velocity decay was the most complete and directly applicable information for this study. No useful data on inflight effects on flap interaction noise was found.

2. Fixed geometry (non-retractable) mixer nozzle design concepts, particularly the multi-lobe design, were considered to offer higher performance and lighter weight than the complex variable geometry designs needed to satisfy similar levels of velocity decay.

3. The mixed flow version of a Quiet TF34 engine was selected over a separate flow version for the following reasons:

   a. Potential for lower flap and jet noise due to lower exhaust velocities.

   b. Availability of space for acoustic suppression treatment.

   c. The internal plus external mixer system for a mixed flow engine is lighter and has higher performance than two external mixers for a separate flow engine (both designed for the same amount of velocity decay).

4. The simplified flap interaction noise prediction procedure developed for this study indicates that 150 m (500 foot) 4 engine sideline noise level at approach will be 2 PNdB lower than the design goal; however, the takeoff noise will be 2 PNdB above the design goal.

   Uncertainties in the system noise prediction procedure are estimated to be $\sim$ +3 DB, -2 DB at both takeoff and approach.

5. A 12-lobe internal and external mixer exhaust nozzle system provides what now appears to be the best balance between flap impingement velocity and interaction noise, performance penalty and weight, as follows:

   - Velocity decay - flap spacing m (in.) 2.5 (100) 2.8 (112) 4 (160)
     velocity ratio 0.68 0.63 0.58
   - 150 m (500 ft) sideline takeoff noise - 94 PNdB (4 engines)
   - 150 m (500 ft) sideline approach noise - 90 PNdB (4 engines)
   - Loss in takeoff net thrust, - 1 %
   - Loss in cruise net thrust, - 8 %
   - Flight weight increment over a conical nozzle - 90 Kg (200 lb)

6. The modifications to this design anticipated to satisfy EBF flight installation considerations should have a negligible influence on velocity decay and performance. However, the elliptical shaped exhaust pattern of the flight design is expected to provide some improvement in EBF wing lift capability, since a larger area of the flap will be in the exhaust stream.

APPENDIX

Detailed curves for mixer optimization shown in simplified form on page 48.

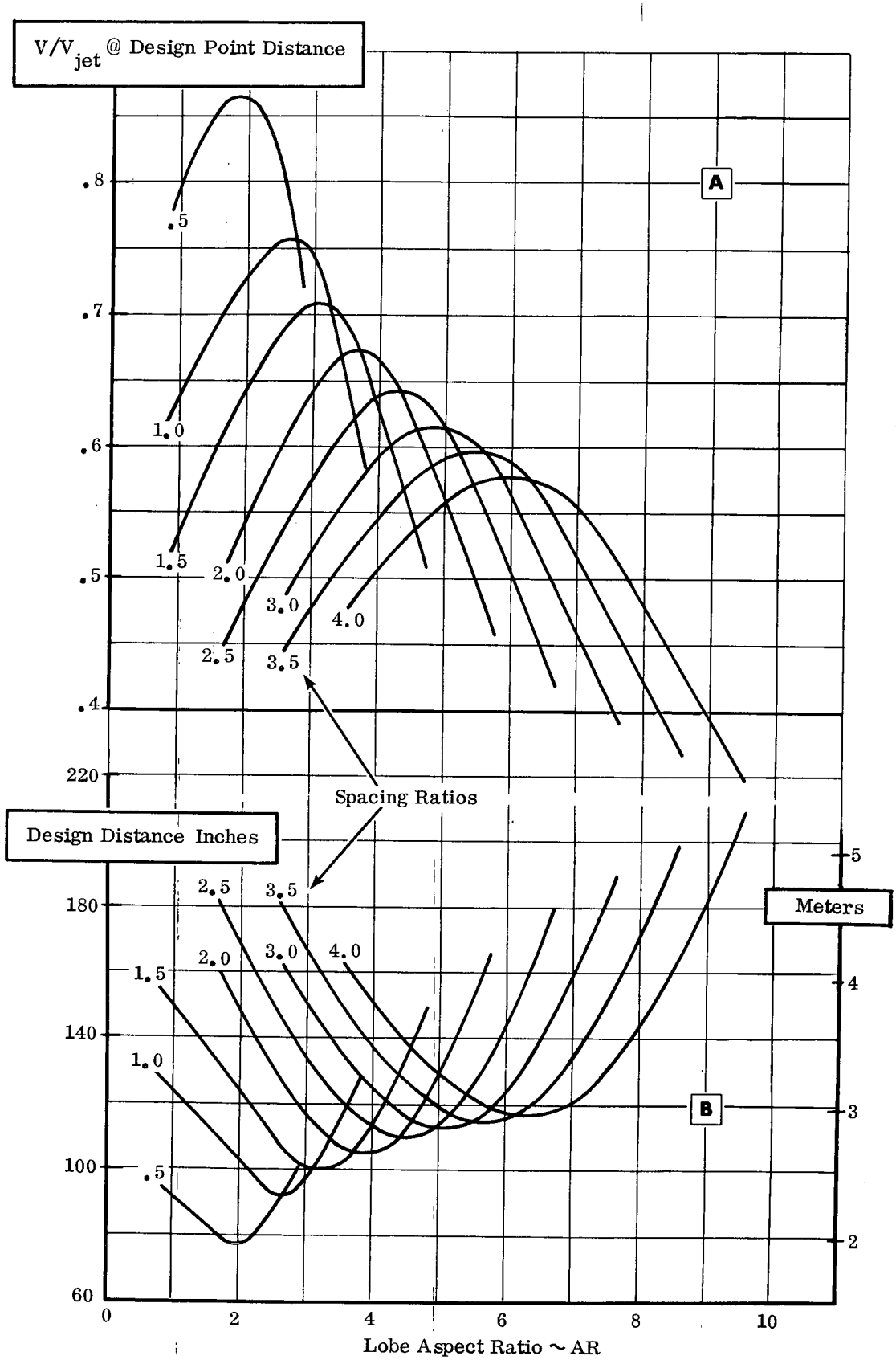

Design Point Distance and Velocity Ratio for a 12 Lobe Velocity Decay Device

Area Ratio Versus Aspect Ratio-Design Curve

12 Lobe Decayer

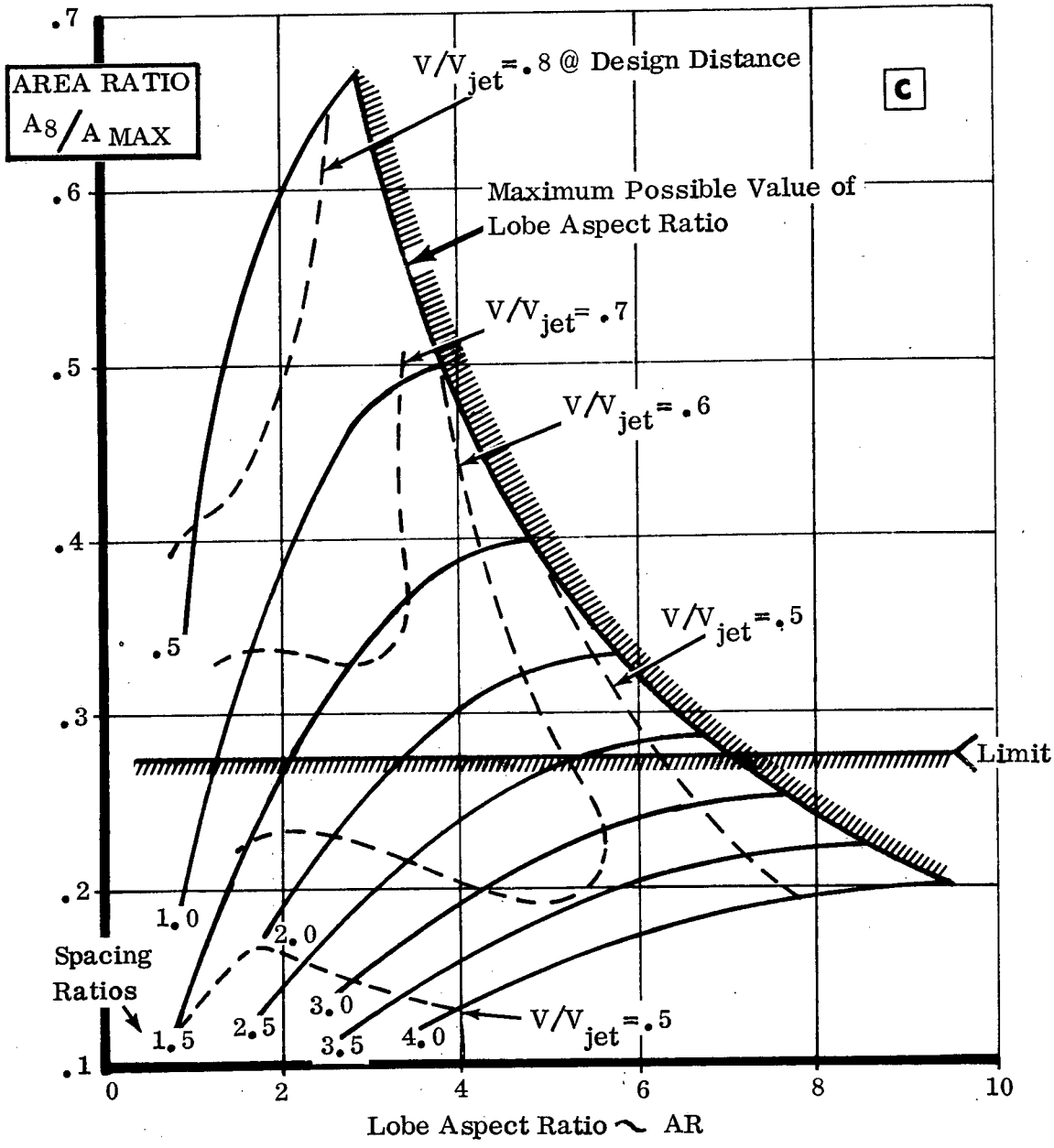

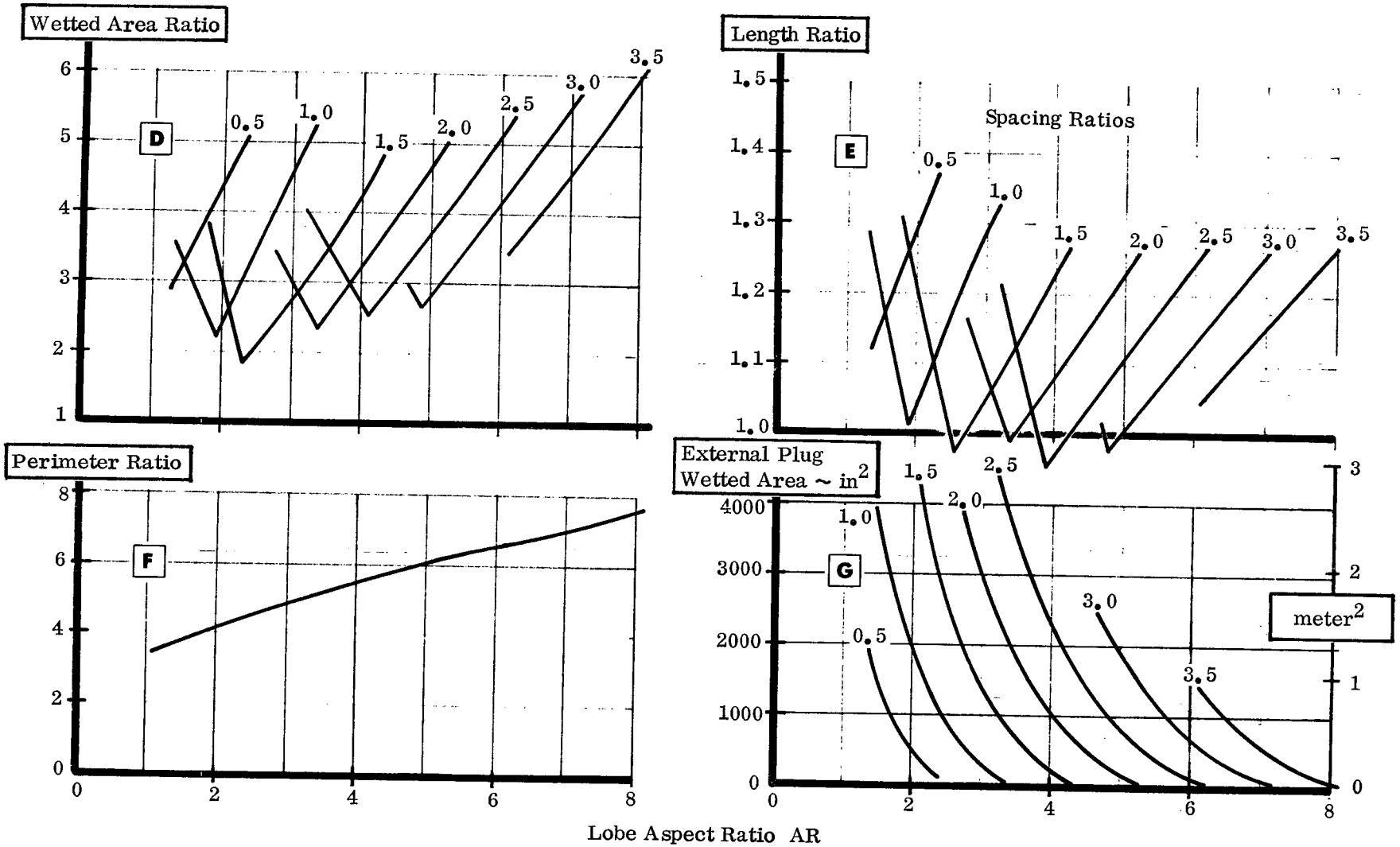
Wetted Area Ratio
D
0.5
1.0
1.5
2.0
2.5
3.0
3.5
Length Ratio
E
Spacing Ratios
Perimeter Ratio
F
External Plug
Wetted Area ~ in²
G
meter²
Lobe Aspect Ratio AR

REFERENCES

* - Indicates direct G. E. experience

1. *AIAA Paper No. 71-4; "Analytical Solution for Free Turbulent Mixing in Compressible Flows", P. H. Heck and D. R. Ferguson; presented at AIAA 9th Aerospace Sciences meeting in N. Y., N. Y., January 25-27, 1971.

2. NASA SP-259, "AIRCRAFT PROPULSION - Blown Flap Noise"; from proceedings of a conference held at NASA Lewis Research Center, November 18-19, 1970.

3. Langley Working Paper No. LWP-989; "Results of Free-Flight Simulation, Noise, and Loads Investigations Related to the NASA Experimental STOL Transport Research Airplane", compiled by R. E. Kuhn and J. L. Hassell, Jr., September 14, 1971.

4. *"GE4/SST Noise Suppression Status Report", J. F. Brausch, March 22, 1971.

5. Boeing Report D6-15071 Vol. II; "Acoustic and Thrust Characteristics of the Subsonic Jet Efflux from Model Scale Sound Suppressors-Part I: Unheated Jets", D. E. Cuadra, et. al., December 21, 1966.

6. Proceedings from a short course on "Noise Generation and Suppression in Aircraft"' The University of Tennessee Space Institute, January 29 - February 2, 1968; edited by H. D. Gruschka.

7. NASA TM X-67850, "Blown Flap Noise Research", R. G. Dorsch, E. A. Krejsa, and W. A. Olsen, June 14-18, 1971.

8. Flight Research Center Working Paper FWP-25, "A Full-Scale Investigation of Externally Blown Flap Impingement Noise"; T. W. Putnam and P. L. Lasagna, August 1971.

9. *"Research Investigation of the Generation and Suppression of Jet Noise" prepared under Navy BuWeps Contract Nos. 59-6160-C; R. Lee, et. al., January 16, 1961.

10. *G. E. TM No. 69-457, "Jet Plume Characteristics of 72-Tube and 72-Hole Primary Suppressor Nozzles"; (FAA Contract FA-SS-67-7), P. H. Heck, July 10, 1969.

11. NACA TN4261, "Acoustic, Thrust, and Drag Characteristics of Several Full-Scale Noise Suppressors for Turbojet Engines", C. C. Ciepluch, et. al., April 1958.

12. NACA TN4269, "Transonic Drag of Several Jet-Noise Suppressors", W.J. North.

13. *G.E. TIS Report R58AGT849, "External Aerodynamic Performance of the CJ805 Sound Suppressor Nozzle", J.T. Kutney, November 17, 1958.

14. NACA TN1387; "Full-Scale Investigation of Several Jet-Engine Noise-Reduction Nozzles", W.D. Coles, et. al., 1958.

15. *G.E. TM 70766; 'Review of Current Multi-Element Aerodynamic Characteristics"; E.J. Stringas, February 15, 1971

16. AFFDL ASD-TDR-62-578; "Suppression of Jet Noise with Emphasis on the Near Field" prepared by Western Electro-Acoustic Laboratory, L.A., California, (K.M. Eldred, et. al.), February, 1963.

17. NASA TND-388 "Transonic Performance Characteristics of Several Jet Noise Suppressors", J.W. Schmeer, et. al., July 1960.

18. "Silencing the Jet Aircraft" by H.W. Withington of the Boeing Company, presented at the Aircraft Noise Session, 24th Annual Meeting, I.A.S., in New York, January 23-26, 1956.

19. Boeing Report D6-11237, "Performance of Several Jet Wake Noise Suppressors", J.E. Postlewaite, January 4, 1967.

20. ASME Paper No. 59 AV49; "Noise Suppressors for Avon and Conway Engines", F.B. Greatrex, March 1959.

21. LWP 981 (Langley Working Paper); "Noise Measurement Studies of Several Model Jet Augmented Lift Systems", F.W. Gibson, August 1971.

22. *G.E. PD&TPO Report No. 6; "Advanced Supersonic Transport Engines (High Noise Suppression Program)", F.A. Schweiger, February 25, 1971.

23. *G.E. TM 71-369; "GE4 High Suppression Exhaust Nozzle Data Correlation", C.D. Wagenknecht, April 13, 1971.

24. NASA TN-D-2263, "Dynamic Pressure and Thrust Characteristics of Cold Jets Discharging from Several Exhaust Nozzles Designed for VTOL Downwash Suppression", C.C. Higgins and T.W. Wainwright, (prepared under contract by the Boeing Company), April 1964.

25. *G.E. Drawing No. 4013153, "Nozzle-Translating Shroud-Cascade Reverser Multiple Tube Suppressor", February 19, 1971.

26. *G. E. Drawing No. 4013153,"Exhaust Nozzle-Translating Shroud, Variable Plug, 32 Chute Sound Suppressor, January 26, 1971.

27. NASA TM X-67934, "Peak Axial-Velocity Decay with Mixer-Type Exhaust Nozzles", D. Grosbeck, R. Huff, and U. von Glahn, September 1971.

28. NASA TM X-67938, "Preliminary Tests of the Mixer Nozzle Concept for Reducing Blown Flap Noise", J.H. Goodykoontz, W. A. Olsen and R.G. Dorsch, October 1971.

29. *Letter from C.Y. Chen to P.R. Knott entitled, "Calculations of Flow Field of a Jet in Flight", dated May 20, 1970.

30. "Research on Jet Noise Generation and Suppression" by W.R. Semrau, April 1964, prepared under Contract No. w 62-0887-d for Department of the Navy.

31. "Momentum Diffusion from a Slot Jet" from Journal of Applied Mechanics, September 1956 by A.S. Weinstein, et. al. pp. 437.

32. General Electric Proposal, M34-0170-006A, "System Proposal for Propulsion of NASA Experimental STOL Transport Research Aircraft".

33. NASA TM X-67979, "Peak Axial-Velocity with Single and Multi-Element Nozzles", U.H. vonGlahn, D.E. Groesbeck, and R.G. Huff, January 17-19, 1972.

34. SAE Air 876A, Jet Noise Predictions, July 1965.

35. SAE Air 923, Method for Calculating the Attenuation of Aircraft Ground to Ground Noise Propagation During Takeoff and Landing, 8/15/66.

ENGINE STATION DESIGNATION

SEPARATE FLOW EXHAUST

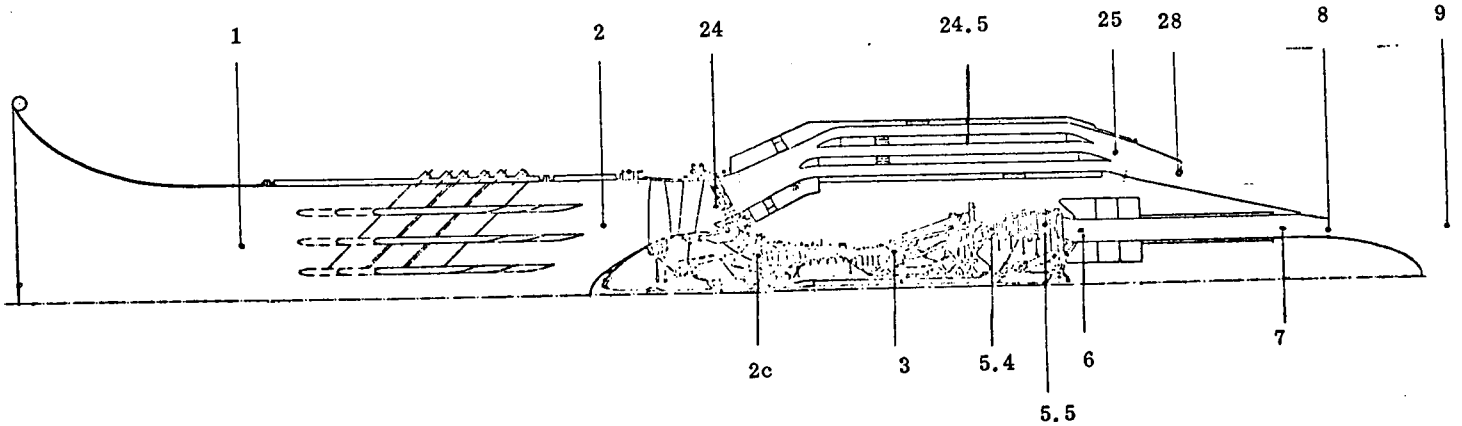

MIXED FLOW EXHAUST